Electrochemical Evaluation of Leaf Composited Membrane with and without Electrolytic salt for Supercapacitors

Thesis submitted in

Partial Fulfilment of the

Degree of Master of Philosophy (M.Phil)

By

V. SUMITHRADEVI

18MPPHF006

DEPARTMENT OF PHYSICS

AVINASHILINGAM INSTITUTE FOR HOME SCIENCE AND HIGHER EDUCATION

FOR WOMEN

COIMBATORE – 641 043

JULY 2019

Electrochemical Evaluation of Leaf Composited Membrane with and without Electrolytic salt for Supercapacitors

Thesis submitted in

Partial Fulfilment of the

Degree of Master of Philosophy (M.Phil)

By

V. SUMITHRADEVI

18MPPHF006

DEPARTMENT OF PHYSICS

AVINASHILINGAM INSTITUTE FOR HOME SCIENCE AND HIGHER EDUCATION FOR WOMEN

COIMBATORE – 641 043

JULY 2019

CERTIFIED AS A BONAFIDE RESEARCH WORK

31/7/2019

Signature of Head of the Department

31/07/19

Signature of the Supervisor

DECLARATION

I declare that the dissertation entitled **Electrochemical Evaluation of Leaf Composited Membrane with and without Electrolytic salt for Supercapacitors** submitted by me for the degree of Master of Philosophy (M.Phil) is the record of work carried out by me during the period from **August 2018 to July 2019** under the guidance of **Dr.(Tmt.) B. Nalini,** M.Sc., Ph.D., M.S (Edu.Mgt.), STA fellow, AIST Fellow (Japan), Assistant Professor (SS), Department of Physics, Avinashilingam Institute for Home Science and Higher Education for Women, Coimbatore and has not formed the basis for the award of any Degree, Diploma, Associateship, Fellowship, Titles in this University or any other University or other similar institution of Higher Learning.

V. Sumithradevi

Signature of the Candidate

CERTIFICATE

I certify that the dissertation entitled **Electrochemical Evaluation of Leaf Composited Membrane with and without Electrolytic salt for Supercapacitors** submitted for the degree of Master of Philosophy (M.Phil.) by **V. Sumithradevi** is the record of research work carried out by her during the period from **August 2018 to July 2019** under my guidance and supervision, and that this work has not formed the basis for the award of any Degree, Diploma, Associateship, Fellowship, Titles in this University or any other University or other similar institution of Higher Learning.

31/7/2019

Signature of the
Head of the Department

31/07/19

Signature of the
Supervisor with designation
ASSISTANT PROFESSOR

CHAPTER - I

INTRODUCTION

1.1 INTRODUCTION

A significant worldwide increase in the consumption of fossilfuels, resulting from the rapid growth of the global economy,produces two major associated issues. The first is the acceleratingdepletion/exhaustion of existing fossil fuel reserves and thesecond is the affiliated environmental problems i.e., increasinggreenhouse gas emissions, general air and water pollution constitute the basis of an urgent,worldwide concern about the future, sustainable developmentand health of our society's ecosystem. The need to develop and scale up sustainable, clean energy sources and their associatedtechnologies is recognized worldwide as an urgent priority.Most renewable clean energy sources are highly dependent onthe time of day and regional weather conditions. Development ofrelated energy conversion and energy storage devices is therefore required in order to effectively harvest these intermittent energysources. In this regard, batteries, electrochemical supercapacitors(ESs) and fuel cells are all recognized as three kinds of the mostimportant electrochemical energy storage/conversion devices. Supercapacitors or an ultracapacitor,has attracted considerable interest in both academia and industrybecause it has some distinct advantages such as higher power density induced by a fast charging/discharging rate (in seconds)and a longer cycle life (<100 000 cycles) when compared to batteriesand fuel cells [1-2].

1.2 ENERGY STORAGE DEVICES

1.2.1 BATTERY

A cell is the fundamental unit of a battery. A single cell consists of an electrode and they are separated by an electrolyte. Battery consist of one or more electrochemical cell which are connected together either in series or parallel. A battery is a device that converts chemical energy within its active material into electrical energy by means of electrochemical oxidation and reduction reaction (redox). In the year of 1800, the first battery was developed by Alessandro Volta. Generally batteries are classified into two types. i.e., Primary batteries and Secondary batteries. Primary batteries can be used once and discarded. Secondary batteries can be recharged electrically after discharge.

Battery consists of two electrodes (anode and cathode) and an electrolyte material. In battery electrode materials are always made up of two dissimilar materials because if one of the electrodes gives the electron and the other will be accepting it. Suppose if both the electrodes are made up of same material there is no electric current flows through the circuit. An electrolyte is placed between two electrodes to prevent contact between them and it act as the ion transfer medium [3-5].

1.2.2 FUEL CELL

A fuel cell is an electrochemical cell that converts chemical energy into electrical energy just like batteries but fuel cell requires continues supply of fuels, often hydrogen. Fuel cell does not require recharging and it produces by products of environmentally friendly water and heat. Fuel cell continuously produces electricity as long as fuel and oxygen are supplied. The first fuel cell was invented in the year of 1838. Fuel cell consists of an electrode (an anode and a cathode) and electrolyte. Fuel cells are classified into several types according to their operating temperature and different electrolyte materials used [6-7]. Mostly used fuel cells are

- Polymer Electrolyte Membrane Fuel Cell (PEMFC)
- Alkaline Fuel Cell (AFC)
- Direct Methanol Fuel Cell (DMFC)
- Molten-Carbonate Fuel Cell (MCFC)
- Phosphoric Acid Fuel Cell
- Solid Oxide Fuel Cell (SOFC)

1.2.3 CAPACITOR

A capacitor is a two terminal electrical component that stores electrical energy in the electric field. Capacitors are constructed by two conductors and they are separated by an insulating material. The conductors can be thin films of metallic foil, aluminium foil, etc. Glass, mica, paper, plastic film, and ceramics can be used as dielectric material. When there is a potential difference across the conductors, static electric field is developed across the dielectric material. The amount of charges stored in the ideal capacitor can be determined using the following relation (1.1).

$$C = {}^{q}/_{V} \longrightarrow (1.1)$$

Where,

C is capacitance, q is charge, and V is voltage.

The conventional capacitor yields capacitance in few pico farads to few thousands of microfarads [8].

1.2.4 SUPERCAPACITOR

A supercapacitor also called as an ultra capacitor is a high-capacity capacitor with capacitance value much higher than conventional capacitor. Energy density (the amount of energy stored per unit volume) of a supercapacitor 10 to 100 times more than that of conventional capacitor but lower than battery. Power density (the amount of energy delivered per unit time) of a supercapacitor is much higher than rechargeable battery. So that supercapacitor acts as a bridge gap between conventional capacitor and rechargeable batteries. Due to high power density supercapacitors are used in the application of a system which requires many rapid charge/discharge cycles rather than long term compact energy storage. Mostly supercapacitors are used in the application of electrical vehicles [9].

1.2.5 COMPARISION OF ENERGY STORAGE DEVICES

Ragone plot is a standard chart to compare the performance of the various energy storage devices [10].

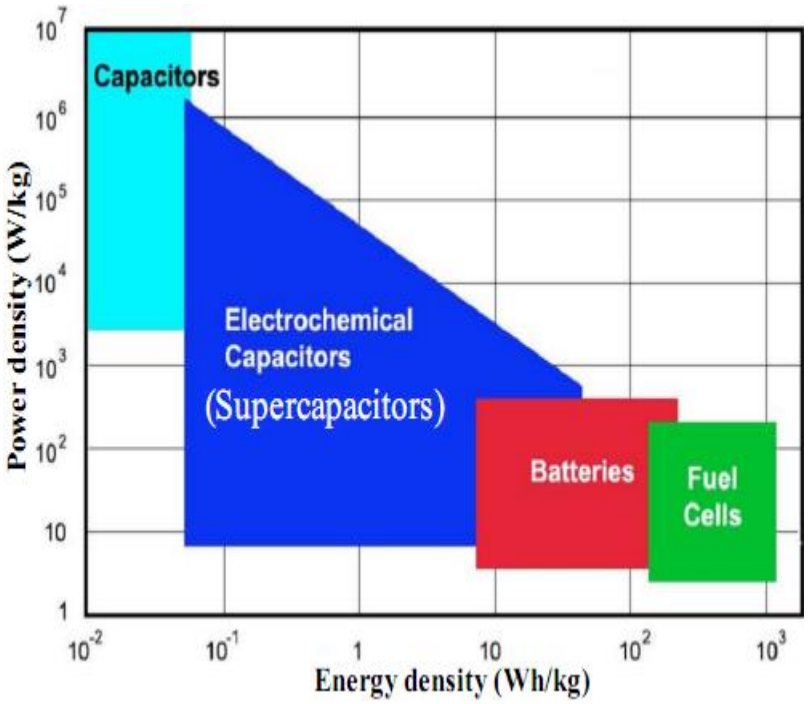

Figure1.1 Ragone plot for various energy storage devices

In this chart (figure 1.1), the values of power density in W/kg versus energy density in Wh/kg is plotted. From the graph in the vertical axis it can be seen that the energy density of the fuel cells and batteries are much higher than conventional capacitor that means they can store large amount of energy than capacitor. But capacitors having high power density which that means they are charged and discharged very fast and produces high power than batteries and fuel cell it is shown in the horizontal axis [11-12].

Table 1.1 Comparison of basic characteristics of energy storage devices

Parameters	**Battery**	**Fuel cell**	**Capacitor**	**Supercapacitor**
Charge /Discharge time	1 to 10 hours	10 to 300 hours instant charge (refuel)	Picoseconds to Milliseconds	Milliseconds to Seconds
Operating temperature	-20 to +65˚C	+25 to +90˚C	-20 to +100˚C	-40 to +85˚C
Operating voltage	1.25 to 4.2V	0.6V	6 to 800 V	2.3 to 2.75V

Capacitance	N/A	N/A	10pF to 2.2mF	100mF to1500F
Life	150 to 1,500 cycles	1,500 to 10,000 hours	>100,000 cycles	50,000+ hrs Unlimited cycles
Weight	1g to > 10g	20g to >5kg	1kg to 10 kg	1g to 230 g
Power density	0.005 to 0.4 kW/kg	0.001 to 0.1 kW/kg	0.25 to 10,000 kW/kg	10 to 120 kW/kg
Energy density	8 to 600 Wh/kg	300 to 3000 Wh/kg	0.01 to 0.05 Wh/kg	1 to 10 Wh/kg

The selection of energy storage device depends on the application, for example the application that requires high power density to energy density, supercapacitors are suitable. [13].Batteries exhibits high energy density so that they are used in the application of mobile phones and laptops. Table 1.1 compares basic characteristics of battery, fuel cell, capacitor and suprcapacitor as shown [14].

Supercapacitors having significant attention due to their higher power density, longer cyclic life and shorter charging and discharging times as compared with batteries [15-16]. According to these desirable properties supercapacitors are mostly used in the application of hybrid electrical vehicles, high power sensor and power electronics [17-18].

1.3 HISTORY OF SUPERCAPACITORS

In the year of 1950, General Electric engineers demonstrate a capacitor with porous carbon electrodes from the design of fuel cells and rechargeable batteries. Mostly activated carbon, also called as activated charcoal is used as electrodes because it consists of extremely porous “spongy” form of carbon with high surface area it increases capacitance value [19, 20, 21]. In 1957, Becker received first patent for capacitor it is based on carbon electrode [U.S. Patent 2 800 616].This energy storage device produces extremely high capacity but the double layer mechanism war not known by him. In 1966, the Standard Oil Company, Ohio (SOHIO) developing another version of energy storage device that is capable of energy storage in double layer interface [22-23].

In earlier electrochemical capacitors consist of activated carbon coated on the aluminium foils acts as the electrodes soaked in an electrolyte and separated by porous insulator. This design gave a capacitor with a capacitance value in farad, significantly higher than electrolytic capacitors. This design remains the basis of electrochemical capacitors.

In 1969, SOHIO demonstrate a disc shaped capacitor, in that capacitor carbon paste soaked in electrolyte which was the first commercialized supercapacitor. In 1971 NEC commercially marketed supercapacitor with low voltage and high internal resistance for memory back up application [23].

In between 1975-1980 Brain Evans Conway conducted extensive fundamental and development on electrochemical capacitors. In 1991 he well defined the difference between "battery" and "supercapacitor". He explained about supercapacitor working mechanism by redox reaction with transfer of charge between two electrodes and ions [24-25].

In 1978, Panasonic produced a "Gold capacitor" for memory backup applications. In 1987, ELNA produced a supercapacitor named "Dyncap". In 1989 United States Department of Energy (DOE) initiated the supercapacitor development. It had set long term and short term goals for 1998-2003 and after 2003. In the production of EDLC number of companies is involved as a part of their commercial activity. Few company names are AVX, Cooper, Evans and Maxwell. The Table 1.2 show the some of the supercapacitor company name, product name, capacitance and voltage value [26].

Table 1.2 Supercapacitor product name, capacitance value and voltage value

Company Name	Country	Product Name	Capacitance value (F)	Voltage value (V)
AVX	USA	Bestcap	0.022-0.56	3.5-12
Cooper	USA	Powerstore	0.47-50	2.3-5
ELNA	USA	Dynacap	0.033-100	2.5-6.3

Epcos	USA	Ultracapacitor	5-5000	2.3-2.5
Evans	USA	Capettery	0.01-1.5	5.5-11
Kold Ban	USA	KAPower	1000	12
Maxwell	USA	Bootcap	1.8-2000	2.5
NEC	Japan	Supercapacitor	0.01-6.5	3.5-12
Panasonic	Japan	Goldcapacitor	0.1-2000	2.3-5.6
ESMA	Russia	Capacitor modules	100-5000	12-52
Cap-XX	Australia	Supercapacitor	0.09-2.8	2.25-4.5
Ness	Korea	EDLC	10-3500	3
Tavirma	Canada	Supercapacitor	0.13-160	14-300

1.4 CLASSIFICATION OF SUPERCAPACITOR

Based on energy storage mechanism and active material supercapacitors can be classified into three types. They are Electrical Double Layer Capacitor (EDLC), Pseudocapacitor and Hybrid capacitor as shown in the figure 1.2.

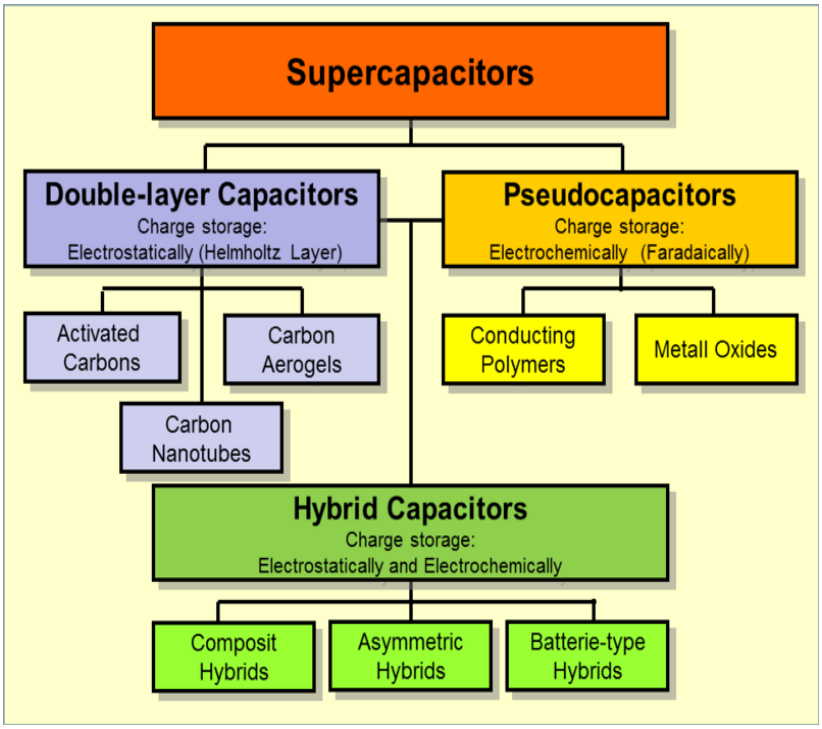

Figure1.2 Classification of supercapacitor

1.4.1 ELECTRIC DOUBLE LAYER CAPACITOR (EDLC):

An electrochemical device consists of two electrodes and they are separated by an electrolyte either solid or liquid. The structure of electrochemical supercapacitor is similar to that of electrochemical cell but there is no electron transfer across the interface. Carbon based materials are found to be suitable electrode materials for supercapacitor due to their high surface area, high electrical conductivity, controllable pore size and low cost than other materials. Various form of carbon based materials such as activated carbon, templated carbon, carbon nanotubes, graphene are mostly used electrode material for supercapacitor. Figure 1.3 shows the diagram of EDLC.

A positive charge accumulates on the positive electrode which attracts equal number of negative charge due to Coulomb force around the electrode and electrolyte interface. The charge balance between the electrode and the electrolyte create an electrical double layer. At the positive electrode side, one double layer is formed. To maintain the neutrality of the whole electrochemical system negative charges accumulates on the negative electrode which attracts equal number of positive charge in the electrolyte. In the negative electrode side another electrical double layer is formed.

Therefore a complete double layer consists of two electrical double layers, one is at positive electrode-electrolyte interface and another one is negative electrode-electrolyte interface. These two electric double layers act as the heart of the supercapacitor [27].

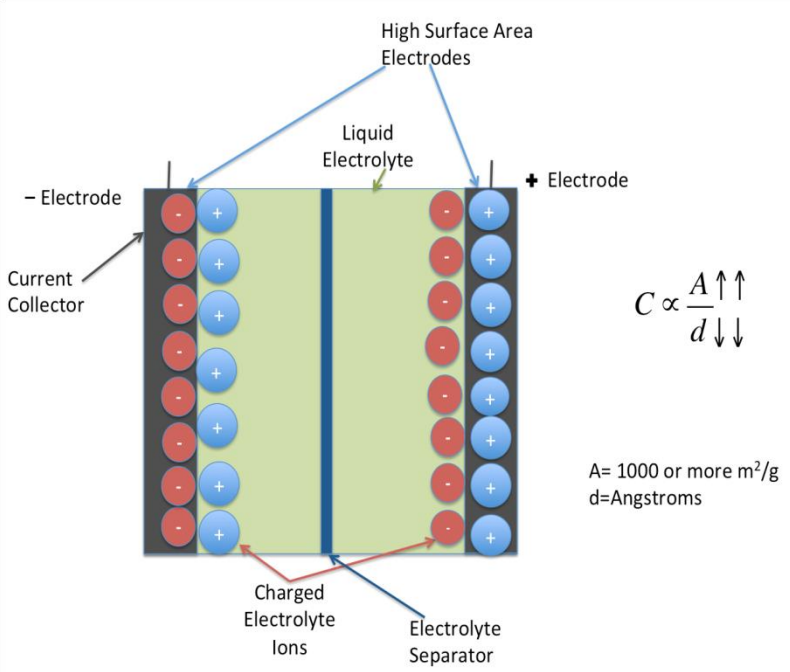

Figure 1.3 Diagram of EDLC

Several models such as Helmholtz model, Gouy-Chapman model, Stern and Granhame model have been proposed to explain about the behaviour observed for electrodes under potentiostatic control in solution.

1.4.1.1 HELMHOLTZ MODEL

In 1879, Helmholtz noticed the double-layer capacitance in supercapacitor. According to the Helmholtz theory the evaluation of double layer is due to the strong interactions between the ions/molecules at electrode and electrolyte interface and reversible ion adsorption on the carbon electrode is responsible for the energy storage in electrochemical capacitors [28]. Since there is no redox reaction occurs in electrochemical capacitor. Due to non faradaic process charge is stored in EDLC at the electrode and electrolyte interface. The capacitance in double layer capacitor can be calculated using the following equation (1.2).

$$\mathbf{C}=\frac{\varepsilon_0 \varepsilon_r A}{d} \longrightarrow \qquad (1.2)$$

where

ε_r is the dielectric constant of the electrolyte

ε_o is the permittivity of free space

A is the surface area of the electrode

d is the thickness of electrical double-layer

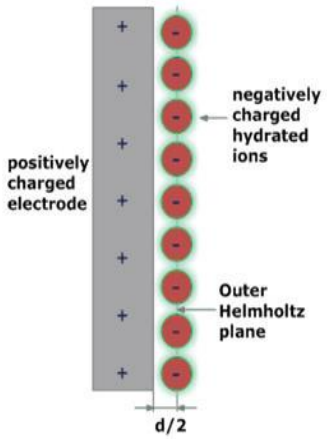

Figure 1.4 Helmholtz model

Thickness (d) depends on the size of the ions and the electrolyte concentration [29]. In EDLC the separation distance d is in the range of angstrom, while in conventional capacitor it is in the micro-meter range. Capacitance in electrochemical capacitor is significantly higher than conventional capacitor. A displacement current has been observed due to the arrangement of charges, which explains the non-faradaic nature of the EDLC due to negligible charge transfer across the interface. Thus oriented polarization of charge species occurs at the electrode and electrolyte interface due to the excess or deficiency of electrons, anions and cations in solution is the reason for the formation of double layer capacitor [30].

1.4.1.2 GUOY-CHAPMAN MODEL

In the year of 1900, Gouy considered that capacitance was not a constant and it depends on the applied potential and the ionic concentration. According to Guoy-Chapman, the electric double layer is divided into two main layers, one layer is Helmholtz layer which arises due to the fact of accumulation of charge carriers at the electrode and electrolyte interface and the another layer is due to the thermal fluctuation in the solution, the net negative ions scattered with a higher concentration near the electrode surface and a lower concentration in a solution. This scattered layer plus electrode positive array is known as the “diffuse double layer” or “diffuse layer”. The thickness of the diffuse layer is depends on the temperature, the concentration of the electrolyte, charge number carried by the ion and the

dielectric constant of the electrolyte. Generally if the temperature is high, the diffusion layer becomes thicker; the electrolyte concentration, charge number carried by the ion and the dielectric constant are high, the diffuse layer becomes thinner. However if the temperature is lowered and the concentration of the electrolyte, the charge number carried by the ion and the dielectric constant of the electrolyte are high, then the diffuse layer become very thin and it forms the negative ions near the electrode surface [27]. In Guoy-Chapman model the total capacitance can be calculated using the following equation (1.3) [31].

$$\frac{1}{\mathrm{C_{total}}} = \frac{1}{C_H} + \frac{1}{C_{diff}} \longrightarrow (1.3)$$

Where,

C_{total} = Total capacitance of the EDLC

C_H = Helmholtz capacitance

C_{diff} = Capacitance of the diffuse layer

From the above equation (1.3) the overall capacitance of the EDLC is the series capacitance of the Helmholtz layer and the diffuse layer.

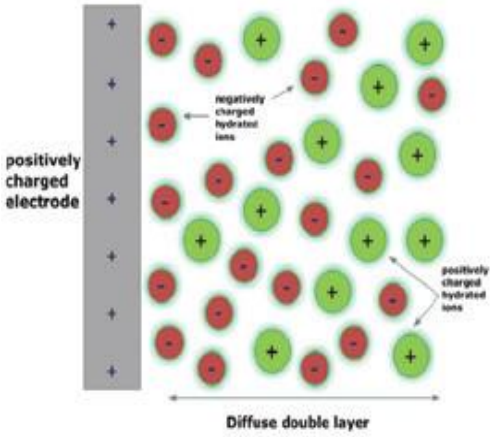

Figure 1.5 Guoy-Chapman model

1.4.1.3 STERN MODEL

Gouy – Chapman model assumes that ions act like point charges and there is no physical limitation for the ions approach to the surface, but which is not true [32]. The capacitance of two separated arrays of charges is inversely proportional to distance between them, so that when point charge ions are closer to the electrode surface it produces an extremely high capacitance which does not meet in the actual case.

To resolve this problem, in 1924 Stern combined the two previous models by adapting the compact layer of ions used by Helmholtz and the diffuse layer of Guoy chapman model. In the Stern layer also called as compact layer, ions are absorbed tightly and that can be divided into two regions depending on the charge polarity of ions. The inner region consists of specifically absorbed ions and the outer region consists of not specifically absorbed ions, as shown in figure. These two regions are distinguished by two plane, they are inner Helmholtz plane and outer Helmholtz plane. The inner Helmholtz plane locates at the distance of closest specifically absorbed anions and the outer Helmholtz plane locates at that of non-specifically absorbed cations. Then the diffuse layer starts after the outer Helmholtz plane [33].

The total capacitance equations were modified including the Stern layer capacitance $C_s$and the diffuse layer capacitance $C_{diff.}$

$$\frac{1}{C_{tot}} = \frac{1}{C_S} + \frac{1}{C_{diff}} \longrightarrow (1.4)$$

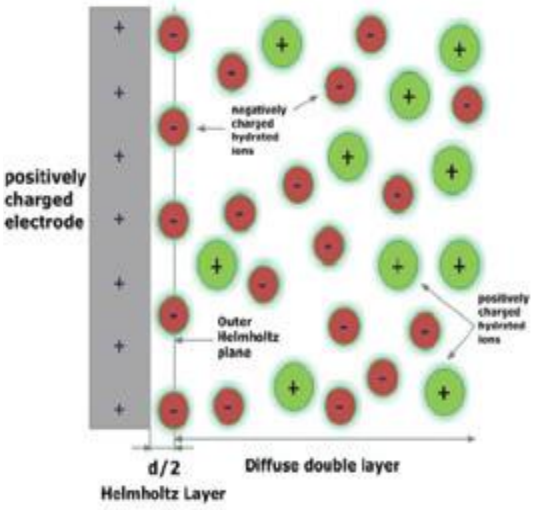

Figure 1.6 Stern model

1.4.2 PSEUDOCAPACITOR

In pseudocapacitor the charge storage mechanism is different from EDLC. The electrode material store charges during charging and discharging process. Metal oxide based electrodes such as MnO_2, RuO_2, Fe_2O_3, SnO_2, MoO_3, $TiO_2$and conducting polymers are mostly used electrode material for pseudocapacitors. Pseudocapacitors store electrical energy by transfer of electron between electrode and electrolyte. When a voltage is applied on the electrode material in the electrochemical capacitor, faradic redox reaction occurs on the

electrode surface just like batteries [34-35]. Generally, the capacitance of the pseudocapacitor is higher than capacitance of the electric double layer capacitor [36-37]. The average specific capacitance of activated carbon is only 150 Fg^{-1}whereas in pseudocapacitor specific capacitance can reach over 1000 Fg^{-1}[38]. The power density of pseudocpacitor is lesser than EDLC because of slower faradic process [39].

1.4.3 HYBRID SUPERCAPACITOR

In order to achieve enhancements in the overall performance of a device, features of EDLC and pseudocapacitors were combined together to develop a new type of capacitor which is called as hybrid capacitors. The hybrid capacitor provides high power and energy density without sacrificing the cycle stability and cyclic life of the device since in hybrid system energy storage mechanism depends on the both faradic and non-faradic processes. In a hybrid system, electrode materials are based on either composite electrode (which is integrated with carbon based materials, conducting polymers) or metal oxide based materials leads to the benefit of physical and chemical storage mechanisms together in a single electrode [40]. The coupling of carbon based electrodes with pseudocapacitor electrodes has gained significant attention due to substantial enhancement in total capacitance of the device.

1.5 SUPERCAPACITOR CONSTRUCTION

This section describes the construction and essential components which are required for the fabrication of supercapacitors. Nowadays, there are many construction methods available for the fabrication of supercapacitors which typically the step by step assembly of the components. Cell components f supercapacitors are similar to batteries except that there is no distinction as anode and cathode. Supercapacitor cell consist of three major parts as given below,

- Electrode
- Electrolyte
- Separator

1.5.1 ELECROLYTE

Electrolyte is the combination of (electrolyte salt + solvent), one of the most important key components of supercapacitor. Electrolyte is placed between the electrode materials, to prevent the contact between them and acts as the ion transfer medium providing

ionic conductivity thus facilitating charge compensation on each electrode in the cell. Nature of the electrolyte includes [41]:

- The ion type and size
- The ion concentration and salt
- Interaction between the ion and solvent
- Interaction between the electrode and electrolyte
- The potential window

1.5.2 IMPORTANCE OF ELECTRLYTE

When the supercapacitors are compared with both batteries and fuel cells, there is an insufficient energy density (for example, EDLCs have an energy density of less than 10 W h kg^{-1}; both pseudocapacitors and hybridcapacitors have an energy density less than 50Wh kg^{-1}) [42], which cannot fulfil the growing demand of the applications where high energy density is required. To overcome this challenge, extensive work has been devoted to increase the energy density of supercapacitor [43-44].

Energy density of the supercapacitor is $E = \frac{1}{2} CV^2$ that is energy density is directly proportional to capacitance (C) and square of the voltage (V). Increasing the capacitance and cell voltage is an effective way to increase the energy density of supercapacitor. This can be achieved through the development of electrode material with high capacitance and electrolyte (salt + solvent) with wide potential windows. In order to make a high capacitive electrode, porous carbon electrode materials should consider the matching between the pour structure and size of the electrolyte ions [45]. Regarding the development of ES electrolytes, widening the potential window of an electrolyte solution, that increase the cell voltage, can effectively increase the energy density of the supercapacitor. In terms of energy density improvement, one important point is increasing the cell voltage would be more efficient than increasing the electrode capacitance, because of energy density is directly proportional to square of the cell voltage. Therefore, developing new electrolytes with wide potential windows should be given higher priority than the development of new electrode materials. In addition to developing the operating voltage window, some other properties such as internal resistance, rate performance, operating temperature, cyclic lifetime, toxicity which is also important in the

practical use of supercapacitor. The effects of electrolytes on the performance of EIS are shown in figure1.7.

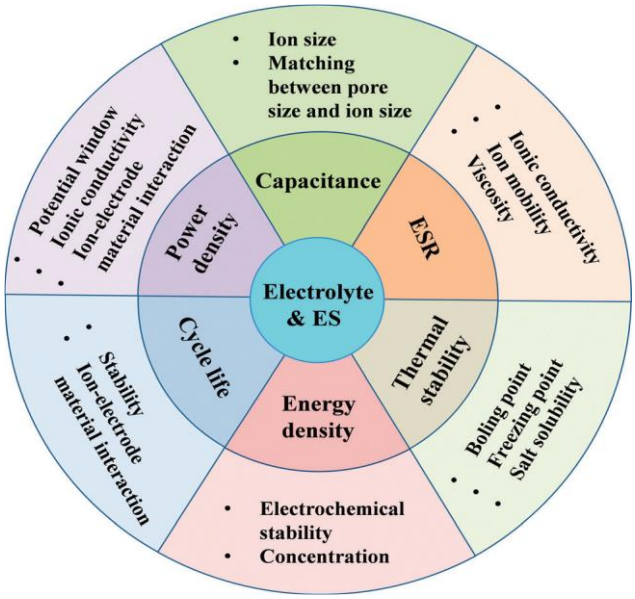

Figure 1.7 Effects of electrolytes on the performance of supercapacitors

1.5.3 REQUIRED PROPERTIES

In general, the required properties for an ideal electrolyte are as follows:

- A wide range of potential window
- High ionic conductivity
- High electrochemical stability
- A wide operating temperature range
- A low volatility and flammability
- Environmentally friendly
- Low cost

Actually, in an electrolyte it is very difficult to meet all of these required properties and each electrolyte has its own advantages and disadvantages.

1.5.4 PARAMETERS OF ELECTROLYTE MATERIAL

(i) Energy density and Power density

When a supercapacitor is charged, a cell voltage (V) is developed across the electrode materials. The energy density (E) and power density (P) can be expressed as follows [46]

$$\text{Energy density } E = \frac{1}{2}CV^2 \longrightarrow (1.5)$$

Where,

C-capacitance (Farad)

V-voltage (Volt)

$$\text{Power density P} = \frac{1}{4WR} V^2 \longrightarrow (1.6)$$

Where,

W-weight of the device

R- Equivalent series resistance ESR (Ohm)

V-voltage (Volt).

The unit of energy density is W h kg^{-1} and the unit of power density is Wkg^{-1}. Energy density and power density depends on the four important variables determining the performance of supercapacitors. The variables are C, V, W and R. In order to improve both the energy and power densities, increasing the values of both voltages and capacitance and simultaneously decreasing the values of weight of the device and resistance are necessary. Increasing a cell voltage should have a great contribution to the improvement of the ES's energy and power densities than increasing the capacitance or reducing resistance, because of both energy and power densities are proportional to square of the voltage. In general, the operating voltage of the supercapacitor is strongly depends on the potential window of the electrolyte [47-48].

(ii) Equivalent series resistance

When a sinusoidal alternative current is applied on an ideal capacitor, the output voltage should be 90˚ out of phase. However, in a supercapacitor, the output voltage is normally out of phase fewer than 90°, suggesting that an equivalent series ohmic resistor is coupled. This ohmic component is defined as the equivalent series resistance (ESR) [49]. ESR is an important parameter for determining the ES's power density as indicated by equation (1.6), which shows that the power density increases with a decreasing ESR value. ESR is the sum of various types of resistances including intrinsic resistance of the electrode material and electrolyte solution, mass transfer resistance of the ions, and contact resistance between the current collector and the electrode and the resistance caused by the dielectric loss of the interphasal solvent and ions when the AC frequency is higher than hundreds of megahertz (MHz) [50]. Normally, as identified, the resistances of the bulk electrolyte

solution and the electrolyte inside the electrode layer pores tend to dominate the ESR, especially when non-aqueous electrolytes such as organic, IL and solid-state electrolytes are used in the ESs. Therefore, in order to achieve a high power density from the ES, it is necessary to use anelectrolyte with high ionic conductivity. However, there is often a trade-off between the ionic conductivity and the operatingpotential window of the electrolytes.

(iii) Cycle-life

Cycle-life, a necessary indicator of thestability of the ES, is also one of the important parameters formeasuring the overall ES performance. General test proceduresfor stability analysis involve the electrode undergoing chargeand discharge cycling in a certain electrolyte to compare theinitial and final capacitance. For example, EDLCs using carbonelectrodes generally have a very high cycling stability. However,when pseudocapacitive reactions are introduced, the cyclic stabilityis generally reduced due to the non-ideal electrochemical reversibilityresulting from the interactions between the electrolyteions and the electrode materials. Actually, the cycle-life of theES depends on many factors such as the cell type, electrodematerial, electrolyte, charging/discharging rate and operating voltage and temperature.

(iv) Self-discharge rate

Another issue concerning the ES performance is self-discharge rates, which are related to potential losses of a charged electrode over a period of storage time. During the self-discharge process, current leakage leads to a decrease of the cell voltage, which in turn may limit the use of ESs for some applications requiring a fixed amount of energy retention for a relatively long time. The ES self-discharge rate and its mechanism are dependent onthe type of electrolyte, its impurities and residual gases.

(v) Thermal stability

Most potential applications forESs occur in the temperature range of -30 to 70˚C, thereforeexpanding the current working temperature range of ESs canfurther widen the scope of applications. For example, mostelectronics related to space avionics applications are requiredto operate at temperatures as low as -55 ˚C.Fuel cell vehicles,on the other hand, may

require a high working temperature forESs. The application of working temperature can affect severalproperties of ESs such as the energy and power densities, rateperformance, ESR, cycle life and self-discharge rate. In particular,the temperature-dependent performance of ESs is strongly dependenton the nature of the electrolyte such as the concentrationand the type of conducting salt, and the specific properties ofthe solvent (e.g., freezing point, boiling point and viscosity).

In summary, based on the above comments, it can be seen that the primary characteristics of ESs are strongly dependenton the specific electrolytes employed.

1.6 CLASSIFICATION OF ELECTROLYTES

In general, various types of electrolytes have been developed and reported in the literature to date. As shown in Figure 1.8, these electrolytes are mainly classified as liquid electrolytes and solid/ quasi-solid-state electrolytes.

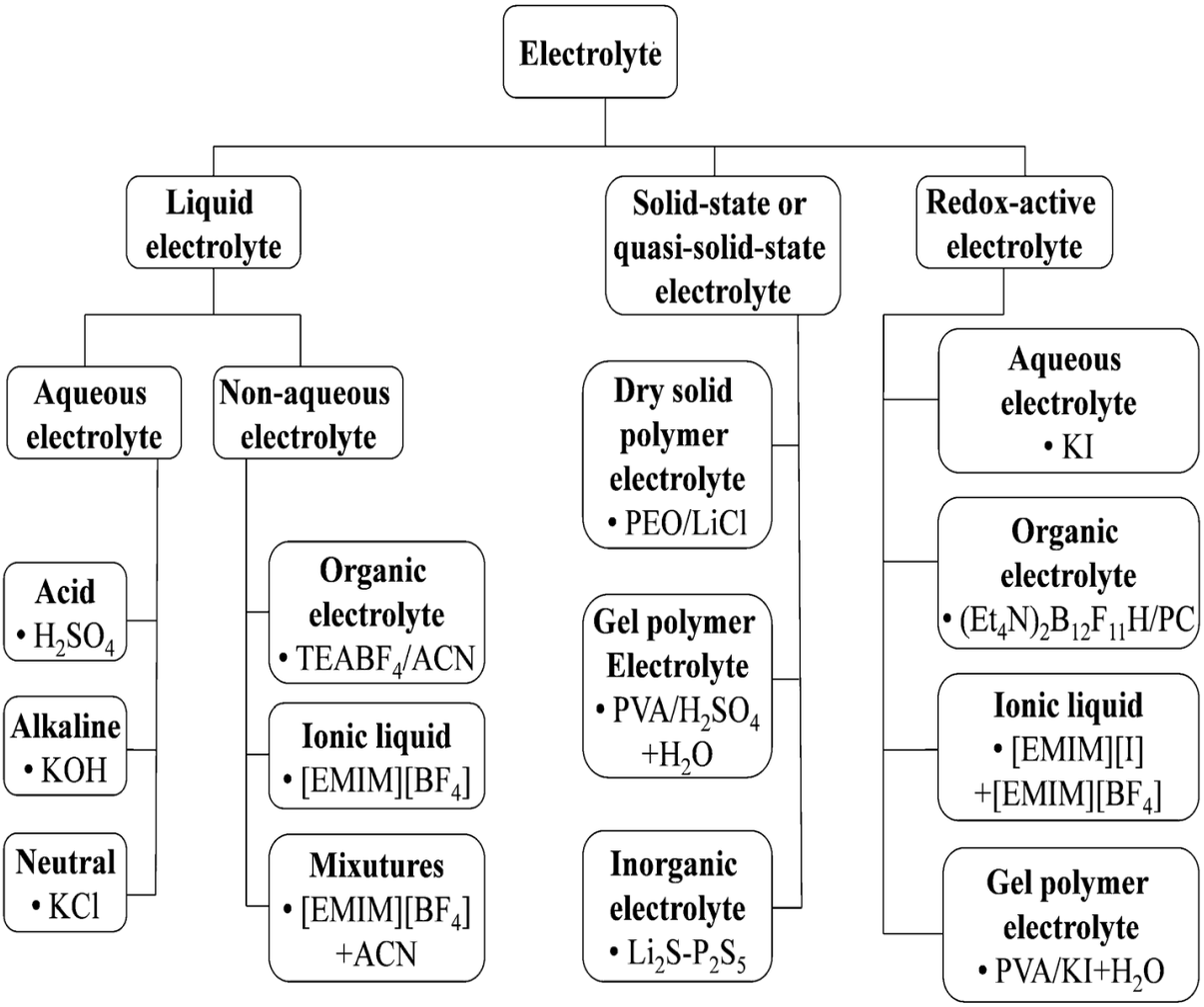

Figure 1.8 Classification of electrolytes

1.6.1 LIQUID ELECTROLYTES

In general, liquid electrolytes can be further grouped into aqueous electrolytes, organic electrolytes and ionic liquids (ILs).

(i)AQUEOUS ELECTROLYTE

Generally, in consideration of energy density, aqueous electrolytes are a low choice for commercial ES products due to their narrow voltage windows. However, aqueous electrolytes have been used extensively in research and development in the literature reported from 1997 to 2014. For example, in 2014, about 84.8% of the published literature employed aqueous electrolytes for ESs due to the fact that aqueouselectrolytes are inexpensive and can be easily handled in the laboratory without needing special conditions thus greatlysimplifying

the fabrication and assembly processes. Organicelectrolytes and ILs, on the other hand, generally requirecomplicated purification procedures under a strictly controlledatmosphere to avoid introduction of moisture.In general, aqueous electrolytes can be grouped into acid,alkaline, and neutral solutions in which H_2SO_4, KOHand $Na_2SO_4$are the most frequently used electrolyte. The main disadvantage of an aqueous electrolyte is their relatively narrow potential window, restricted by the decomposition of water.

(ii) ORGANIC ELECTROLYTE

Organic electrolyte-basedESs is currently dominating the commercial market owing totheir high operation potential window typically in the range of2.5 to 2.8 V. The increased operation cell voltage can provide asignificant improvement in both the energy and power densities.Furthermore, using organic electrolytes allows the use of cheapermaterials (e.g., Al) for the current collectors and packages.Typical organic electrolytes for the commercial EDLCs consistof the conductive salts (e.g., tetraethylammonium tetrafluoroborate($TEABF_4$)) dissolved in the ACN or PC solvent. Compared to ESs using aqueous electrolytes, ESs with organic electrolytes usuallyhave a higher cost, a smaller specific capacitance, a lowerconductivity, and safety concerns related to the flammability,volatility and toxicity. Furthermore, an organic electrolyterequires complicated purification and assembling processesin a strictly-controlled environment to remove any residual impurities (e.g., water) that can lead to large performance degradation and serious self discharge issues.

(iii) IONIC LIQUID ELECTROLYTE

Ionic liquids (low temperature or room temperature molten salts) are generally defined as those salts composed solely of ions (cations and anions) with melting points below 100 ˚C. An IL usually consists of a large asymmetric organic cation and an inorganic or an organic anion, and this special combination of certain cations and anions contributes to a low melting point. Owing to the unique structures and properties, ILs has recently received significant interest as alternative electrolytes for ESs. Normally, ILs has several potential advantages including high thermal, chemical and electrochemical stability, negligible volatility, and non-flammability (depending on the combination of cations andanions).Furthermore, ILs' physical and chemical properties can be highly tunable due to their large variety (virtually unlimited) of combinations of cations and anions. In this sense, ILs are also regarded as ''designer solvents''. This property tenability of ILs is very attractive for ES electrolytes because the electrolyte compositions can be optimized or customized to

meet certain requirements of ES performance such as operative cell voltage, the working temperature range, ESR (related with the ionic conductivity), and so on. The ILs employed forESs are commonly based on imidazolium, pyrrolidinium, ammonium, sulfonium, phosphonium cations and anions of ILs are tetrafluoroborate ($BF4^-$), hexafluorophosphate($PF6^-$),bis(trifluoromethanesulfonyl)imide($TFSI^-$),dicyanamide (DCA^-) and bis(fluorosulfonyl)imide (FSI^-). Unfortunately, there are several main drawbacks with most ILs, such as high viscosity, low ionic conductivity and high cost, which can limit their practical use in ES's.

1.6.1.1 ADVANTAGES

- high ionic conductivity
- high diffusion rate
- low viscosity

1.6.1.2 DISADVANTAGES

- High volatility
- Expansion through heat absorption
- Corrosion of electrodes leading to serious safety concerns
- Narrow operation temperature range
- Difficulty in packaging
- The assembly of supercapacitors requires the use of an ion-selective membrane and a five-layer sandwiched structure (electrode/electrolyte/separator/electrolyte/electrode).

1.6.2 SOLID- OR QUASI-SOLID-STATE ELECTROLYTES

Solid-state electrolyte based electrochemical energy devices have attracted great interest in recent years. The solid-state electrolytes can not only serve as the ionic conducting media but also as the electrode separators. The major advantages when using solid-state electrolytes are the simplification of packaging and fabrication processes of ESs and liquid-leakage free. To date, major types of the solid-state electrolytes developed for ESs have been based on polymer electrolytes, and only very limited work has been focused on inorganic solid materials (e.g., ceramic electrolytes). The polymer-based solid electrolytes for ESs can be further grouped into three types:

- Solid polymer electrolyte (dry polymer electrolytes)
- Gel polymer electrolyte (GPE)

- Polyelectrolyte.

1.6.2.1 SOLID POLYMER ELECTROLYTE

The SPE is composed of a polymer (e.g., PEO) and a salt (e.g., LiCl), without any solvents (e.g. water). The ionic conductivity of SPE is provided by the transportation of salt ions through the polymer.

1.6.2.2 GEL POLYMER ELECTROLYTE (GPE)

Incontrast, the GPE consists of a polymer host (e.g., PVA) andan aqueous electrolyte (e.g., H_2SO_4) or a conducting salt dissolvedin a solvent. In this case, the polymer serves as a matrix,which can be swollen by the solvent, and the ions transport inthe solvent instead of in the polymer phase, which is differentfrom that of SPE.Due to the presence of a liquid phase in GPEs, some studies called them as quasi-solid-state electrolytes. As mentioned previously,GPEs are currently the most extensively studied electrolytes forsolid-state ESs due to their high ionic conductivity. A GPE istypically composed of a polymer matrix (host polymer) and aliquid electrolyte (e.g., aqueous electrolyte, organic solventcontaining conducting salt and IL).

Regarding the host polymer,various polymer matrices have been explored for preparing GPEs, including poly(vinyl alcohol) (PVA), poly(acrylic acid) (PAA),potassium polyacrylate (PAAK), poly(ethyl oxide) (PEO), poly-(methylmethacrylate) (PMMA), poly(ether ether ketone) (PEEK),poly(acrylonitrile)-block-poly(ethylene glycol)-block-poly(acrylonitrile)(PAN-b-PEG-b-PAN), and poly(vinylidene fluoride-co-hexafluoropropylene)(PVDF-HFP), Carboxy methyl cellulose(CMC). When water is used as a plasticizer, theresulting GPE is also called a hydrogel polymer electrolyte,which has some three-dimensional polymeric networks whichcan trap water in the polymer matrices mainly through surfacetension. Besides water, organic solvents such as PC,ECand DMF or their mixtures (e.g., PC–EC, PC–EC–DMC,and PC–EC) have also been commonly used as the plasticizersin GPEs. The composition ratio between a polymer and a plasticizernormally plays an important role in the degree of plasticization,thus affecting the glass-transition temperature of GPEs.

One of the most significant advantages of using solid-stateelectrolytes including GPEs in ESs is that they allow thedevelopment of diverse and bendable structures and tuneableshapes for various desired applications. For example, basedon the PVA-based hydrogels, various solid-state ESs have been developed, including flexible ESs, stretchable

ESs, flexible micro-ESs, printable micro-ESs, on chip micro-ESs, 3D micro-ESs, yarn ESs, wire or fibres shaped ESs, transparent ESs, ultrathin ESs, weaveable ESs, paper-like ESs, and integrated ESs with other devices [51] .

1.6.2.3 POLYELECTROLYTE

In the polyelectrolyte, the ionic conductivity is contributed by the charged polymer chains.

As identified, eachtype of these solid-state electrolytes has their own advantagesand disadvantages. Normally, GPEs have the highest ionicconductivity among these three types of solid-state electrolytes.Due to the presence of a liquid phase in a GPE, its ionicconductivity is significantly higher than that of the dry SPE.Due to this reason, GPE-based ESs currently dominates thesolid electrolyte-based ES products, and studies on ESs usingdry SPEs are very limited. However, depending on theircomposition, GPEs may suffer from relatively poor mechanicalstrength and a narrow operative temperature range particularlywhen water is used as the solvent. Furthermore, the weakmechanical strength of some GPEs is the main concern, as itmay lead to internal short circuits, causing safety issues.Although dry SPEs normally have low ionic conductivities, theyhave relatively high mechanical strength when compared toGPEs. It should be noted that these solid-state electrolytes forESs normally have some common disadvantages including thelimited contact surface area between solid-state electrolytes andelectrode materials especially for the nanoporous materials.This issue could increase the ESR value, reduce the rate performance,and limit the utilization of active electrode materials,resulting in a low specific capacitance of ESs.When developing solid-state electrolytes for ESs, the followingcritical requirements should be considered:

(1) High ionicconductivity,

(2) High chemical, electrochemical and thermal stability

(3) Sufficient mechanical strength and dimensionalstability.

In practice, it is difficult for a solid-sateelectrolyte to meet all of these requirements. In this aspect, several reviews have been publishedrecently (i.e., focusing on the solid-stated electrolytes forESs).

1.6.3 ENVIRONMENTALLY FRIENDLY GEL POLYMER ELECTROLYTE

Natural polymers are a promising class of materials for gel formation because of their renewability and their nontoxic often biodegradable properties. Consideringthe environmental impact, the use of environmentallyfriendly materials from renewable nature sources such as cornstarch, gelatin, acacia gum, xanthan gum and chitosan or biodegradable materials (e.g.,poly(epsilon-caprolactone)) as polymer hosts for solid-stateelectrolytes has also been received increasing attention. However,natural polymers such as starch films generally suffer from lowmechanical properties. To improve the mechanical propertyof natural polymers, blended materials such as a blend ofchitosan and starch, and a blend of chitosan and PEG,were developed.

1.7 OVERCOMING THE CHALLENGES IN ES ELECTROLYTE

- Improving electrolyte's ESPW values to increase the ES's energy density.
- Enhancing the charge capacity by utilizing the pseudocapacitive contribution.
- Increasing the purity of the electrolyte.
- Decreasing ESR values to further increase the ES's power density.
- Optimizing the matching between the electrolyte and electrode materials to improve the overall performance.
- Increasing the working temperature range for ES operation.
- Further fundamental understanding through both theoretical and experimental investigations.
- Development of standard methods to evaluate the performance of electrolytes.

1.8 ADVANTAGES OF SUPERCAPACITOR

- Long life: It works for a large number of cycles without wear and aging.
- Rapid charging: It takes a few seconds to charge completely.
- High power storage: It store huge amount of energy in a small volume.
- Fast release: Release the energy much faster than battery.
- Low toxicity of materials used.
- High cycle efficiency (95% or more).

1.9 DISADVANTAGES OF SUPERCAPACITOR

- High self-discharge: The rate is considerably higher than that of a battery.
- The energy density is considerably lower than that of an electrochemical battery.
- Cells have low voltages: Series connections are needed to obtain higher voltages.

- Price of supercapacitors is more than Li-ion batteries for the same capacity.

1.10 APPLICATIONS OF SUPERCAPACITOR

- The supercapacitor mainly used in where very fast charging and discharging needed.
- The supercapacitor is used in digital cameras for flashing of light.
- Supercapacitors are used in electric vehicles and the regenerative braking mechanism is used for charging the supercapacitor. The regenerative braking helps to charge in a very short time.
- They also used in defibrillators to shock the human heart.
- They are used to provide power back up to the low power devices like PC Cards, automated meter reading equipment.
- Nowadays the supercapacitors are used in many electrical and electronic tools.
- They are also used in many portable gadgets and devices [52].

1.11 OBJECTIVE

- Prepare conducting membrane using natural products for using as separator cum electrolyte carrier in supercapacitors.

1.12 METHODOLOGY

- Preparation of various concentration of Sodium Carboxymethyl Cellulose (CMC) and Bovine Bone (BB) composited membrane for supercapacitor.
- To reduce the resistance and improve the ionic conductivity of the membrane by the addition of varied weight percentage of NaCl.
- To use rubber leaf vein skeleton to improve the electrical properties of the membrane under study.

CHAPTER-II

REVIEW OF LITERATUTE

2.1 NATURAL MATERIALS

Natural materials have shown great interest in the production of devices for generating and storing energy at low cost. Natural based electrolyte materials are cost effective and eco-friendly derived from renewable sources and become a promising replacement for synthetic polymers. There are a wide variety of natural polymers used for making polymer electrolytes like- agar- agar, cellulose, chitosan, gelatin, pectin, starch, etc. In these natural polymers based electrolytes glycerol and water are widely used as plasticizer. The ionic conductivity has been found in the order of 10^{-4} S/cm at room temperature.

2.1.1 CELLULOSE BASED ELECTROLYTES

Cellulose and its derivatives are important as they have good viscosimetric, emulsifying stabilizing, dispersing and agglutinant properties. They are highly soluble in some organic solvents and water. They also have ability to form films with desirable mechanical strength. These characteristics make them appropriate for applications in ink, paper, food, pharmaceutical, cosmetic, ceramic, textile and agricultural products. Some researchers also used cellulose and its derivatives for making SPEs by doping different salts and obtained conductivity in the range of 10^{-6} to 10^{-4} S/cm at room temperature.

2.1.2 GELATIN BASED ELECTROLYTES

Gelatin is a form of protein and was the first materials to be used in the production of movies. This protein is very promising in the area of development of new materials, since it is abundantly available, has low cost, good film-forming properties, nontoxic and forms transparent solutions with high viscosity. Gelatin films are generally obtained by solubilization, heat and dehydration of collagen, which leads to a distortion of a partial triple helix of this macromolecule. However to improve its functional properties formaldehyde and glutaraldehyde are used as crosslinking agents. It is observed that in SPEs based on gelatin the conductivity lies in between 10^{-5} to 10^{-4} S/cm.

2.1.3 STARCH BASED ELECTROLYTES

Starch is an interesting natural polymer. It is abundantly present in nature in various forms and can be obtained from various renewable sources. It is the major reserve material of many plant storage tissues. Starch is a mixture of two units; linear amylose and highly branched amylopectin. It is soluble in some organic solvents and hot water. It has an ability to form film with good mechanical strength.

2.1.4 NATURAL GUM BASED ELECTROLYTES

Natural gums are polysaccharides of natural origin. They can increase the viscosity of the solutions even at small concentration. They are used as thickening agents, gelling agents, emulsifying agents, and stabilizers. Most often these gums are found in the woody elements of plants or in seed coatings. They are classified according to their origin as well as they are categorized as uncharged and ionic polymers or polyelectrolytes. For example gum arabica and gellan gum are polyelectrolytes whereas xanthan and guar gums are uncharged.

S.No	Reported by	Electrolyte	Ionic conductivity	Reference
1.	Vieira et.al 2007	Gelatin-CH_3COOH	4.5×10^{-5} S/cm	[53]

2.	Avellanedaa et.al 2008	Gelatin-$LiClO_4$	1.5x 10^{-5} S/cm	[54]
3.	Andrade et.al 2009	Pectin-Gly-LiClO4	4.7 x 10-4 S/cm	[55]
4.	Khiar et.al 2010	Starch -NH_4NO_3	2.83×10^{-5} S/cm	[56]
5.	Rozely et.al 2010	Rice Starch-Gly-$LiClO_4$	1.10×10^{-4} S/cm	[57]
S.No	**Reported by**	**Electrolyte**	**Ionic conductivity**	**Reference**
6.	Tiwari et.al 2011	Potato starch - NaI - glutaraldehyde –PEG	1.3×10^{-4} S/cm	[58]
7.	Leones et.al 2012	Gelatin-(C_2mim)(OAc)	1.18×10^{-4} S/cm	[59]
8.	Sit et.al 2012	HEC-NH_4Br	3.61×10^{-4}S/cm	[60]
9.	Noor et.al 2013	Gellan-$LiCF_3So_3$	5.4x 10^{-4}S/cm	[61]

10.	Ramlli et.al 2013	CMC-OA-PC	2.52 x 10^{-7} S/cm	[62]
12.	Chai et.al 2013	CMC-Oleic acid	2.11 x 10^{-5} S/cm	[63]
13.	Khanmirzaei et.al 2013	Rice Starch-LiI	4.68 × 10^{-5} S/cm	[64]
14.	Rani et.al 2014	CMC- CH_3COONH_4	5.77x 10^{-4}S/cm	[65]
15.	Ramlli et.al 2014	CMC-NH_4F	2.68 x 10^{-7}S/cm	[66]
S.No	**Reported by**	**Electrolyte**	**Ionic conductivity**	**Reference**
16.	Shukur et.al 2014	Corn starch- LiOAc	1.04 × 10^{-3} S/cm	[67]
17.	Arora et.al 2014	Xanthan gum-NH_4Cl	0.86 ×10^{-3}S/cm	[68]
18.	Vijaya et.al 2014	Pectin-NH_4SCN	4.505 x10^{-4}S/cm	[69]
19.				[70]

	Leones et. al 2014	Pectin-KCl	1.45×10^{-3}S/cm	
20.	Sudhakar et.al 2015	Xanthan gum (XG)-Gly-Li_2B4O_7	6.4×10^{-2}S/cm	[71]
21.	Zhu et.al 2015	CMC-$LiPF_6$	0.4×10^{-3} S/cm	[72]
22.	Sohaimy et.al 2015	CMC-AC	7.71×10^{-6} S/cm	[73]
23.	Sudhakar et al 2015	HEC-H_3PO_4	$4.1\ 9 \times 10^{-3}$ S/cm	[74]
24.	Ledwon et.al 2015	HPC-Dichloromethane	3.5×10^{-5}S/cm	[75]
S.No	**Reported by**	**Electrolyte**	**Ionic conductivity**	**Reference**
25.	Kavitha et.al 2016	Pectin-NH_4NO_3	6.64×10^{-5} S/cm	[76]
26.	Chai et.al 2016	CMC-Oleic acid-Gly	1.64×10^{-4} S/cm	[77]
27.	Ahmad and Isa et.al 2016	CMC-NH_4Cl	1.4×10^{-3} S/cm	[78]

28.	Teoh et.al 2016	Corn starch-$LiClO_4$ - $BaTiO_3$	1.28×10^{-2} S/cm	[79]
29.	Hemalatha et.al 2016	Potato starch - NH_4SCN	3.93×10^{-4} S/cm	[80]
30.	Samsudin et.al 2018	CMC-DTAB	$7{\cdot}72 \times 10^{-4}$ S/cm	[81]
31.	Saadiah et.al 2018	CMC:PVA	9.12×10^{-6} S/cm	[82]
32.	Perumal et.al 2018	Pectin/LiC	2.08×10^{-3} S/cm	[83]
33.	Noor et.al 2019	CMC-NH_4SCN	6.48×10^{-5} S/cm	[84]
S.No	**Reported by**	**Electrolyte**	**Ionic conductivity**	**Reference**
34.	Muthukrishnan et.al 2019	Pectin -(NH_4SCN)	1.5×10^{-3} S/cm	[85]
35.	Perumal et.al 2018	Pectin-lithium perchlorate	3.89×10^{-4} S/cm	[86]

CHAPTER-III

MATERIALS AND METHODS

3.1 INTRODUCTION

The present work aims to prepare a membrane for supercapacitor application. A brief description of preparation of various concentrations of CMC and BB membrane and experimental details followed in the present study are given in this chapter. The electrochemical properties of the membrane depend on the concentration of the material, area of the film and its thickness. In this chapter, preparation of various concentrations of

electrolytes and details of Electrochemical Impedance Analyzer and Fourier Transform Infra Red Spectroscopy (FTIR) are briefly discussed.

3.1.1 MATERIAL OF INTEREST

For the preparation of membrane Sodium Carboxymethyl Cellulose (CMC) and gelatin powder (Bovine bone) are taken as the starting materials. In order to improve the ionic conductivity of the prepared membranes, Sodium Chloride (NaCl) and rubber leaf vein are used with different concentrations.

3.1.1.1 SODIUM CARBOXYMETHYL CELLULOSE (CMC)

Carboxymethyl cellulose (CMC) is used in this present work due to its superior properties such as good filming ability, high mechanical property, and bio-compatibility and abundance in nature. Carboxymethyl cellulose (CMC) is a cellulose derivative with carboxymethyl groups (-CH_2-COOH) bound to some of the hydroxyl groups of the glucopyranose monomers that make up the cellulose backbone[87].The pure Sodium Carboxymethyl Cellulose is white or milk white fibrous powder or particles, odourless and tasteless. It is insoluble in organic solvents such as methanol, alcohol, diethyl ether, acetone, chloroform and benzene but soluble in water. Degree of substitution is an important factor influencing water solubility and the viscosity of Sodium carboxymethylcellulose also has a great effect on the water solubility.

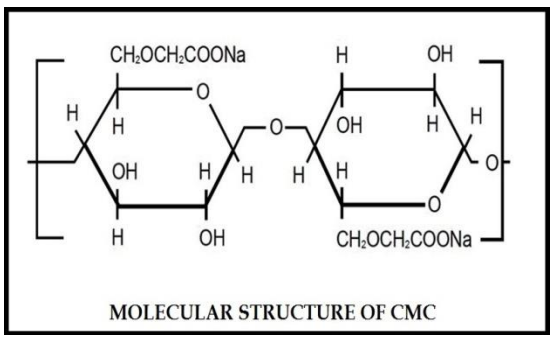

MOLECULAR STRUCTURE OF CMC

3.1.1.2 GELATIN

Gelatin is a form of protein and this protein is very promising in the area of development of new materials, since it is abundantly available, has low cost, has good film-forming property, nontoxic and forms transparent solutions with high viscosity. Gelatin films

are generally obtained by solubilisation, heat and dehydration of collagen, which leads to a distortion of a partial triple helix of this macromolecule. However, to improve its functional properties formaldehyde and glutaraldehyde are used as crosslinking agents. It is observed that Solid Polymer Electrolyte (SPE) based on gelatin has conductivity between 10^{-5} to 10^{-4} S/cm. In the present work, Bovine Bone (BB) gelatin powder is used.

3.1.1.3 INTERACTION BETWEEN PROTEIN AND POLYSACCHARIDES

Interactions of different origins betweenproteins and polysaccharides result in tailor-made functionalproperties. Depending on the molecular charge and concentration,different phenomena including co-solubility, thermodynamic incompatibility,depletion flocculation and thermodynamic compatibilitytake place in a mixture of protein and polysaccharide. When twopartners are oppositely charged, soluble complexes are developed atthe first stage, followed by formation of inter-polymeric (insoluble)complexes. Different factors including composition, concentrationand ratio of reagents, order of mixing, pH, charge distribution, molecular weight, and conformation, ionic strength and ion type affect the complexationphenomenon.

3.1.2 SOLUTION CASTING TECHNIQUE

This is the most commonly used and simple method for the preparation of membrane films. The preparation of electrolytic films is generally done by simple casting technique. The solute is dissolved in suitable solvents (e.g. acetonitrile, methanol, ethanol, triple distilled water etc) and the solution is stirred for several hours to achieve complete mixing. Then the solution cast into polypropylene or glass dishes and slowly evaporated to obtain films. Polymer films with required thickness can be obtained from this method.

3.1.3 PREPARATION OF SODIUM CARBOXYMETHYL CELLULOSE (CMC) AND BOVINE BONE MEMBRANE (BB):

After optimization of Carboxymethyl cellulose (CMC) and Bovine Bone (BB), the following tabulated (Table 3.1) membranes are prepared by solution casting technique.

Table 3.1Various concentrations of CMC and BB

S.No	CMC (gram)	BB (gram)	Ratio (wt%)
1.	0.1	0.9	10:90
2.	0.2	0.8	20:80

3.	0.3	0.7	30:70
4.	0.4	0.6	40:60
5.	0.5	0.5	50:50
6.	0.6	0.4	60:40
7.	0.7	0.3	70:30
8.	0.8	0.2	80:20
9.	0.9	0.1	90:10

For the preparation of membrane initially, an appropriate amount of Sodium Carboxymethyl cellulose (CMC) is dissolved in 10 ml of deionised water. The solution is stirred at 40˚C. Simultaneously, an appropriate amount of Bovine Bone (BB) is dissolved in 10ml of deionised water and the bovine bone is stirred at 40˚C. After 15-20 minutes, bovine bone got dissolved in deionised water and resulted is a homogeneous solution. After that homogeneous bovine bone solution is mixed with the CMC solution. Finally, the entire solution is stirred well and maintained at 40˚C for 1 hour. Inner surface of the petri dish is swapped with Glycerol (3-4 drops) andthesolutions obtainedwere poured into glass petri dishes and are left to evaporateslowly at room temperature for the drying process until membrane is formed. After drying, the membrane films are peeled out from the petri dish and preserved for further studies. All the samples are prepared at identical conditions of temperature and pressure. Figure 3.1 is the flow chart for preparation of membrane. Figure 3.2 shows the prepared membrane solution poured into the petri dish. Figure 3.3 shows the prepared membrane peeled out from the petri dish.

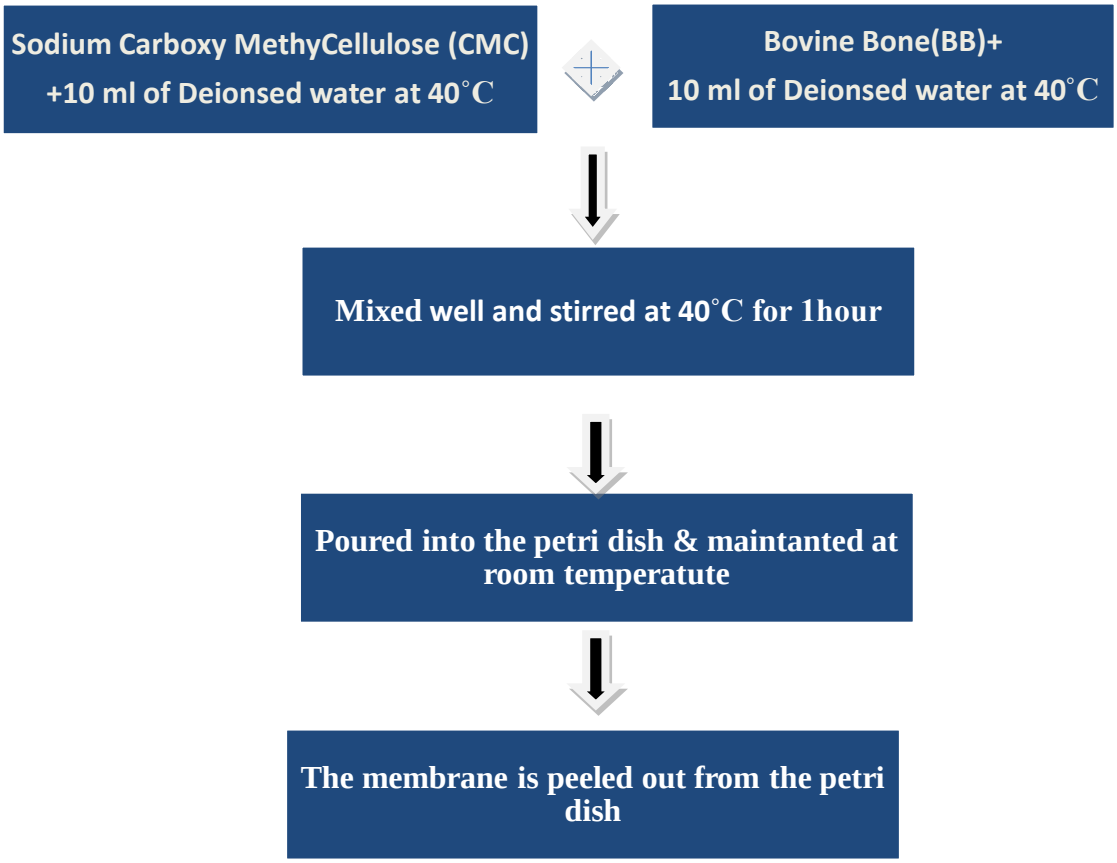

Figure 3.1 Flow chart for preparation of polymer membrane

Figure 3.2 Prepared solution poured into the petridish

Figure 3.3 Peeled CMC : BB membrane

3.1.4 PREPARATION OF CMC:BB MEMBRANE WITH VARIOUS CONCENTRATIONS of NaCl :

To improve the ionic conductivity and to reduce the resistivity of the as prepared CMC and BB membranes, Sodium chloride is added at different concentrations into the host material. Sodium chloride is one of the most well-known and widely used chemicals, also known as common salt.The chemical formula of sodium chloride is NaCl and its molar mass is 58.44 g/mol. It is an ionic compound consisting of a sodium cation (Na^+) and a chloride anion (Cl^-). Solid NaCl has a crystalline structure, in which each Na^+ ion is surrounded by six chloride ions in an octahedral geometry. Sodium chloride is a white crystalline solid with a density of 2.16 g/mL, and a melting point of 801 °C. Sodium chloride is readily soluble in water and other polar solvents. It is a stable solid.

From the above table three ratios (10:90, 50:50, 90:10) are particularly taken for further improvement of ionic conductivity. Adding the NaCl salt with different concentration such as (0.01g, 0.03g, 0.05g, 0.07g and 0.09g) into the host material can effectively improves the ionic conductivity of the film.

Table 3.2 CMC:BB (10:90) with NaCl

S.No	CMC (gram)	BB (gram)	NaCl (gram)
1	0.1	0.9	0.01
2	0.1	0.9	0.03
3	0.1	0.9	0.05
4	0.1	0.9	0.06
5	0.1	0.9	0.07

Table 3.3 CMC:BB (50:50) with NaCl

S.No	CMC (gram)	BB (gram)	NaCl (gram)
1	0.5	0.5	0.01
2	0.5	0.5	0.03
3	0.5	0.5	0.05
4	0.5	0.5	0.06
5	0.5	0.5	0.07

Table 3.4 CMC:BB (90:10) with NaCl

S.No	CMC (gram)	BB (gram)	NaCl (gram)
1	0.9	0.1	0.01
2	0.9	0.1	0.03
3	0.9	0.1	0.05
4	0.9	0.1	0.06
5	0.9	0.1	0.07

The Table (3.1), (3.2), (3.3) shows the various ratios of CMC: BB with different concentration of NaCl. All the tabulated samples are similarly prepared by solution casting technique.

3.1.5 PREPARATION OF LEAF COMPOSITED MEMBRANE

RUBBER LEAF VEIN

Numbers of rubber leaves are collected and the process to remove chlorophyll to obtain leaf vein is carried out for the preparation of rubber leaf composted membrane. Rubber leaf vein is shown in Figure (3.4). In 50:50 (CMC+BB) ratio and (50:50) + NaCl ratio, rubber leaf vein is casted to enhance the ionic conductivity of the polymer membrane.

Figure 3.4 Rubber leaf vein

3.1.5.1 SINGLE CASTING

In single casted membrane, as prepared homogeneous solution is entirely poured into the glycerol swapped petri dish, after that finally at the surface of the solution rubber leaf is placed. The leaf remains on the surface of the membrane.

3.1.5.2 DOUBLE CASTING

In double casted polymer membrane, half of the prepared polymer solution is poured into the petri dish followed by placing leaf vein and remaining solution is poured on the leaf surface. The leaf is located at the centre of the membrane is referred as double casted. After the drying process, double casted skeleton leaf is preserved for further studies. Figure (3.5) shows the leaf composited CMC: BB membrane.

Figure 3.5 Leaf composited membranes

3.2 CHARACTERIZATION TECHNIQUES

3.2.1 INTRODUCTION

The characterization of certain materials is an essential for understanding their properties and applications. Some characterization methods are used to study the sizes, shapes and morphology of nanostructures, whereas others are used to obtain detailed structural information. This chapter mainly discusses in briefly about the various characterization techniques and analysis have carried out for prepared films.

3.2.2 FOURIER TRANSFORM INFRARED SPECTROSCOPY

3.2.2.1 ITRODUCTION

Infrared spectroscopy is nondestructive technique for materials analysis and used in the laboratory for over seventy years. Infrared absorption spectroscopy is the study of interaction of infrared radiation with matter as a function of photon frequency. Fourier

Transform Infrared Spectroscopy (FTIR) provides specific information about the vibration and rotation of the chemical bonding and molecular structures, making it useful for analyzing organic materials and certain inorganic materials.

An infrared spectrum represents a fingerprint of a sample with absorption peaks which correspond to the frequencies of vibrations between the bonds of the atoms making up the material. Because each different material is a unique combination of atoms, no two compounds produce the exact same infrared spectrum. Therefore, infrared spectroscopy can result in a positive identification (qualitative analysis) of every different kind of material. In addition, the size of the peaks in the spectrum is a direct indication of the amount of material present. With modern software algorithms, infrared is an excellent tool for quantitative analysis.

The IR region is commonly divided into three smaller areas: near - IR (400 - 10 cm^{-1}), mid - IR (4000 - 400 cm^{-1}), and far - IR (14000 – 4000 cm^{-1}). Infrared photons have enough energy to cause groups of atoms to vibrate with respect to the bonds that connect them. Like electronic transitions, these vibrational transitions correspond to distinct energies, and molecules absorb infrared radiation only at certain wavelengths and frequencies. Chemical bonds vibrate at characteristic frequencies, and when exposed to infrared radiation, they absorb the radiation at frequencies that match their vibration modes. Measuring the radiation absorption as a function offrequency produces a spectrum that can be used to identify functional groups and compounds. Some impurities produce their own characteristic bands in infrared region. Spectral measurements of these bands are used to determine concentration of the impurities and their bonding with the host materials. In order to make identification, the measured interferogram signal cannot be interpreted directly. A means of “decoding” the

individual frequencies is required. This can be accomplished via a well-known mathematical technique called the Fourier transformation.

3.2.2.2 CONSTRUCTION AND WORKING

Construction

There are three basic spectrometer components in an FTIR system: a radiationsource, an interferometer, and a detector.

Interferometer divides radiant beams, generates an optical path difference between the beams, and then recombines them in order to produce repetitive interference signals measured as a function of optical path difference by a detector. As its name implies, the interferometer produces interference signals, which contain infrared spectral information generated after passing through a sample. The most commonly used interferometer is a Michelson interferometer. It consists of three active components: a moving mirror, a fixed mirror, and a beam splitter. The two mirrors are perpendicular to each other. The beam splitter is a semi-reflecting device and is often made by depositing a thin film of germanium onto a flat KBrsubstrate. Radiation from the broadband IR source is collimated and directed into the interferometer, and impinges on the beam splitter.

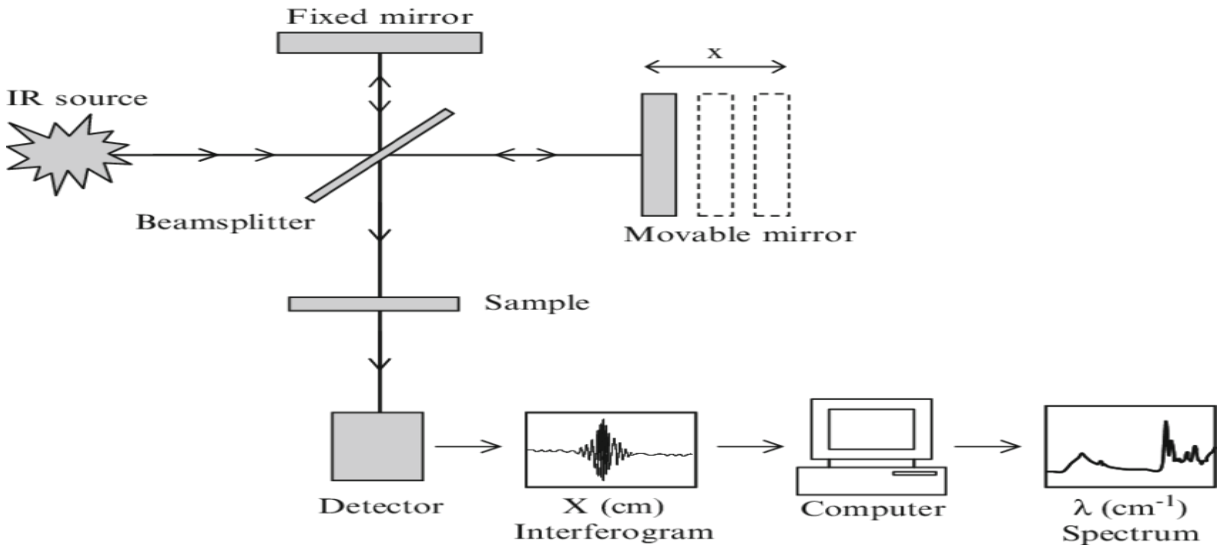

Figure 3.6 Schematic diagram for Fourier Transfer Infrared Spectroscopy

Working

The normal instrumental process is as follows:

1. The Source: Infrared energy is emitted from a glowing black-body source. This beam passesthrough an aperture which controls the amount of energy presented to the sample (and ultimately, to the detector).

2. The Interferometer: The beam enters the interferometer where the "spectral encoding" takesplace. The resulting interferogram signal then exits the interferometer.

3. The Sample: The beam enters the sample compartment where it is transmitted through or reflected off of the surface of the sample, depending on the type of analysis being accomplished. This is where specific frequencies of energy, which are uniquely characteristic of the sample, are absorbed.

4. The Detector: The beam finally passes to the detector for final measurement. The detectors used are specially designed to measure the special interferogram signal.

5. The Computer: The measured signal is digitized and sent to the computer where the Fouriertransformation takes place. The final infrared spectrum is then presented to the user for interpretation and any further manipulation [88-89].

3.2.2.3 APPLICATIONS

- Identification of simple mixtures of organic and inorganic compounds both as solids or liquids.
- Identification of polymers and polymer blends.
- Indirect verification of trace organic contaminants on surfaces.
- Routine qualitative & quantitative FTIR Analysis.
- Thin film analysis.
- Analysis of adhesives, coatings and adhesion promoters or coupling agents.
- Small visible particle chemical analysis.
- Analysis of stains and surface blemishes remnant from cleaning and degreasing processes combined with optical microscopy, SEM/EDX, XPS and SIMS techniques.
- Analysis of resins, composite materials and release films .
- Solvent extractions of leach ables or contaminants, plasticizers, mould release agents and weak boundary layers coupled with XPS surface chemical analysis techniques.
- Identification of rubbers and filled rubbers.
- Determination of degrees of crystallinity in polymers (eg LDPE and HDPE).
- Compararive chain lengths in organics.

- Extent of thermal, UV or other degredation or depolymerisation of polymers and paint coatings.
- Analysis of a gaseous sample using a gas cell for headspace analysis or environmental monitoring.
- Analysis of unknown solvents, cleaning agents and detergents.
- Assessment of degradation and oxidation of polymers.

3.2.2.4 STRENGTH

The FT-IR spectrometer has several major advantages over the dispersive instrument.

- Its sensitivity is better because it measures all frequencies simultaneously rather than scanning through the individual frequencies.
- Less energy is needed from the source and less time (typically 1 to 2 seconds) is needed for a scan.
- Several scans can be completed in a few seconds and averaged to improve the signal.
- Resolution and accuracy are also improved because a laser beam is used alongside the IR beam to control the speed of the moving mirror and to time the collection of data points.
- The light beam is a precise frequency reference that keeps the spectrometer accurately calibrated.

3.2.2.5 LIMITATIONS

Few limitations of FTIR spectrometer are listed below:

- Minimal elemental information is given for most samples.

- Background solvent or solid matrix must be relatively transparent in the spectral region of interest.
- Molecule must be active in the IR region; i.e. when exposed to IR radiation, a minimum of one vibrational motion must alter the net dipole moment of the molecule in order for absorption to be observed [90].

3.2.3 AC IMPEDANCE SPECTROSCOPY

3.2.3.1 INTRODUCTION

The electrochemical impedance method was developed in the 1950s, based on earlier studies of dielectric systems [91]. In the early 1980s frequency response analyzers came into the market. Meanwhile, acimpedance spectroscopy belongs to the routine techniques in electrochemistry [92]. By imposing potential sweeps, potential steps or current steps, the electrochemical cell is generally driven to a condition far from equilibrium, and a transient response signal is observed [93]. The ac impedance method perturbs the cell with an alternating signal of small magnitude.

3.2.3.2 IMPEDANCE

The terms resistance and impedance both denote an opposition to the flow of electrons or current. In direct current (dc) circuits, only resistors produce this effect. However, in alternation current (ac) circuits, two other circuit elements, capacitors and inductors, impede the flow of electrons. Impedance can be expressed as a complex number, where the resistance is the real component and the combined capacitance and inductance is the imaginary component. The total impedance in a circuit is the combined opposition of all

its resistors, capacitors, and inductors to the flow of electrons. The opposition of capacitors and inductors is given the same name reactance, symbolized by X and measured in ohms. Since the symbol for capacitance is C, capacitive reactance is symbolized by X_C. Similarly, since the symbol for inductance is L, inductive reactance is symbolized by X_L. Capacitors and inductors affect not only the magnitude of an alternating current but also its time-dependent characteristics or phase. When most of the opposition to current flow comes from its capacitive reactance, a circuit is said to be largely capacitive and the current leads the applied voltage in phase angle. When most of the opposition to current flow comes from its inductive reactance, a circuit is said to be largely inductive and the current lags the applied voltage in phase angle. The more inductive a circuit is, the closer the difference in phase angle approaches 90 degrees.

It's sometimes easier to perform calculations using admittance, the reciprocal of impedance. Admittance is symbolized by Y and measured in siemens (S). Like impedance, admittance can be expressed as a complex number, where the conductance, the reciprocal of resistance, is the real component, and the susceptance, the reciprocal of reactance, is the imaginary component.

3.2.3.3 PRINCIPLE

If a potential (voltage) is applied across an electrochemical cell (corroding material, battery etc.) a current is caused to flow through the cell, with a value determined by the mechanisms of the reaction taking place. The reaction is the formation of new chemical speciesas result of the movement of ions through the electrolyte. The ionic movements are caused by the applied potential difference, and constitute a flow of electric current.

If the applied potential is a sinusoid *(ΔE*sinω*t)* then the subsequent current will also be sinusoidal, with a value Δisin(ω*t* + φ). Harmonics of this current (2ω, 3ω . . . etc.) will also flow. The relationship between the applied potential and the current flow is known as the impedance, which is analogous to the resistance-current-potential relationship of a dc circuit. The impedance (Z) has a magnitude *(ΔE/Δi)* and phase (φ) and is thus a vector quantity.

3.2.3.4 REPRESENTATION OF IMPEDENCE PARAMETERS

In general electrical characterizations can be done by DC and AC measurement techniques. Though the DC measurement technique is straightforward, it cannot be implemented for solid electrolytes for the following reason:

- As the DC field is applied to the electrolyte, the material gets polarized and ionic conductivity ceases giving only electronic conductivity
- It is difficult to find an electrode material compatible with the solid electrolyte that does not give polarization effects at electrode-electrolyte interface. Therefore for solid electrolytes, AC measurement of electrical conductivity is done to avoid polarization of the sample

On applying a sinusoidal voltage $V=V_{max}\sin\omega t$, where ω ($2\pi f$) is the angular frequency, a current will flow within the electrolyte with identical frequency to that of applied voltage. Due to capacitive and inductive effects, however the current is typically out of phase with voltage.

$$I=I_{max}\ \mathrm{Sin}\ (\omega t+\theta) \qquad (3.1)$$

where I_{max} is the maximum current and θ is the phase angle.

The relationship between applied voltage and resultant current can be written as:

$$Z=V_{max}/ I_{max} \quad (3.2)$$

where, V_{max} is maximum voltage. Z is the total impedance or opposition to the charge flow within electrolyte.

The admittance, the ease of charge flow through the material can be written as:

$$Y=1/Z = I_{max}/ V_{max} \quad (3.3)$$

With a phase difference between V_{max} and I_{max}, the impedance and admittance are vector quantities, processing magnitude and phase and as such may be represented in the vector plane. Similarly both quantities may be represented in the complex plane, where X and Y axes are designated as the real and imaginary components respectively.

$$Z^* = Z'_{real} - jZ''_{imaginary} \quad (3.4)$$

$$Y^* = Y'_{real} - jY''_{imaginary} \quad (3.5)$$

However to obtain a more accurate characterization of the material under study is often necessary to use two other formalisms, closely related to those mentioned above; i.e., the complex electric modulus and complex permittivity. They are given by

$$M^* = M'_{real} - M''_{imaginary} = j\omega C_0 Z^* \quad (3.6)$$

$$\epsilon^{**} = E'_{real} - E''_{imaginary} = (j\omega C_0)^{-1} Y^* \quad (3.7)$$

where C_0 is the vacuum capacitance of the cell.

3.2.3.5 REPRESENTATION OF COMPLEX IMPEDANCE

In the electrochemical impedance analysis, an AC potential is applied to a solid electrolyte and the current through the sample is measured. The response to this potential is an AC current signal containing the excitation frequency and harmonics. By observing the current response, the resistance within different frequencies can be examined.

The electrochemical impedance is measured from this small excitation signal and the data can be represented as Nyquist plot.

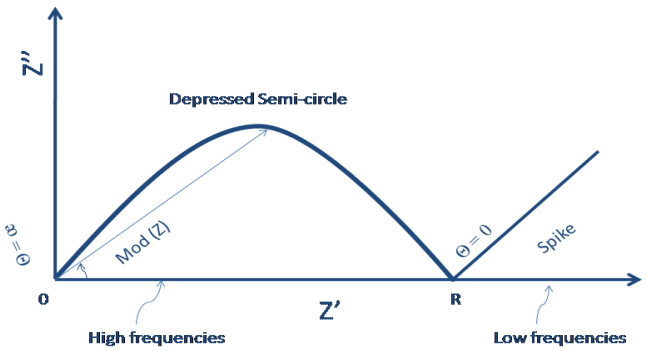

Figure 3.7A typical Nyquist plot

On the Nyquist plot the impedance can be represented as a vector (arrow) of length |Z|. The angle between this vector and the X-axis, commonly called as the "phase angle", f (=arg Z). Another common representation is Bode plot where impedance is plotted with log frequency on the X-axis and both the absolute values of the impedance ($|Z|=Z_0$) and the phase-shift on the Y-axis.

Unlike the Nyquist plot, the Bode plot gives the frequency information. The Nyquist plot could be fitted using an equivalent circuit called the Randles circuit made up of series or parallel combination of resistors and capacitors. Each circuit element represents a component of the electrochemical cell and thus the model will stimulate the experimental impedance spectrum.

3.2.3.6 EQUIVALENT CIRCUIT MODELING

Equivalent circuit modeling of EIS data is used to extract physically meaningful properties of the electrochemical system by modeling the impedance data in terms of an electrical circuit composed of ideal resistors (R), capacitors (C) and inductors (L).

The generalized Constant Phase Element (CPE) and Warburg Element (Z_W) are also used to represent the diffusion or mass transport impedances of the cell [94].

In the equivalent circuit analog, resistors represent conductive pathways for ion and electron transfer. Resistors are also used to represent the resistance to the charge-transfer process at the electrode surface. Capacitors and Inductors are associated with space-charge polarization regions, such as the electrochemical double layer and adsorption/desorption processes at an electrode, respectively.

3.2.3.7 NYQUISTPLOT

The Nyquist complex impedance plane plot is for evaluating electrochemical data. Here the plot is between Z' and Z" of impedance data. This plot shows slightly depressed semicircle which corresponds to the bulk resistance. The ionic conductivity can be determined from resistance were the semicircle crosses the X-axis. From the plot, one can infer about the polarization nature of the sample. For a material which obeys Debye law, the centre of semicircle lies exactly on the real axis and one can distinguish Debye and non-Debye nature of the materials.

The frequency corresponding to the top of the semicircle ω_{max} can be used to calculate the capacitance, if R_b is known,

$$C_b = 1 / 2\pi \omega_{max} R_b \qquad (3.8)$$

The electrical conductivity of the bulk electrolyte is obtained by

$$\sigma_0 = \frac{l}{A} (1/R_b) \qquad (3.9)$$

where, A is the area of the sample, $l$is the thickness of the sample and R_b is the bulk resistance. The bulk resistance can be determined from the Nyquist plot where the semicircles

intercept on the Z' axis. Hence by using Nyquist plot, the values of the relasxation time, the bulk capacitance of the sample can also be obtained.

3.2.3.8 ADVANTAGES OF EIS

Measurements can be made under real-world fuel cell operating conditions, *e.g.*, open circuit voltage or under load (DC voltage or current).

1. Multiple parameters can be determined from a single experiment.
2. Relatively simple electrical measurement that can be automated.
3. Can verify reaction models, and characterize bulk and interfacial properties of the system, e.g., membrane resistance and electrocatalyst.
4. Measurement is non-intrusive – does not substantially remove or disturb the system from its operating condition.
5. A high precision measurement – the data signal can be averaged over time to improve the signal-noise ratio.

CHAPTER-IV

RESULTS AND DISCUSSION

4.1 INRODUCTION

The present work aims to prepare and study electrical properties of prepared membrane for supercapacitor application. To the bestof our knowledge, this is the first attempt to synthesis of various ratios of CMC and Bovine bone membrane with different concentration NaCl with leaf composited membranes were prepared by solution casting method and applied it as an electrolytecum separator for supercapacitor application.Prepared films are characterized by Fourier Transform Infrared spectroscopy (FTIR) and Electrochemical Impedance Analysis.

4.2 ELECTROCHEMICAL IMPEDANCE ANALYSIS

Using the electrochemical impedance spectrometer, electrochemical behaviour of the prepared films is evaluated. For exploration of electrolytic conductivity and dielectric propertiesof the prepared membranes, it is necessary to carry out impedance spectra measurements throughout a large range of frequencies from 1mHz to 10 KHz. To analyse the impedance spectra of the membrane, the films were cut into a suitable size of (2 x 2 cm^2) placed between the copper electrodes which are connected by leads to the electrochemical workstation.

4.2.1 CONDUCTIVITY MEASUREMENTS OF CMC:BB MEMBRANES OF VARIOUS RATIOS:

The plot drawn between real impedance and imaginary impedance is called the Nyquist plot and the frequency response of the real and imaginary are called Bode plot. Figure 4.1 shows the Nyquist and Bode plot of imaginary alone is shown as the information rendered by the Bode plot of real is negligible when compared the Nyquist. The Nyquist plot consists of a high-frequency semicircle and low frequency spike. The high-frequency semicircle is due to the parallel combination of resistance corresponding to the solution/ electrolyticmigration of ions through the host matrix and capacitance component due to the immobile carriers in the insulating matrix of CMC:BB. The low frequency spike can be attributed to the effect of migration species blocked at the electrodes. It means that the conducting species in the electrolyte gets terminated at the interface of electrolyte and

electrode. They do not diffuse into electrode and hence they are readily available during reversibility. The resistance due to the electrolytic conduction of the samples can be calculated from difference between the low frequency intercept of semicircle and the high frequency intercept of the high frequency semicircle of the Nyquist plot [95].

The complex impedance plots reveal that the behaviour of solution conduction, interfacial capacitancedue to the insulating matrix and the electrode electrolyte conduction phenomenon. The inclined line emerging at the low frequency regime corresponds to the blocking or non-blocking / diffusion process of the charge carriers between the contact electrodes and sample. The Bode plot of the CMC:BB Membrane of ratio 10:90 shows a relaxation 106mHz indicating that the resistance formed due to the conducting species and the capacitance formed due to the insulating matrix formulates periodic release of charges to the electrode.

The accurate conductivity of the samples has been determined by fitting the experimental data using Z-view software and equivalent circuits are provided. The solid circle indicates the experimental data and the line represents the fitted plots. The value of the conductivity can be calculated from the resistance obtained from fitting the equivalent circuit. This equivalent circuit is a combination of resistance, capacitance, as well as a few specialized electrochemical elements such as constant phase element (CPE) and Warburg diffusion element.

The electrical conductivity of the sample can be calculated by using the equation

$$\sigma = \frac{d}{R^{*}A} \longrightarrow (4.1)$$

where,

R_b= bulk resistance of the sample (ohm)

d = Thickness of the film (mm)

A = Area of analysis of film ($4cm^2$)

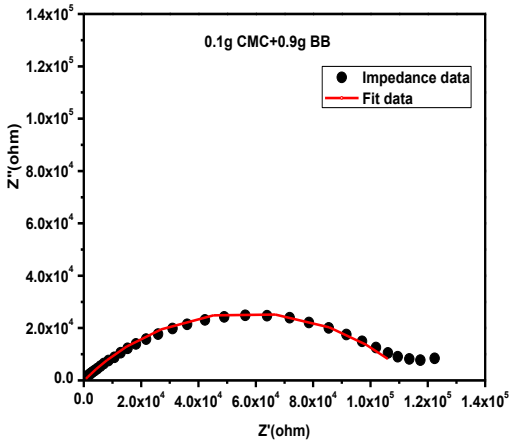

(a)

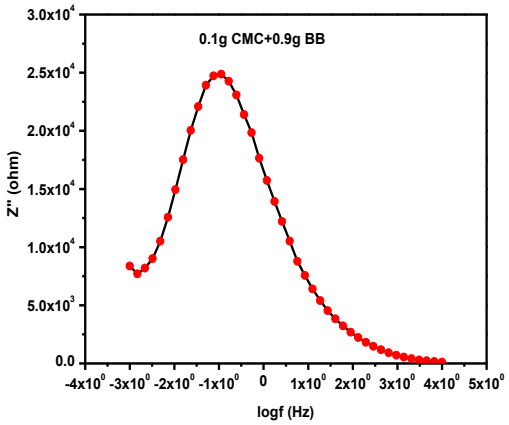

(b)

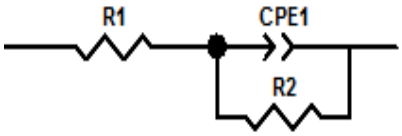

(c)

Figure 4.1(a) Nyquist plot (b) Bode plot of imaginary impedance (c)Equivalent circuitCMC:BB membrane with a ratio of 10:90

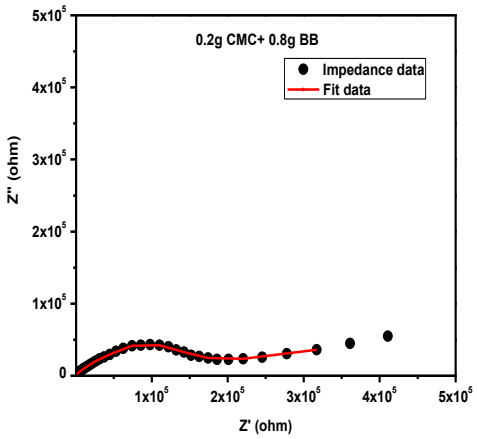

(a)

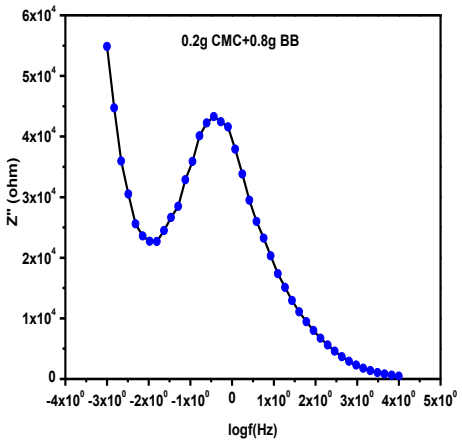

(b)

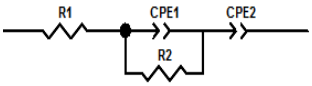

(c)

Figure 4.2 (a) Nyquist plot (b) Bode plot of imaginary impedance (c) Equivalent circuit CMC:BB membrane with a ratio of 20:80

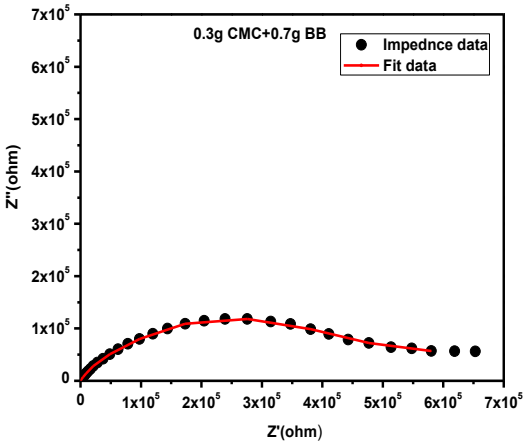

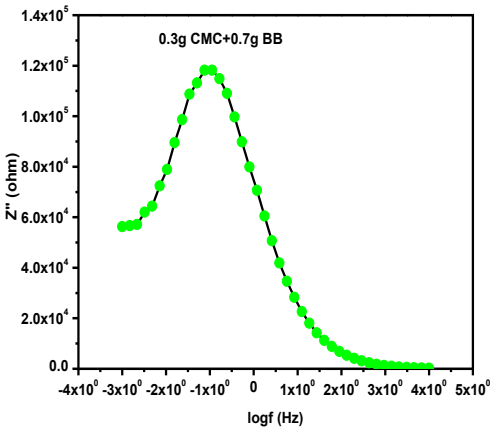

(a) (b)

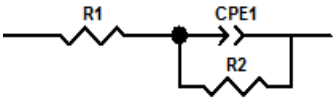

(c)

Figure 4.3 (a) Nyquist plot (b) Bode plot of imaginary impedance (c) Equivalent circuit CMC:BB membrane with a ratio of 30:70

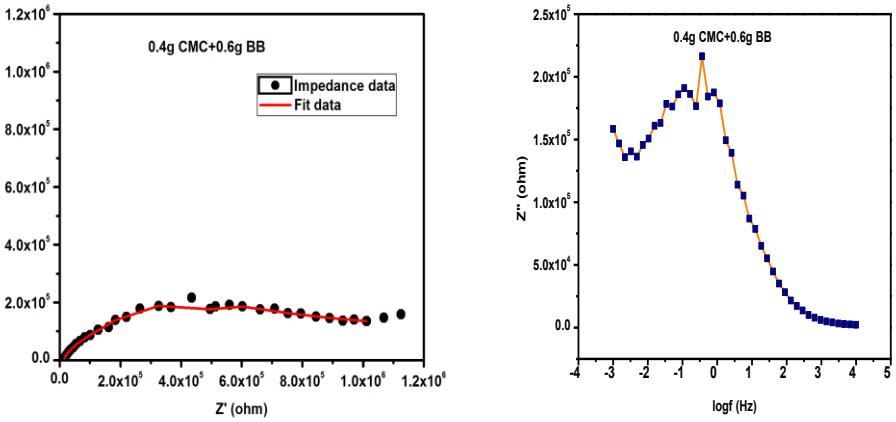

(a) **(b)**

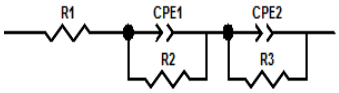

(c)

Figure 4.4 (a) Nyquist plot (b) Bode plot of imaginary impedance (c) Equivalent circuit CMC:BB membrane with a ratio of 40:60

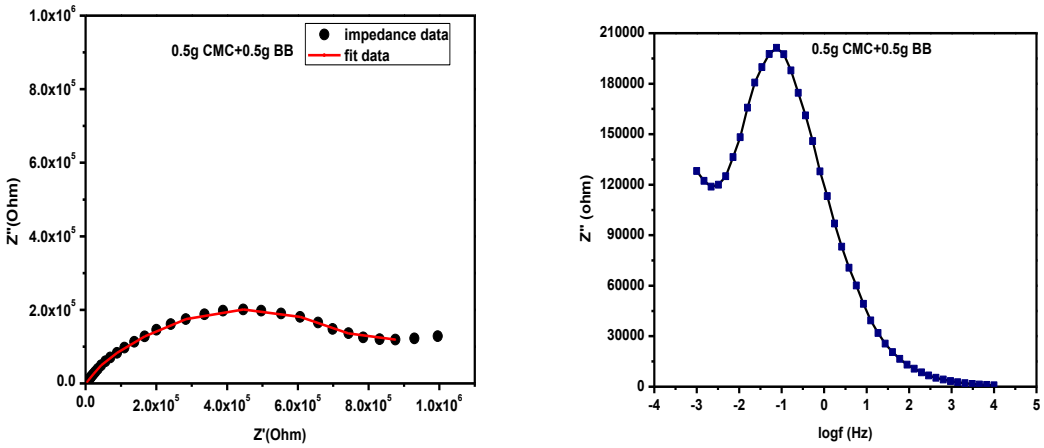

(a) (b)

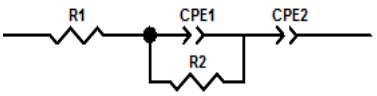

(c)

Figure 4.5 (a) Nyquist plot (b) Bode plot of imaginary impedance (c) Equivalent circuit CMC:BB membrane with a ratio of 50:50

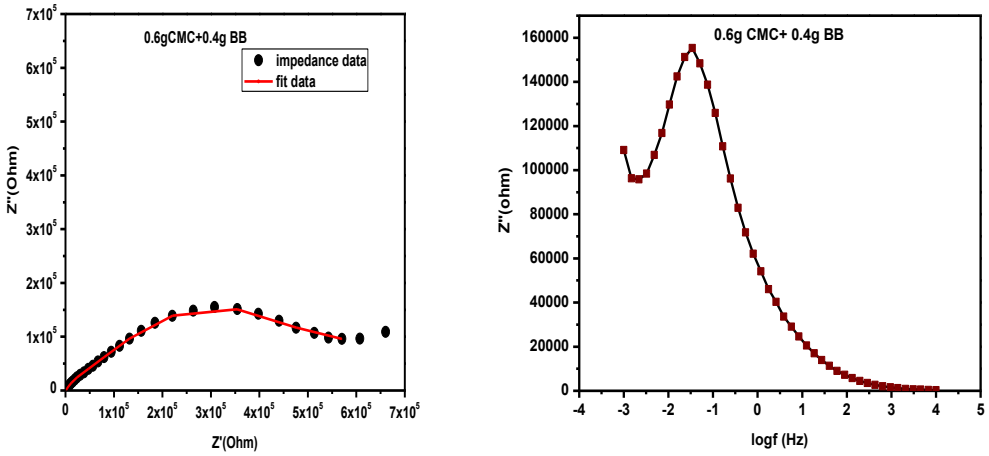

(a) (b)

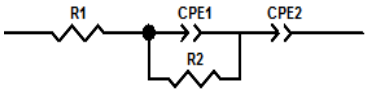

(c)

Figure 4.6 (a) Nyquist plot (b) Bode plot of imaginary impedance (c) Equivalent circuit CMC:BB membrane with a ratio of 60:40

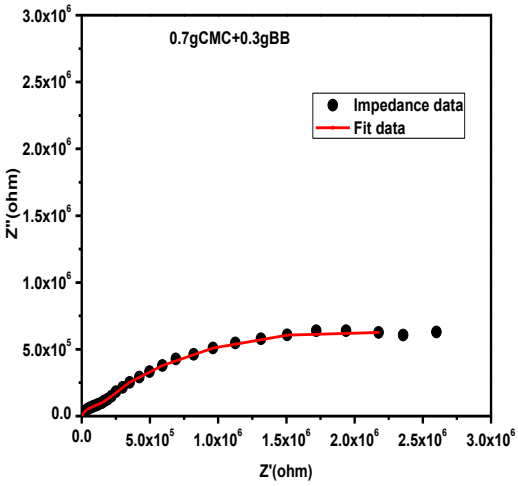

(a)

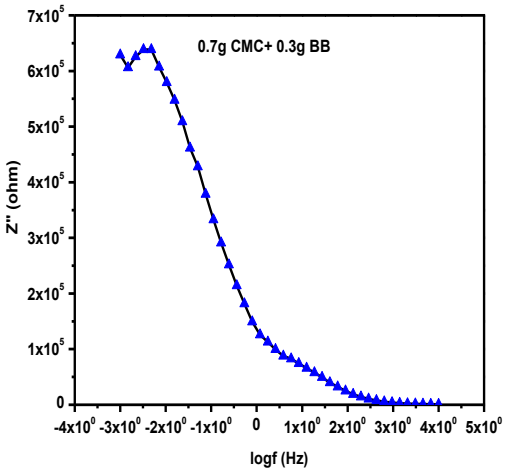

(b)

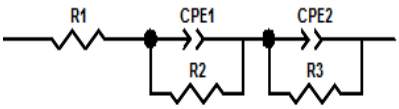

(c)

Figure 4.7 (a) Nyquist plot (b) Bode plot of imaginary impedance (c) Equivalent circuit CMC:BB membrane with a ratio of 70:30

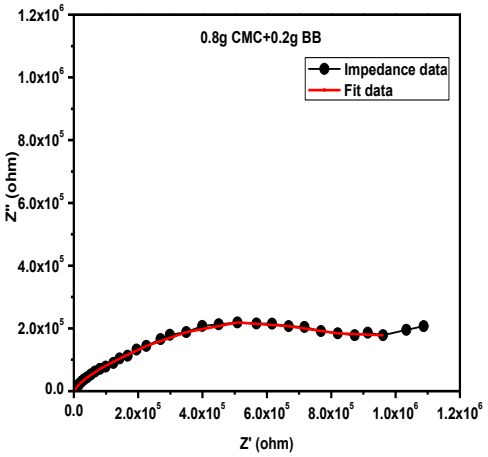

(a)

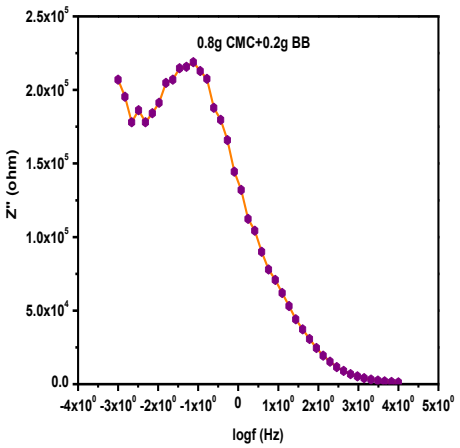

(b)

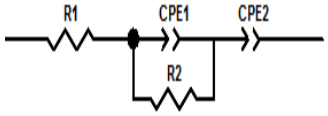

(c)

Figure 4.8 (a) Nyquist plot (b) Bode plot of imaginary impedance (c) Equivalent circuit CMC:BB membrane with a ratio of 80:20

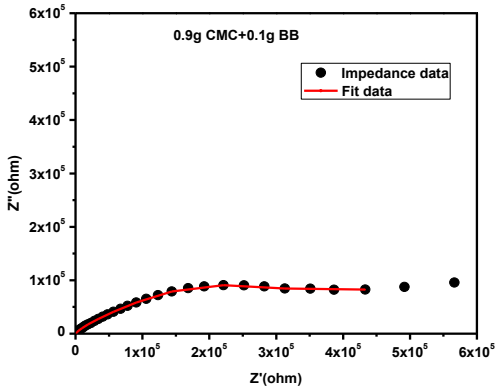

(a)

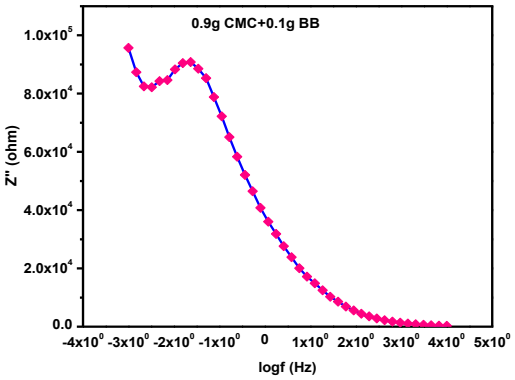

(b)

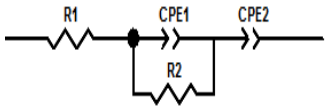

(c)

Figure 4.9 (a) Nyquist plot (b) Bode plot of imaginary impedance (c) Equivalent circuit CMC: BB membrane with a ratio of 90:10

Table 4.1 Comparision of CMC and BB membrane with varied ratios

S. No	Ratio of CMC : BB	Thickness of the membrane (10^{-3} m)	Area of the film (10^{-4} m^2)	R_1 (Ω)	R2 (Ω)	R3 (Ω)	CPE1-T (µF)	CPE1-P	CPE2-T (µF)	CPE2-P
1.	10 : 90	0.180	4	206.7	114090	-	9.9072	0.54	-	-
2.	20 : 80	0.114	4	11.6	208790	-	3.7181	0.51	0.9531	0.45
3.	30 : 70	0.180	4	69.3	518900	-	2.3317	0.63	-	-
4.	40 : 60	0.164	4	10655	566100	577870	0.89940	0.58	6.3739	0.61
5.	50 : 50	0.140	4	4.47	722550	-	1.6841	0.59	0.2539	0.34
6.	60: 40	0.136	4	66.02	602310	-	3.6106	0.54	0.0222	0.53
7.	70 : 30	0.114	4	1573	2714100	95593	2.0488	0.57	0.2430	0.88
8.	80 : 20	0.136	4	10.6	721090	-	1.0837	0.54	0.2051	0.33
9.	90 : 10	0.144	4	10	439260	-	5.3964	0.51	0.0882	0.73

Figures 4.2 (a,b,c) to 4.9(a,b,c) shows the Nyquist plot, Bode plot of the imaginary impedance and equivalent circuit for the CMC: BB membranes of ratios 20:80, 30:70, 40:60, 50:50, 60:40,70:30, 80:20 and 90:10 respectively. The total resistance appears to depend on the ratio of CMC until the ratio of 50:50 ratio however, higher than this inconsistent change is observed which may be due to the poor homogenizing capacity of BB as the ratio of BB is smaller in these membranes. It is to be noted that the ratio of 80:20 is almost similar to 40:60 and 50:50 which proposes that the homogeneity plays a role. While the 90:10 shows extremely smaller resistance compared to the 50:50 but not smaller enough as 10:90. Thus, it is understood that by compositing the CMC and BB, a rational behaviour is expected only upto 50:50. However, as 90:10 have behaved peculiar further analyses are made on this composition also. The Bode plots of imaginary resistance of the ratios indicate the relaxation frequencies to be 358mHz, 106mHz, 346mHz, 75mHz, 357mHz, 4.8mHz, 23mHz for the compositions 20:80, 30:70, 40:60, 50:50, 60:40,70:30, 80:20 and 90:10 respectively. All the relaxations are in the mHz range and hence it is understood that the relaxation is caused only in the electrode electrolyte interface due to the blocking of charge carriers at the electrode interface. Hence the matrix conduction is extremely through for incorporating electrolytic salt for improvisation of conduction. Table 4.1 shows the consolidated data of CMC and BB membranes of various ratios. The table includes the values of solution or electrolytic resistance (R1), resistance due to the insulating matrix (R2), Resistance due to the electrode electrolyte interfacial (R3) and the values of Constant Phase Element (CPE-T, CPE-P) due to the dispersion of conduction caused similar to the dispersive capacitance. The CPE1 corresponds to the capacitive component caused due to the insulating matrix with the conducting charge carrier and CPE2 refers to the polarization effects in the electrode electrolyte interface.

From the Table 4.1, among all the samples, 50:50 ratio of CMC and BB exhibit the lowest value of R1 (solution/electrolytic resistance)value 4.47 Ω. The electrolytic conduction is in the order of 50:50 < 90:10< 80:20< 20:80< 60:40< 30:70 <10:90 < 70:30 <40:60. Among all the last two ratios given above exhibits exorbitantly higher resistance whilst all the other have a meagre difference of few tens which need not be looked into very seriously. Looking into the CPE values, the ratios 10:90 and 30:70 did not exhibit the relaxation at the interface of electrode and electrolyte. All the ratios exhibited the matrix to carrier relaxation. The order of capacitance of matrix to carrier relaxation is 40:60< 80:20 < 50:50 <70:30 <60:40 <20:80 < 90:10 <10:90. The dispersion component of the Constant Phase element is

almost the same for all these capacitances. The capacitance caused due to the interface blocking is of the order of 70:30< 40:60 < 20:80 < 50:50< 80:20 < 90:10 < 60:40. Overall view of all the three factors indicate that the more suitable ratio considering optimal electrolytic resistance, charge carrier capacitance due to the insulating matrix and the interfacial capacitive component is with 50:50.

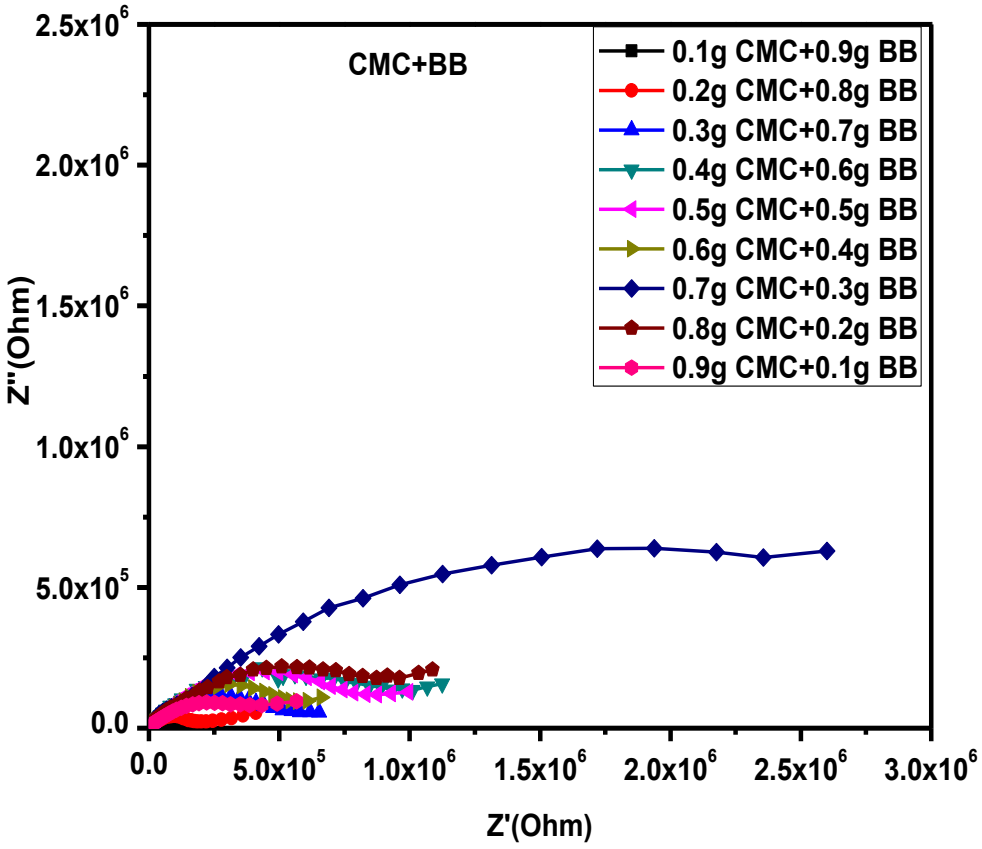

Figure 4.10Comparison of Nyquist plot of all ratios

4.2.2CONDUCTIVITY MEASUREMENTS OF CMC:BB MEMBRANES WITH DIFFERENT CONCENTRATIONS OF ELECTROLYTIC SALT NaCl:

To increase the conductivity of CMC: BBmembranes, electrolytic salts can be composited with the membrane. Hence, in this work, various concentrations of NaCl (0.01g 0.03g, 0.05g, 0.07g, 0.09g) areaddedto the three ratios of CMC: BB Membrane namely 10:90, 50:50 and 90:10 ratios. The three are chosen on the following basis (i) 50:50 is chosen for the reasons stated already in the previous section such as this ratio exhibits an optimal

electrolytic conduction, and their electrical properties are studied (ii) 10:90 is chosen as the membrane did not show any interfacial relaxation and (iii) 90:10 as it has all the three components, namely electrolytic resistance, resistance and relaxation due to the insulating matrix and also the interfacial relaxation, prominent.

4.2.2.1. CONDUCTIVITY MEASUREMENTS OF CMC:BB (10:90) MEMBRANES WITH DIFFERENT CONCENTRATIONS OF ELECTROLYTIC SALT NaCl:

Figure 4.11a,b,c to 4.15 a,b,c shows the Nyquist, Bode of the imaginary impedance and the equivalent circuit fit for the CMC:BB membrane of ratio 10:90 incorporated with 0.01, 0.03, 0.05, 0.07 and 0.09 g of NaCl. Similar to the analysis of the CMC:BB membranes in the previous section, a Table 4.2 is consolidated for convenience to look into the resistance and capacitive components. All the concentrations of NaCl shows relaxation in the Bode Plot at frequencies 275mHz, 10mHz, 718mHz, 34mHz and 78mHz for the NaCl concentrations of 0.01,0.03,0.05,0.07 and 0.09g respectively. As all the frequencies are in mHz of relaxation, it is clear that the relaxation originates from the electrode electrolyte interfacial polarization and not due to the insulating matrix to the electrolytic salt included in the matrix. The order of the electrolytic resistance is 0.01g < 0.09g < 0.05g < 0.07g < 0.03g. But the total conductivity inclusive of the matrix resistance is of the order of 0.05> 0.09 > 0.07 > 0.03 > 0.01. It is understood that the matrix resistance plays a vital role in the contribution of conduction in these membranes.

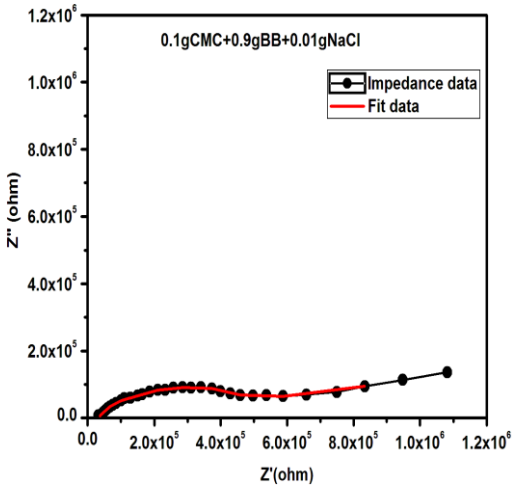

(a)

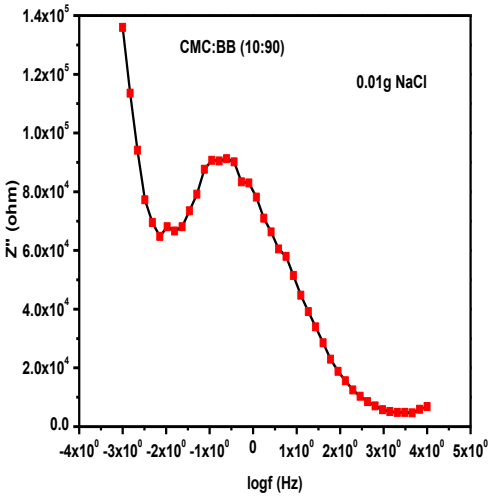

(b)

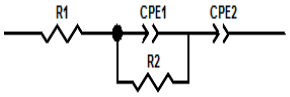

Figure 4.11 (a) Nyquist plot (b) Bode Plot of the imaginary impedance (c) fitted equivalent circuit of the CMC:BB (10:90) membrane with 0.01g of NaCl electrolytic salt

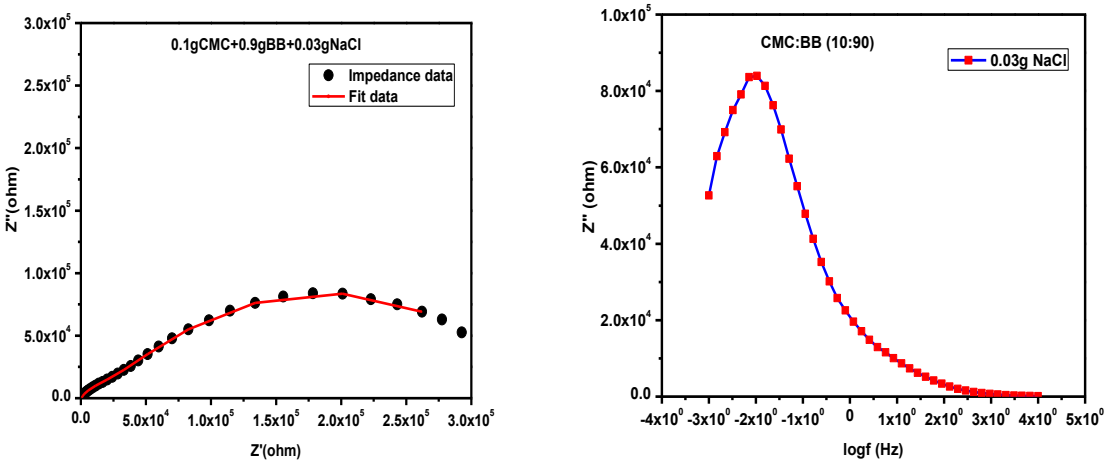

(a) (b)

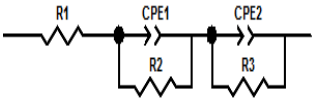

(c)

Figure 4.12 (a) Nyquist plot (b) Bode Plot of the imaginary impedance (c) fitted equivalent circuit of the CMC:BB (10:90) membrane with 0.03g of NaCl electrolytic salt

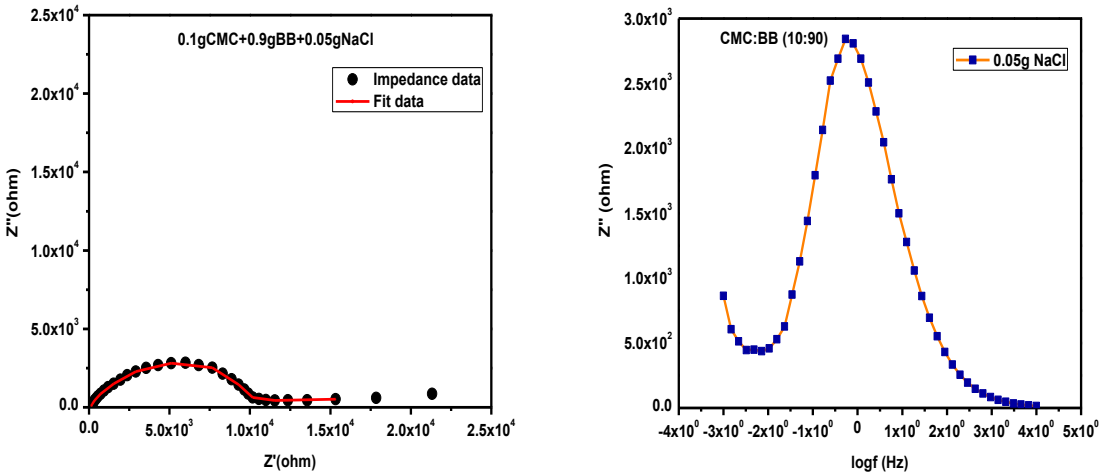

(a) (b)

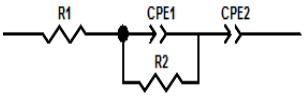

(c)

Figure 4.13 (a) Nyquist plot (b) Bode Plot of the imaginary impedance (c) fitted equivalent circuit of the CMC:BB (10:90) membrane with 0.05g of NaCl electrolytic salt

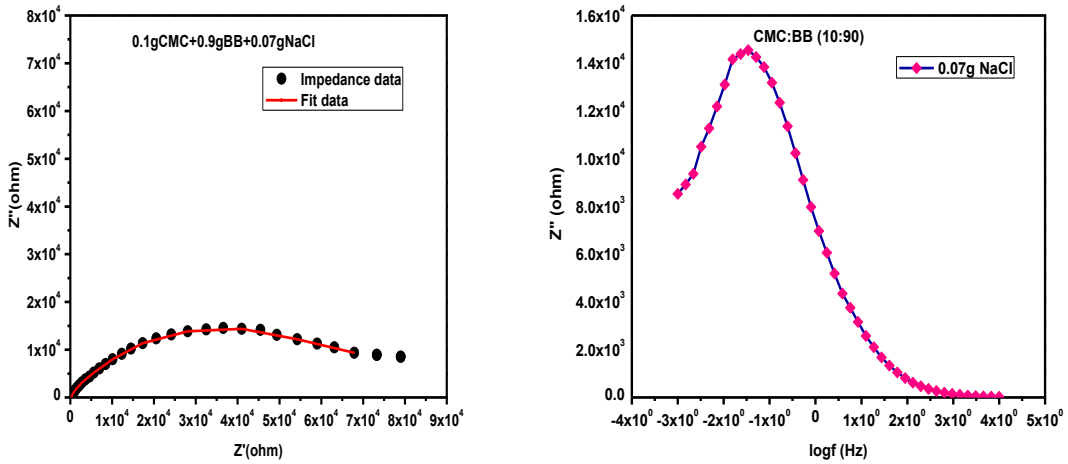

(a) (b)

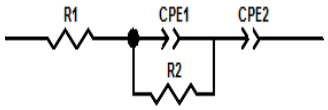

(c)

Figure 4.14 (a) Nyquist plot (b) Bode Plot of the imaginary impedance (c) fitted equivalent circuit of the CMC:BB (10:90) membrane with 0.07g of NaCl electrolytic salt

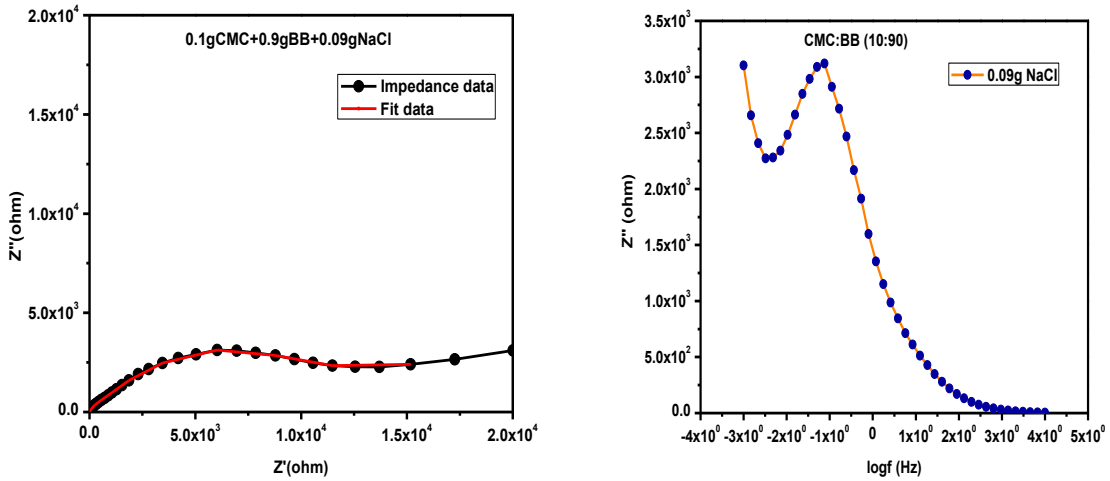

(a) **(b)**

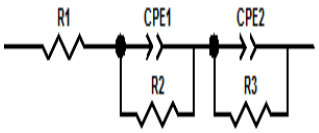

(c)

Figure 4.15 (a) Nyquist plot (b) Bode Plot of the imaginary impedance (c) fitted equivalent circuit of the CMC:BB (10:90) membrane with 0.09g of NaCl electrolytic salt

Among these five concentrations, the 0.05g and 0.09g of NaCl shows high conductivity of the order of 10^{-5} Sm^{-1}. Both electrolytic and insulating matrix resistances are the least among the five concentrations. The insulating matrix resistance of 10:90 CMC:BB membrane was 114090 ohms where as that has been reduced to 10440 ohms when incorporating 0.05g of NaCl , 13460 ohms in the case of 0.09 g of NaCl. Figure 4.16 a and b consolidates the results for the convenience of the reader.

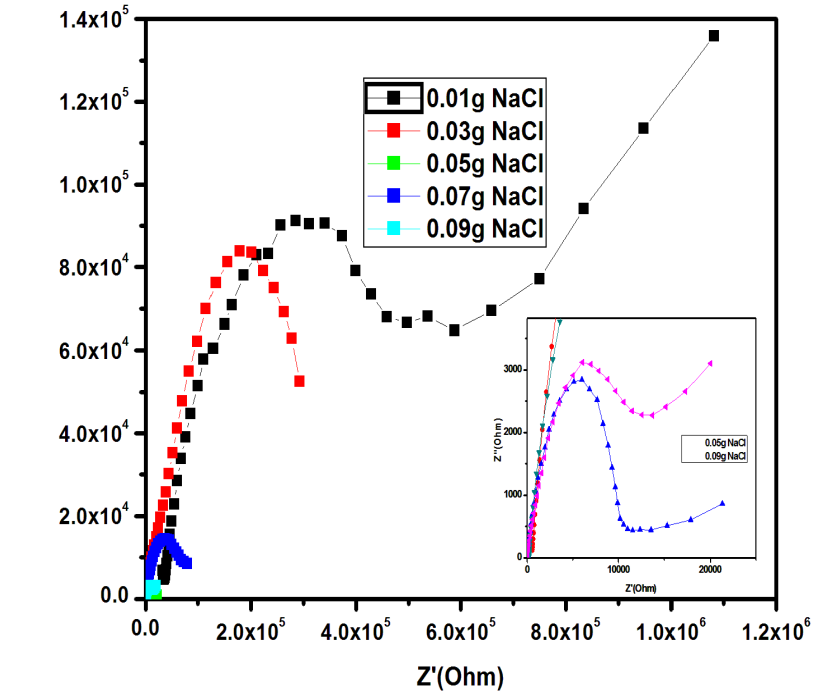

Figure 4.16 (a) Comparisionof Nyquist plot of CMC:BB (10:90) membrane for different concentrations of NaCl

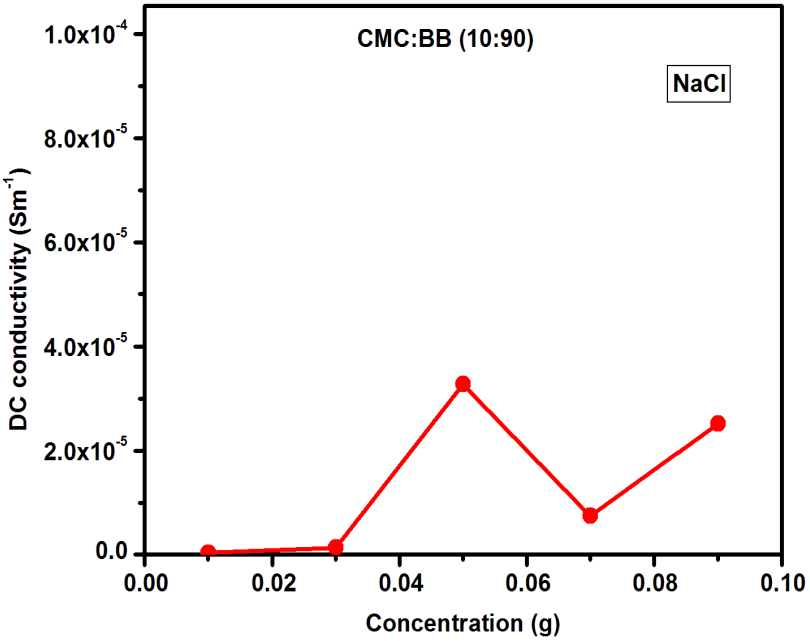

Figure 4.16 (b) Concentration versus conductivity-Comparision for all membranes

Table 4.2 Comparison of CMC: BB membrane of ratio 10:90 with different concentrations of NaCl

S. No	Concentration of NaCl (g)	Thickness of the membrane (10^{-3}m)	Area of analysis of film $10^{-4}m^2$	R1 (Ω)	R2 (Ω)	R3 (Ω)	CPE1-T (µF)	CPE1-P	CPE2-T (µF)	CPE2-P	DC conductivity (Sm^{-1})
1.	0.01	0.114	4	15	841230	-	2.0877	0.41	39.876	0.001	0.3387×10^{-7}
2.	0.03	0.196	4	85.76	366280	2519	0.1123	0.50	0.783	0.42	1.3283×10^{-6}
3.	0.05	0.204	4	66.7	10440	5053	0.3347	0.64	115.44	0.40	3.2776×10^{-5}
4.	0.07	0.174	4	76.62	58160	-	0.2635	0.58	955.00	0.52	7.4695×10^{-6}
5.	0.09	0.144	4	18.62	13460	800.9	0.0178	0.67	47.877	0.83	2.5210×10^{-5}

4.2.2.2. CONDUCTIVITY MEASUREMENTS OF CMC:BB (50:50) MEMBRANES WITH DIFFERENT CONCENTRATIONS OF ELECTROLYTIC SALT NaCl:

The results obtained for the CMC:BB (50:50) membrane with different concentrations of NaCl is discussed here. Figure 4.17 a,b,c to Figure 4.22 a,b,c presents the Nyquist, Bode plot of imaginary impedance and equivalent circuit of the CMC:BB (50:50) membrane with 0.01g, 0.03g, 0.05 g, 0.07 g and 0.09g NaCl. Here, electrolytic resistance is in the order of 0.01g< 0.07g <0.09g < 0.05g < 0.03g. However, looking into the total resistance, the resistance of 0.03g is exorbitantly high and incomparable to all the other concentrations. The 0.09g shows the least resistance among the five concentrations. Comparing the values of fitting of the 0.09g of 50:50 membrane, the total conductivity has not changed but there is a play off between the resistance due to insulating matrix and the interfacial resistance. In the 50:50 membrane, the interfacial resistance is higher.

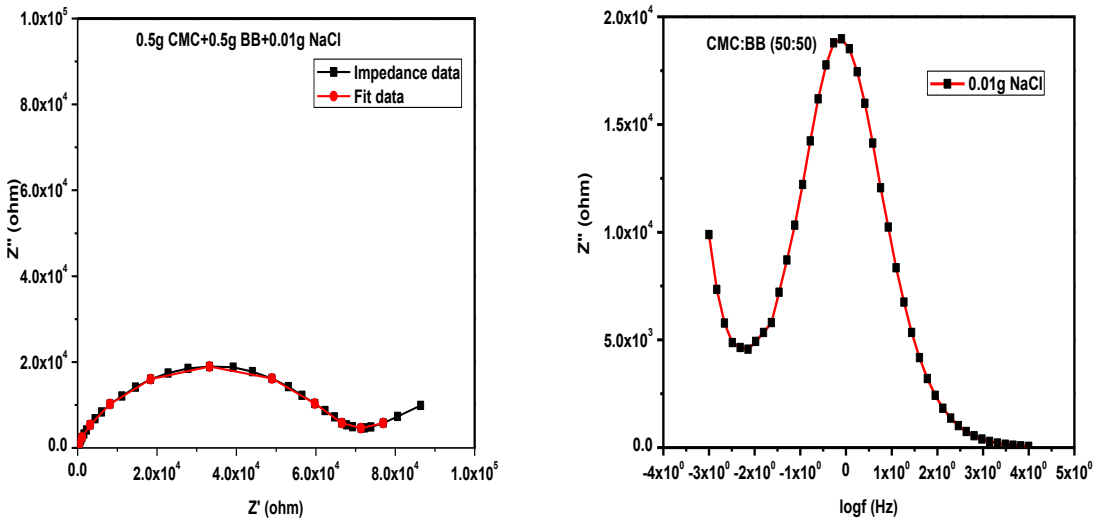

(a) (b)

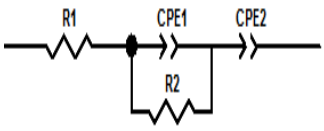

(c)

Figure 4.17 (a) Nyquist plot (b) Bode Plot of the imaginary impedance (c) fitted equivalent circuit of the CMC:BB (50:50) membrane with 0.01g of NaCl electrolytic salt

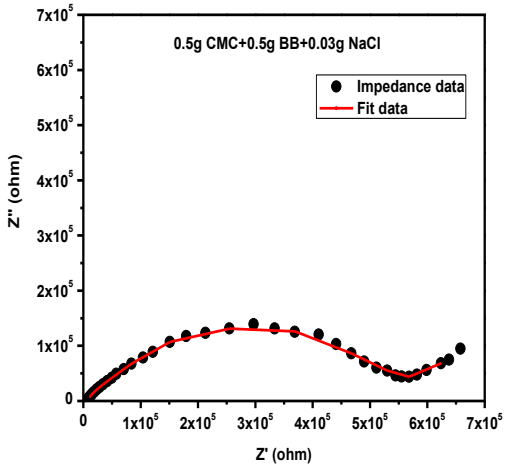

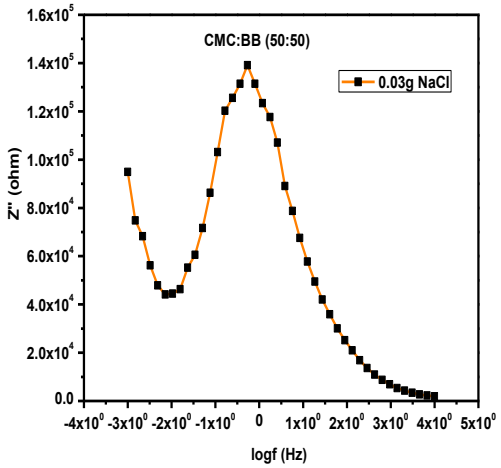

(a) **(b)**

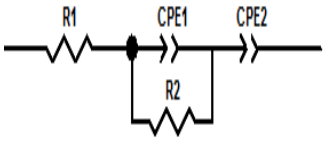

(c)

Figure 4.18 (a) Nyquist plot (b) Bode Plot of the imaginary impedance (c) fitted equivalent circuit of the CMC:BB (50:50) membrane with 0.03g of NaCl electrolytic salt

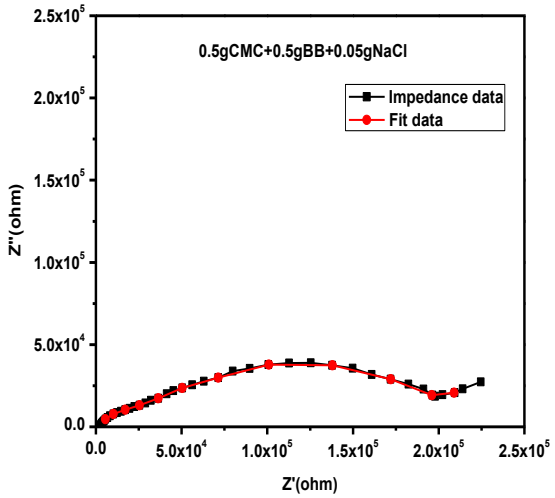

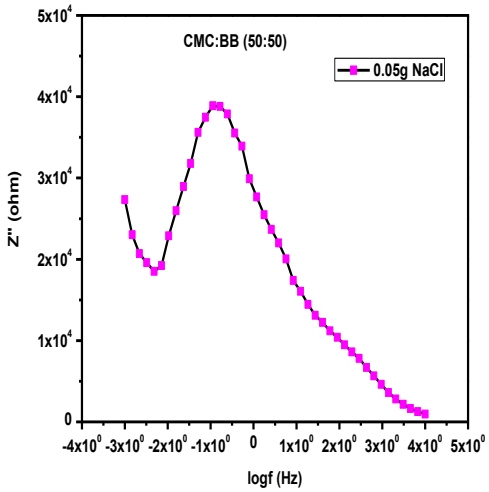

(a) (b)

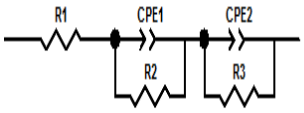

(c)

Figure 4.19(a) Nyquist plot (b) Bode Plot of the imaginary impedance (c) fitted equivalent circuit of the CMC:BB (50:50) membrane with 0.05g of NaCl electrolytic salt

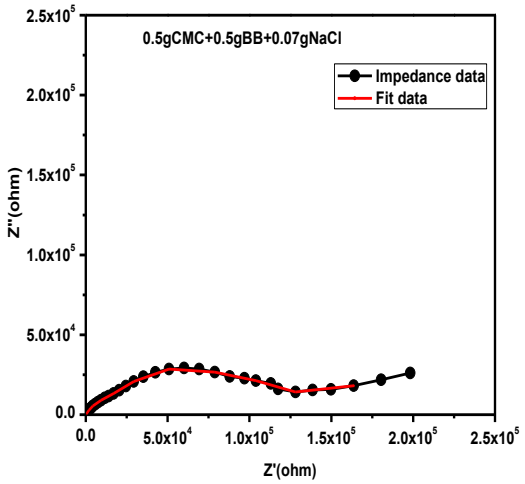

(a)

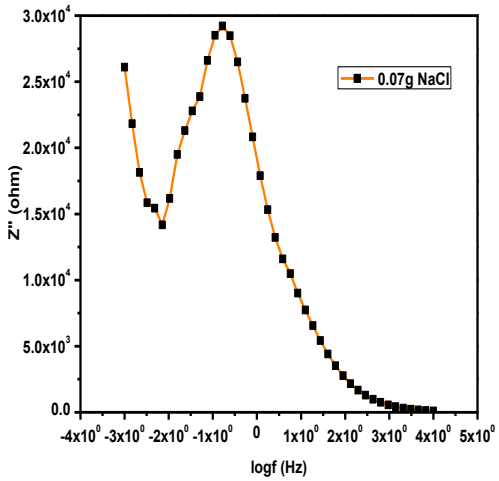

(b)

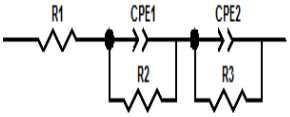

(c)

Figure 4.20 (a) Nyquist plot (b) Bode Plot of the imaginary impedance (c) fitted equivalent circuit of the CMC:BB (50:50) membrane with 0.07g of NaCl electrolytic salt

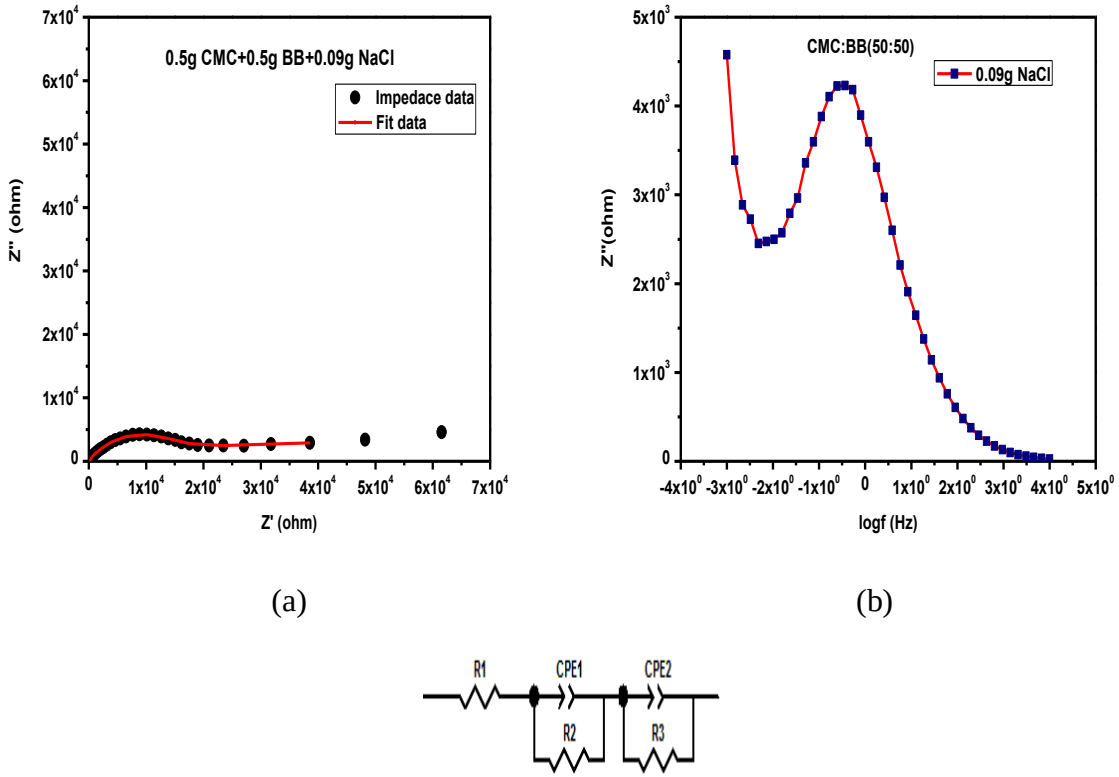

Figure 4.21 (a) Nyquist plot (b) Bode Plot of the imaginary impedance (c) fitted equivalent circuit of the CMC:BB (50:50) membrane with 0.09g of NaCl electrolytic salt

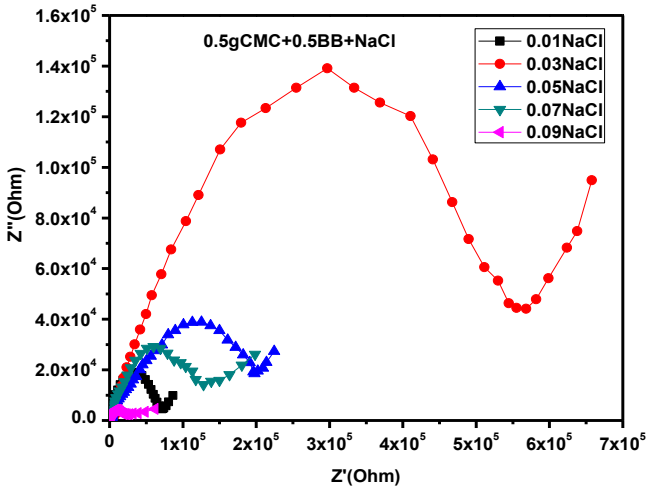

Figure 4.22 (a)Comparison of the Nyquist plot of the CMC:BB (50:50) membranes with different concentrations of NaCl

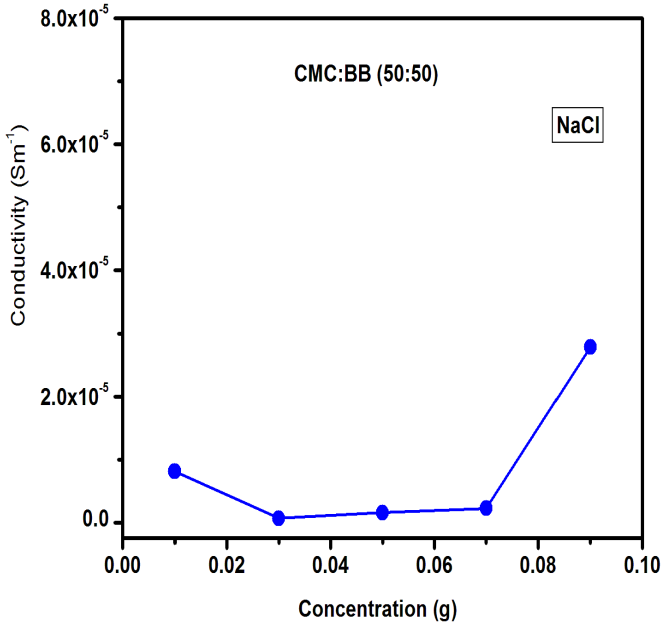

Figure 4.22 (b) Comparison of the CMC:BB (50:50) membranes with different concentrationsof NaCl

Table 4.3 Comparison of CMC:BB membrane of ratio 50:50 with different concentrations of NaCl

S. No	Ratio of NaCl (g)	Thickness of the membrane x 10^{-3} m	area of the film x 10^{-4} m^2	R1 (Ω)	R2 (Ω)	R3 (Ω)	CPE1-T (μF)	CPE1-P	CPE2-T (μF)	CPE2-P	DC Conductivity (S m^{-1})
1.	0.01	0.206	4	41.91	63556	-	3.8866	0.73228	0.0076	0.53445	8.09775 x 10^{-6}
2.	0.03	0.160	4	4140	585260	-	0.92599	0.54269	158.38	0.49891	6.78656 x 10^{-7}
3.	0.05	0.170	4	3648	22757	246340	12.373	0.76400	5.1316	0.32969	1.55823 x 10^{-6}
4.	0.07	0.142	4	62.2	149530	9530	12.123	0.58659	5.0087	0.79146	2.23098 x 10^{-6}
5.	0.09	0.216	4	69.8	2223	17122	31.012	0.70800	49.710	0.61918	2.78130 x 10^{-5}

When compared with the 10:90 ratio 0.09g of NaCl membrane, the present membrane have an interfacial resistance value of 17122 ohm which is higher than the other one. Among the 50:50 membranes with NaCl, only 0.09g of NaCl have comparable conductivity. The relaxation occurs in all the five samples and are rated as 0.05 (120mHz) < 0.07 g (186mHz) < 0.09g (275mHz) < 0.03g (552mHz) < 0.01g (783mHz) indicates that the relaxation is only due to the interfacial polarization.

4.2.2.3. CONDUCTIVITY MEASUREMENTS OF CMC:BB (90:10) MEMBRANES WITH DIFFERENT CONCENTRATIONS OF ELECTROLYTIC SALT NaCl:

Various concentrations of NaCl such as 0.01g, 0.03g, 0.05g, 0.07g, 0.09g are added to CMC:BB (90:10) ratio and their conductivity studies are made.

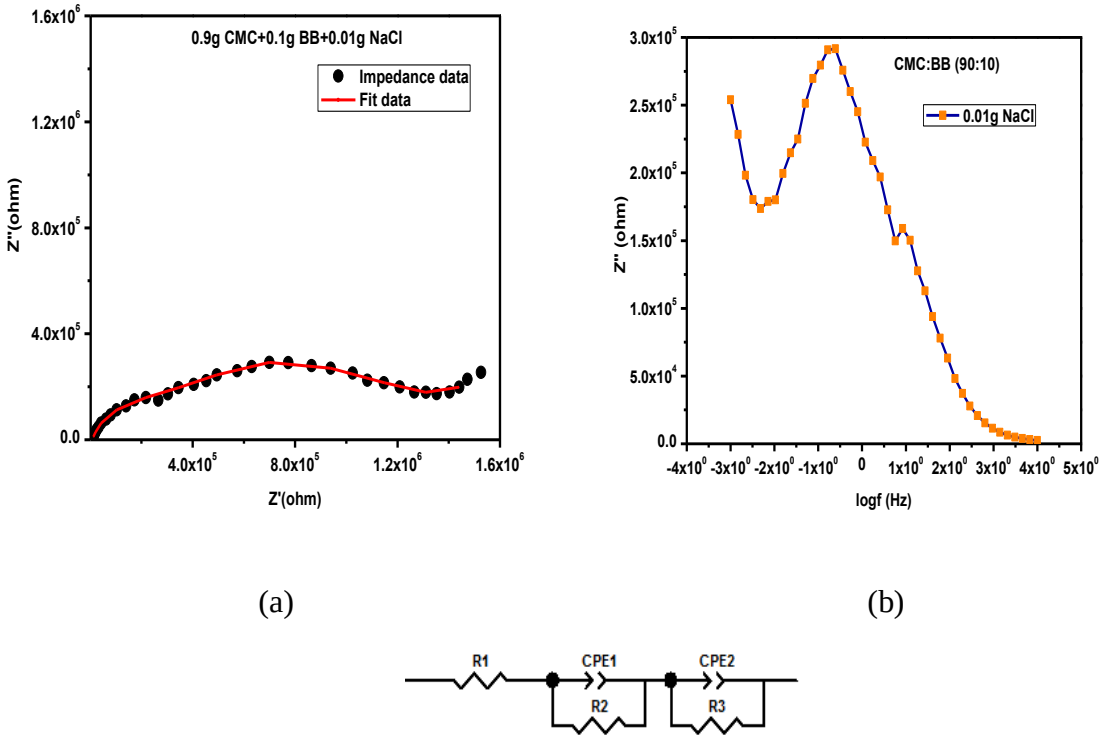

Figure 4.23 (a) Nyquist plot (b) Bode Plot of the imaginary impedance (c) fitted equivalent circuit of the CMC:BB (90:10) membrane with 0.01g of NaCl electrolytic salt

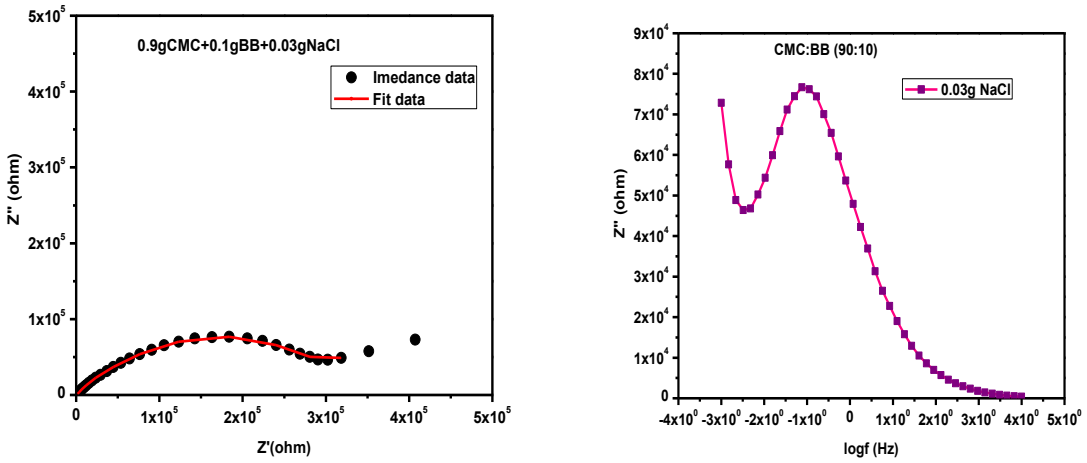

(a) (b)

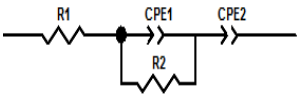

(c)

Figure 4.24 (a) Nyquist plot (b) Bode Plot of the imaginary impedance (c) fitted equivalent circuit of the CMC:BB (90:10) membrane with 0.03g of NaCl electrolytic salt

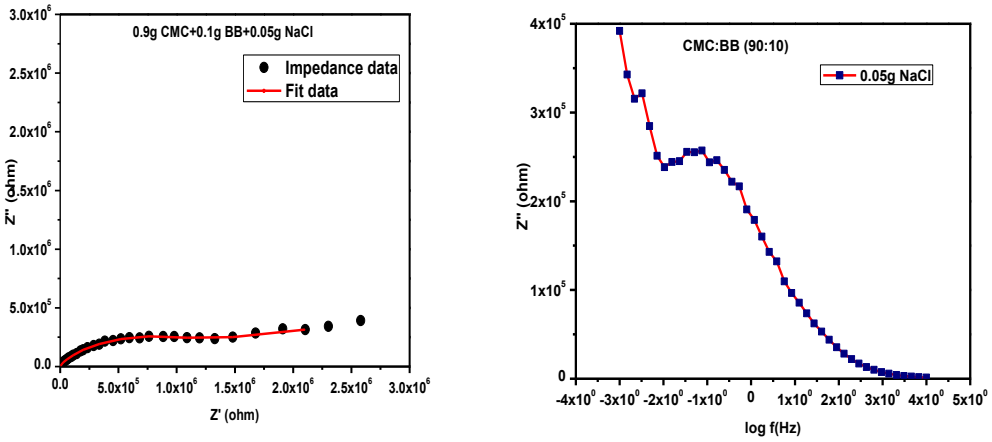

(a) (b)

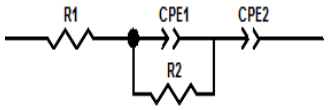

(c)

Figure 4.25 (a) Nyquist plot (b) Bode Plot of the imaginary impedance (c) fitted equivalent circuit of the CMC:BB (90:10) membrane with 0.05g of NaCl electrolytic salt

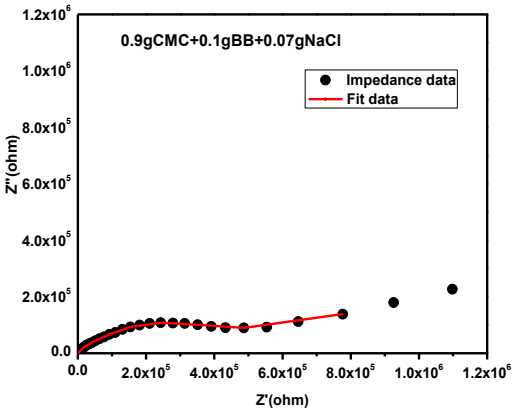

(a)

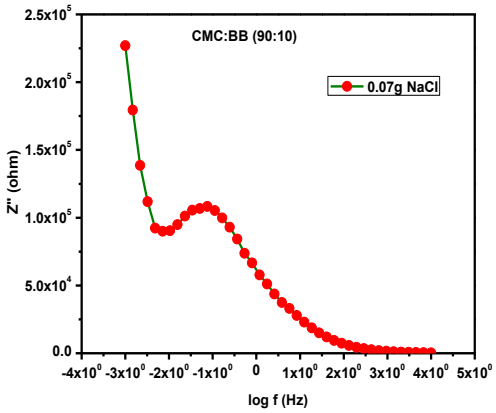

(b)

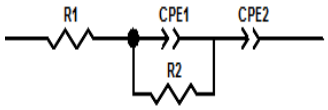

(c)

Figure 4.26 (a) Nyquist plot (b) Bode Plot of the imaginary impedance (c) fitted equivalent circuit of the CMC:BB (90:10) membrane with 0.07g of NaCl electrolytic salt

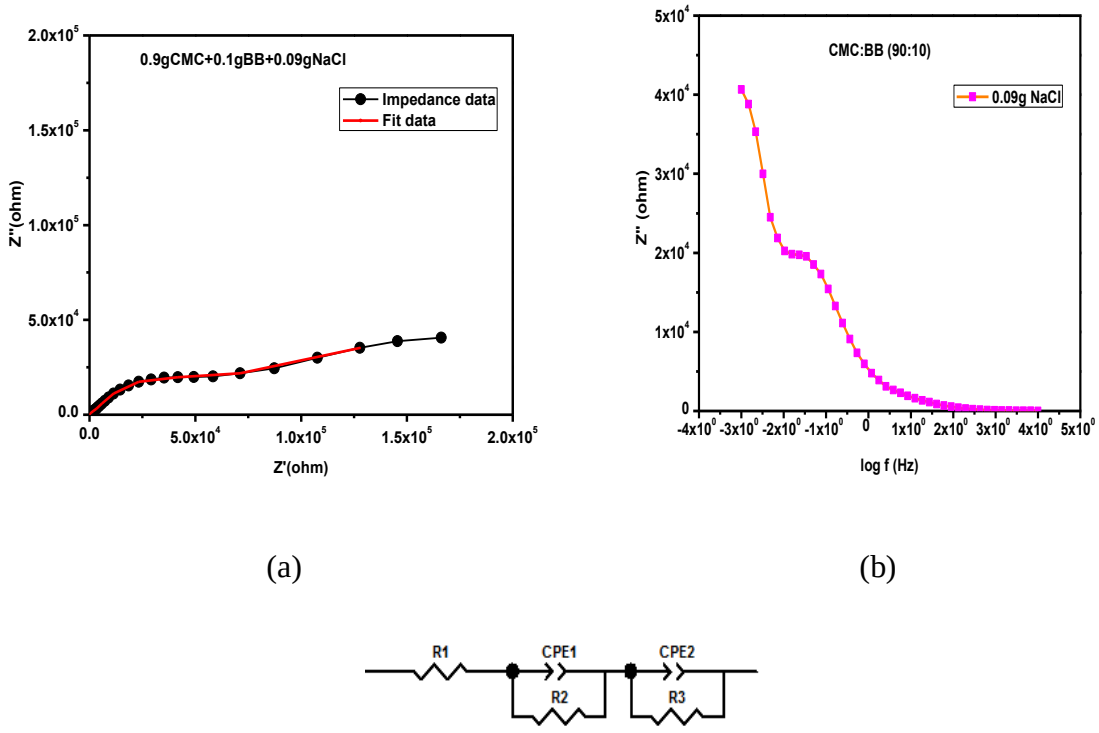

Figure 4.27 (a) Nyquist plot (b) Bode Plot of the imaginary impedance (c) fitted equivalent circuit of the CMC:BB (90:10) membrane with 0.09g of NaCl electrolytic salt

Table 4.4 Comparison of CMC:BB membrane of ratio 90:10 with different concentrations of NaCl

S. No	Ratio of NaCl (g)	Thickness of the membrane (10^{-3} m)	area of the film (10^{-4} m^2)	R1 (Ω)	R2 (Ω)	R3 (Ω)	CPE1-T (μF)	CPE1-P	CPE2-T (μF)	CPE2-P	Ionic conductivity (Sm^{-1})
1.	0.01	0.194	4	5569	1252700	238890	0.9892	0.56674	0.1196	0.81944	3.23946×10^{-7}
2.	0.03	0.200	4	312.6	297330	-	3.4487	0.54666	168.87	0.49381	1.67986×10^{-6}
3.	0.05	0.190	4	1454	1055300	-	0.0748	0.57826	9.7769	0.49174	4.49489×10^{-7}
4.	0.07	0.180	4	243	520680	-	2.9774	0.56382	7.6754	0.4187	8.63851×10^{-7}
5.	0.09	0.304	4	1.5	140700	1450	49.218	0.62684	0.16047	0.90047	5.34640×10^{-6}

Figures 4.23 a,b,c to 4.27 a,b,c shows the Nyquist plot, bode plot of imaginary impedance and equivalent circuit for the CMC: BB 90:10 Membrane with 0.01g, 0.03g, 0.05g, 0.07g and 0.09g of NaCl salt incorporated in the membrane. Figure 4.28 consolidates the Nyquists and the Table 4.4 compares the conductivity of the membranes, fitting parameters of the NaClincorporated CMC: BB 90:10 ratio membranes. Among all the five concentrations, 0.09g of NaCl with CMC: BB (90:10) membrane exhibits higherDC conductivity of $5.3464 \times 10^{-6} Sm^{-1}$. For 0.01g of NaCl with CMC: BB (90:10) membrane exhibit the lowest conductivity value of $3.23946 \times 10^{-7} Sm^{-1}$. It reveals that, when the concentration of NaCl increases in the host material, the conducting species increases and it effectively increases the conductivity of the membrane.

For 0.01g of NaCl with CMC: BB (90:10) ratio, electrode/electrolyte interfacial resistance value is high. It effectively decreases the total conductivity of the membrane. For 0.09 g of NaCl with CMC: BB (90:10) ratio, electrode/electrolyte interfacial resistance value is 1450 ohm.For 0.05g of NaCl, insulating matrix resistance is high.

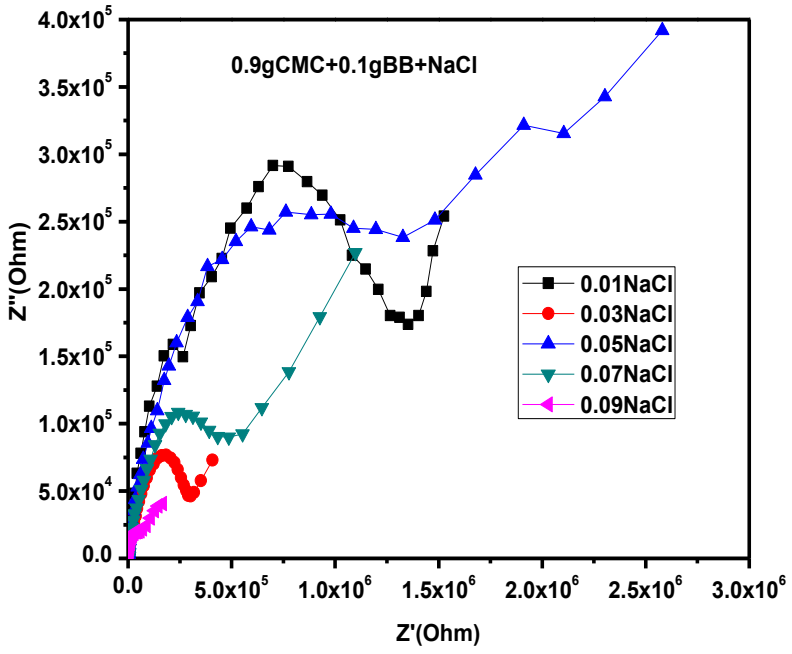

Figure 4.28 (a) Comparison of the Nyquist plot of the CMC:BB (90:10) membranes with different concentrations of NaCl

From the bode plot,the relaxation frequencies are of the order of 3.4mHz (0.5g) < 71.9mHz (0.07g) < 81.4mHz (0.09g) < 231mHz (0.01g) < 781mHz (0.03g). All the frequencies are in mHz and hence the relaxation is due to the interfacial component only. The matrix does not relax due to the impeded motion.

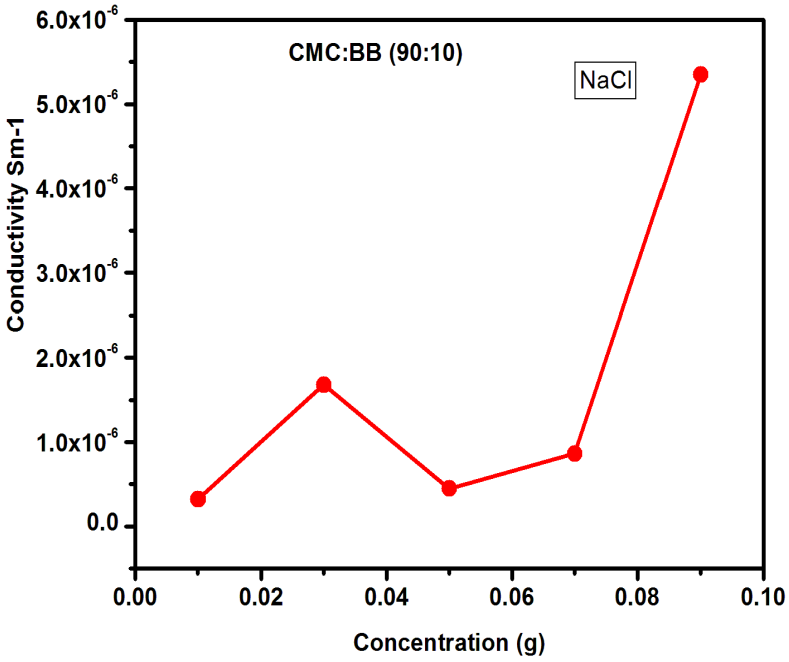

Figure 4.28 (b) Comparison of the CMC:BB (90:10) membranes with different concentrations of NaCl

Figure 4.28 (b) shows the comparison of conductivity at different concentrationsof NaCl in CMC: BB (90:10) membrane. For 0.09 g of NaCl with CMC:BB (90:10) exhibit the highest conductivity due to the increase of conducting species in the host matrix.

Consolidating all the conductivity data, it is noted that the highest conduction is obtained with CMC:BB (50:50) membrane with 0.09g of NaCl. Hence, the CMC:BB ratio of 50:50 with 0.09g of NaCl is chosen for attempting with the leaf reinforced membrane and its analysis.

4.2.3DIELECTRIC ANALYSIS

Study on the relative permittivity in membranes films help to understand the polarization effect at the electrode/electrolyte interface.

Complex dielectric constant and dielectric loss are evaluated from the recorded complex impedance data. The complex permittivity [96]

Dielectric constant $\epsilon' = Z''/\omega C_0 (Z'^2 + Z''^2)$ → **(3.2)**

Dielectricloss $\epsilon'' = Z'/\omega C_0 (Z'^2 + Z''^2)$ → **(3.3)**

Here, $C_0 = \varepsilon_0 A / d$

ε_0 is permittivity of free space, A is electrode–electrolyte contact area, and dis the thickness of the electrolyte)

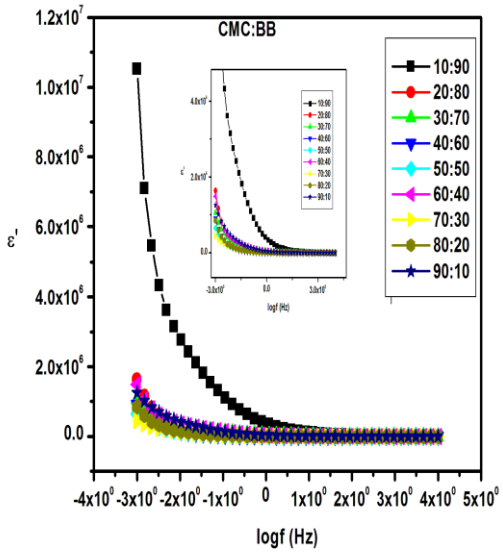

(a)

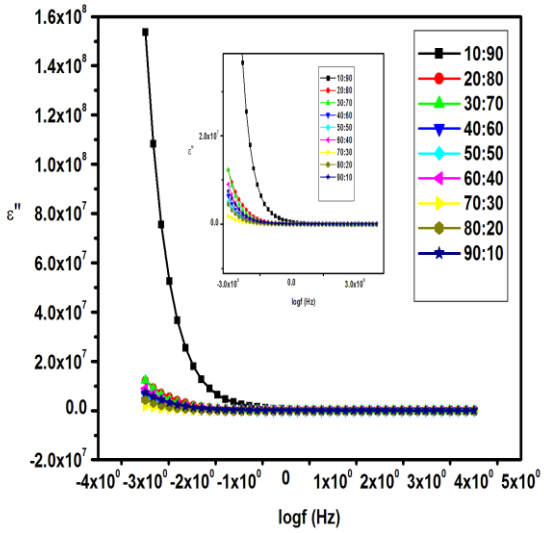

(b)

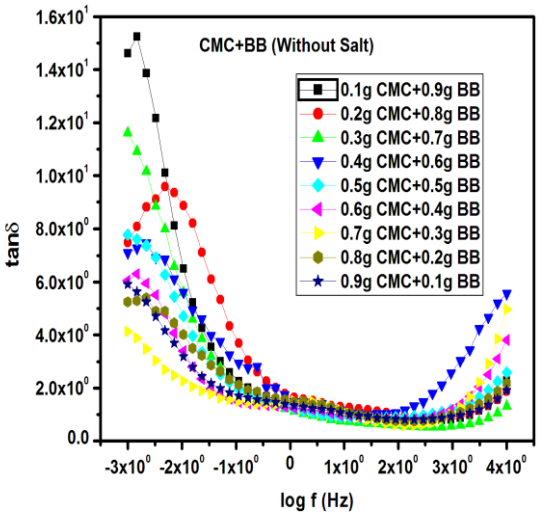

(c)

Figure 4.29(a) Dielectric constant (b) Dielectric loss and (c) tan δ of the various concentration of CMC:BB

Figure 4.29 shows the frequency dependence (a) dielectric constant (b) dielectric loss and (c)tan**δ**graph of CMC: BB (without salt). The complex dielectric permittivity has two parts; real part (ϵ') describes storage capacity or dielectric constant while the imaginary part (ϵ") is the dielectric loss. All the membranes confirm the non-Debye dependence based on the sharp rise of the dielectric value towards low frequencies which indicate that the electrodepolarization has occurred. In the high frequency region, dielectric constant decreases rapidly and becomes frequency independent. This is because the charge carriers and dipoles in the membrane find it hard to translate and orient, respectively, according to the direction of theapplied field. At high frequencies, the periodic reversal of the electric field occurs so fast that there is no excess ion diffusion in the direction of the field. The polarization is due to the charge accumulation decrease, leading to the observed decrease in the value of ϵ' and ϵ''.

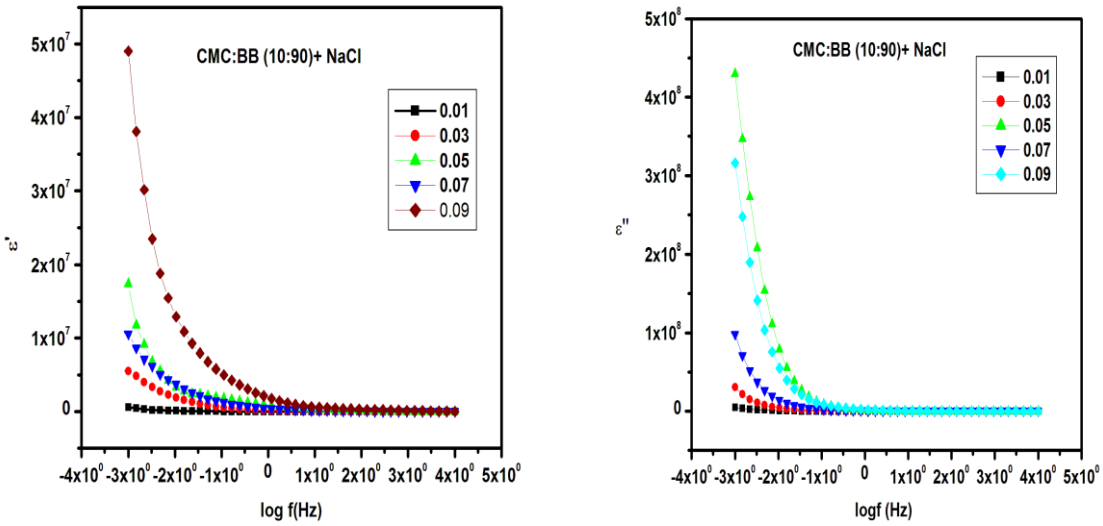

(a) (b)

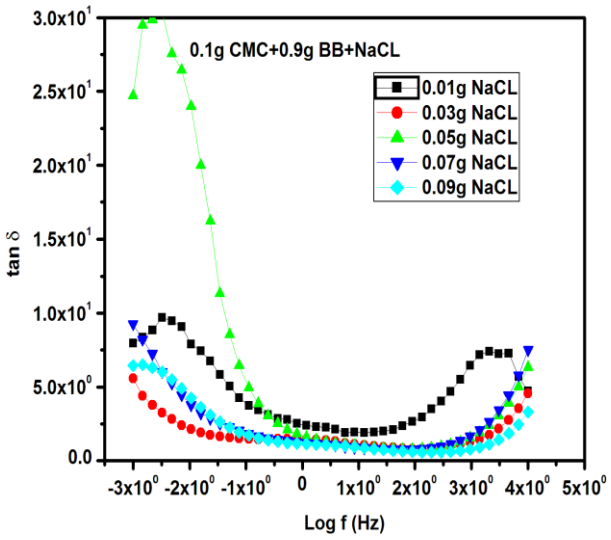

(c)

Figure 4.30 (a) Dielectric constant (b) Dielectric loss and (c) tan δ of the various concentration of NaCl with CMC: BB (10:90)

Figure 4.30 (a, b, & c) shows the frequency dependence dielectric constant and dielectric loss and loss tangent for various concentration of NaCl with CMC: BB (10:90). Both dielectric constant and dielectric loss rise sharply at low frequencies indicating that electrode polarization and space charge effects have occurred confirming non-Debye

dependence implying that the conductivity exhibits relaxation that is non-exponential in time. On the other hand, as frequency increased, the rate of reversal of the electric field increased, and so there was no time for charge to build up at the interface. Therefore, the polarization due to charge accumulation decreased that lead to the decreasing in the value of dielectric loss.

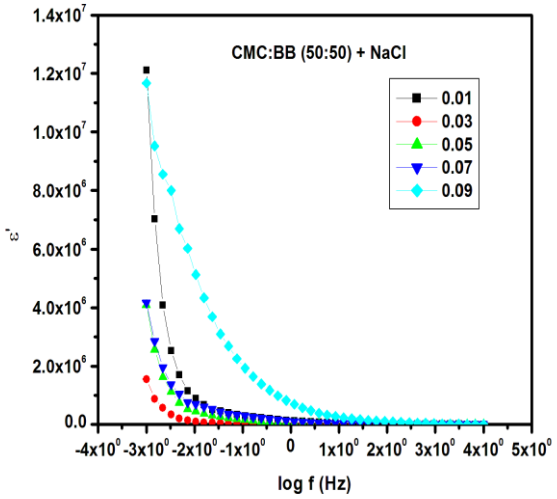

(a)

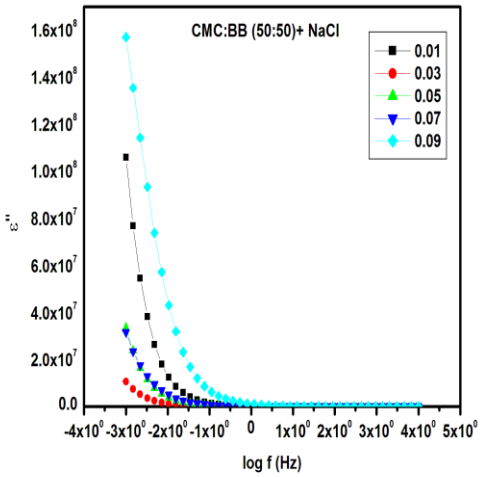

(b)

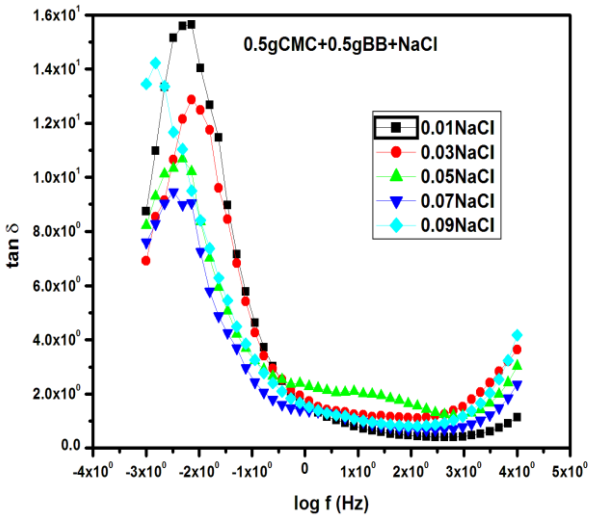

(c)

Figure 4.31 (a) Dielectric constant (b) Dielectric loss and (c) tan δ of the various concentration of NaCl with CMC: BB (50:50)

Figure 4.31 (a, b& c) shows the dielectric constant, dielectric loss and tan δfor various concentration of CMC: BB (50:50) with various concentrations of NaCl. It is observed that the dielectric constant and dielectric loss is maximum at low frequency region and gradually decreases with increasing frequency. Polarization mainly depends on the ability of the dipoles to orient themselves in the direction of the applied electric field. The larger value of ϵ' at lower frequency can be attributed to the large time taken for dipoles to orient themselves in the direction of AC field.

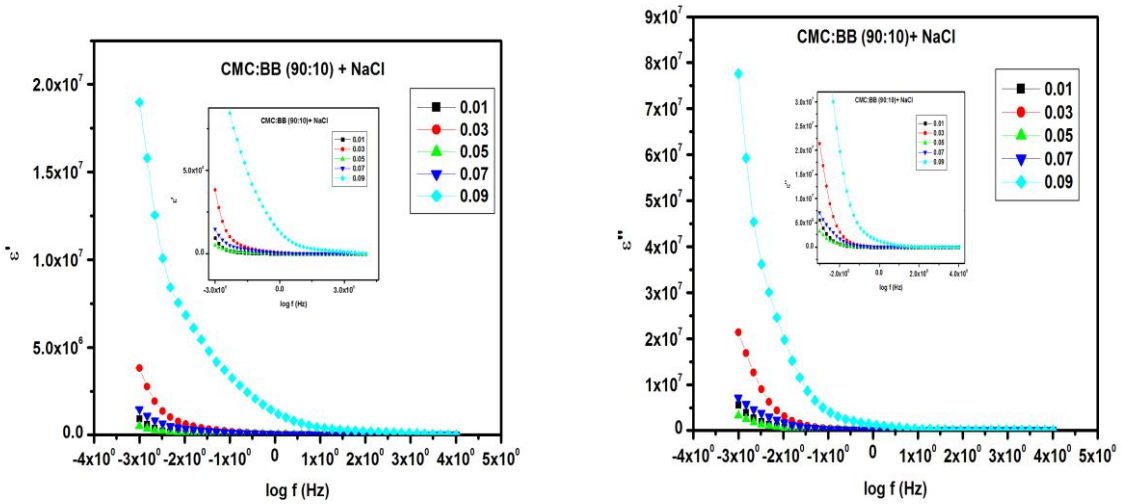

(a) (b)

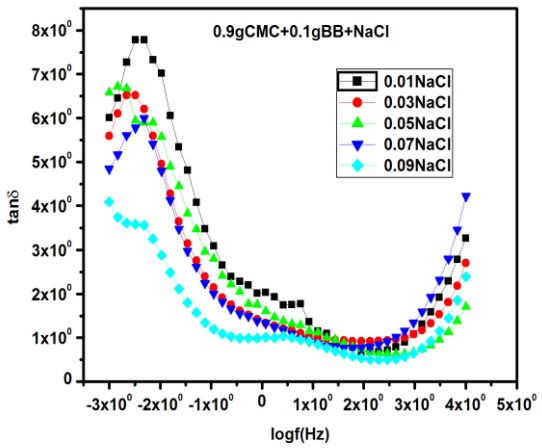

(c)

Figure 4.32 (a) Dielectric constant (b) Dielectric loss and (c) tan δ of the various concentration of NaCl with CMC: BB (90:10)

Figure 4.32 (a, b & c) shows the dielectric constant, dielectric loss and tan δ for various concentration of CMC: BB (90:10) with various concentrations of NaCl.Both dielectric constant and dielectric loss rise sharply at low frequencies indicating that electrode polarization or space charge effects have occurred confirming non-Debye dependence. On the other hand, as the frequency is increased, the rate of reversal of the electric field also increases and so there was no time for charge to and hence they build up at the interface. Therefore, the polarization due to charge accumulation decreased which lead to the decrease in the value of dielectric loss [97]. All the dielectric relaxations observed at various concentrations confirms that the relaxation is due to the electrolyte electrode interfacial capacitance. The membranes which did not have relaxation are considered favourable for the application of supercapacitor.

4.2.4LEAF VEIN CASTED MEMBRANE

The chosen ratio of CMC:BB is 50:50 ratio and the NaCl Concentration of 0.09g is the most favourable one out of all the ratios and concentrations tried so far. Hence, the Leaf vein where chlorophyll is removed and dried is casted with the chosen ratio of CMC:BB and NaCl Concentration. The single casted membrane is evaluated for conduction similar to the membranes. Figure 4.33a and b shows the Nyquist and Bode plot of imaginary impedance of the single casted Leaf membrane. The relaxation frequency is 344 mHz. Hence, the relaxation is only due to the electrode electrolyte interfacial polarization.The total resistance of single casted membrane alone is ~ 8 Megaohms which is extremely high. Hence, a double casting, as explained in the materials and methods chapter, shown in Figure 4.34 a and b, exhibits a total resistance of ~ 0.5 Mega ohms. One order reduction of resistance is seen between single and double casted leaf reinforced membrane which is the most fascinating result in the membranes. The relaxation of single casted membrane is at 316mHz however of the double casted membrane is 12Hz. This indicates that, in the single casted membrane, the relaxation is caused due to the accumulation of charges in the electrolyte- electrode interface. But, in the case of double casted membrane, the relaxation occurs in the insulating medium. This is quite expected as the leaf vein would also be able to conduct which is observed by the drastic reduction of the resistance but the rate of transfer of charges from the insulating matrix to the leaf vein would be different from the rate of transfer of charges within the leaf vein. Hence, a space charge effect would be possible on the surface of the leaf vein thus exhibiting relaxation in the insulating matrix itself. Figure 4.35 shows a comparison between the single casted and double casted membranes with same quantity of NaCl dispersed as an

electrolyte. Comparing with single casting method, double casted method provides the good result.

As the double casting method shows a better result, further improvisation of conduction is attempted with the addition of electrolytic salt, NaCl. As the concentration 0.09g yielded better result in the CMC: BB 50:50 membrane, the same is employed for testing the double casted membrane.

The equivalent circuit fitted data for the double casted membrane is consolidated in Table 4.5. It is to be noted that there is a CPE component alone without electrode electrolyte resistance in all the four membranes namely, CMC:BB (50:50), CMC:BB (50:50) with 0.09g NaCl, CMC:BB (50:50) with Leaf vein and CMC:BB (50:50)with Leaf vein and 0.09g NaCl.

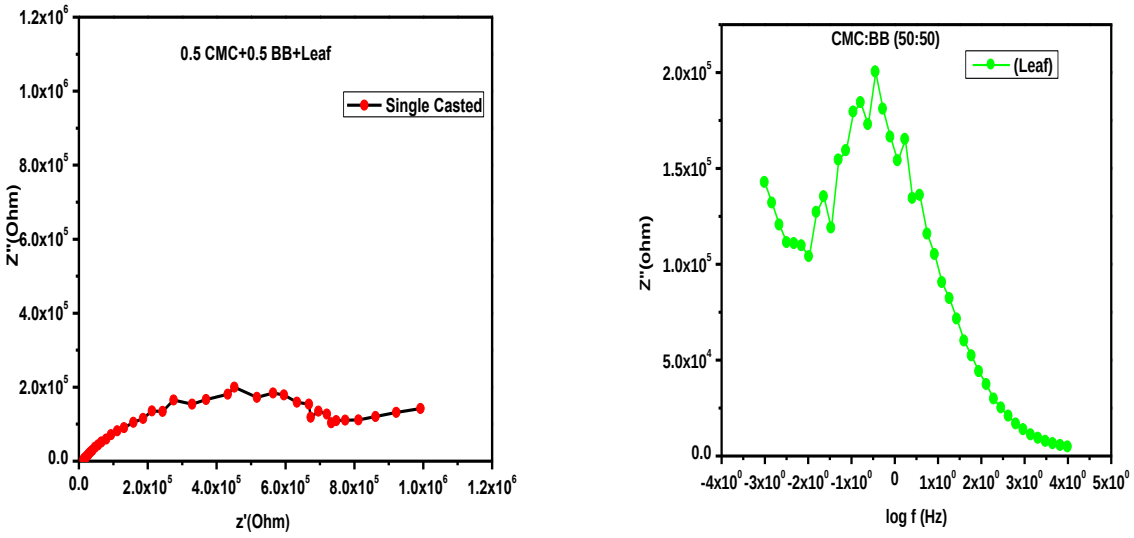

(a) (b)

Figure 4.33 (a) Nyquist plot (b) Bode Plot of the imaginary impedanceof the Single casted CMC:BB (50:50) membrane

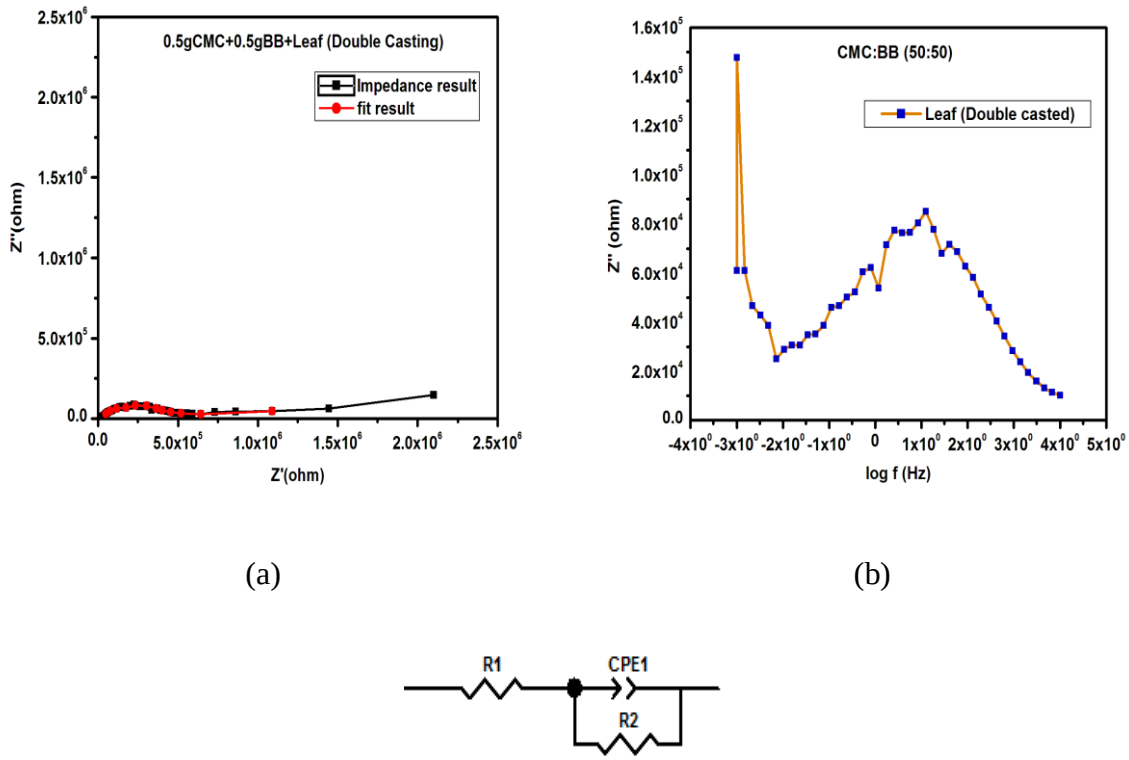

Figure 4.34 (a) Nyquist plot (b) Bode Plot of the imaginary impedance (c) fitted equivalent circuit of the Leaf Double Casted CMC:BB (50:50) membrane

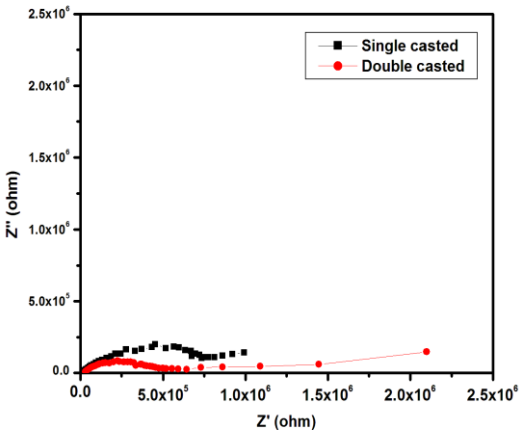

Figure 4.35 (a) Comparison between Single Casted and Double Casted CMC: BB (50:50) membrane

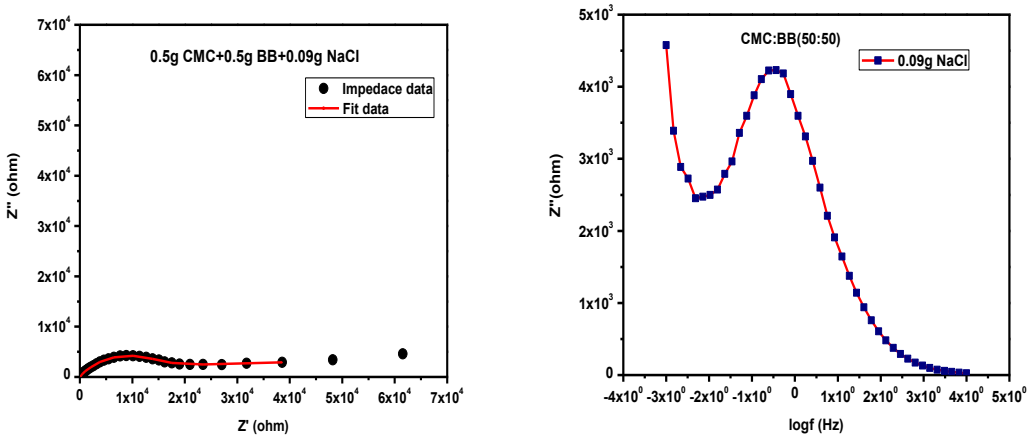

(a) (b)

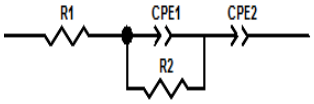

(c)

Figure 4.36(a) Nyquist plot (b) Bode Plot of the imaginary impedance (c) Equivalent circuit of the Double casted CMC:BB (50:50) membrane with electrolytic salt of 0.09g NaCl

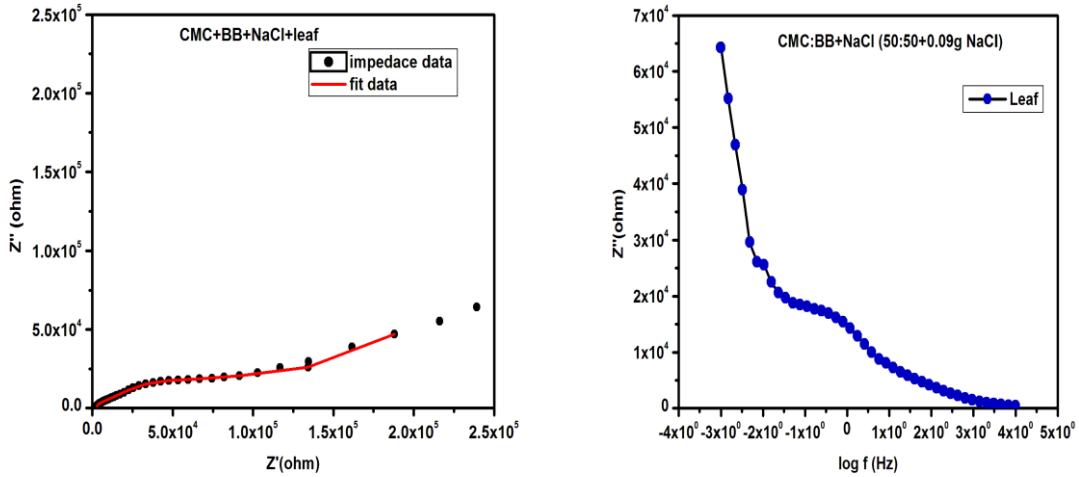

(a) (b)

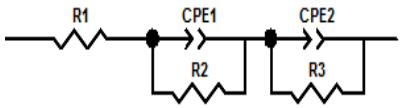

(c)

Figure 4.37(a) Nyquist plot (b) Bode Plot of the imaginary impedance (c) Equivalent circuit of the Double casted CMC:BB (50:50) membrane with electrolytic salt of 0.09g NaCl

The fitted data explicitly shows that the electrolytic resistance is more when the leaf and NaCl are employed simultaneously. However, the insulating matrix resistance is extremely lowered in the case of Leaf and when NaCl is employed alone. It is quiet natural that the conduction increases when NaCl is added to the matrix. But, it is to be specifically noted that just addition of leaf vein brings a conduction more or less similar effect as that of NaCl inclusion in conduction. On contrary, when both are employed together a huge resistance of the interface is observed which indicates that the rate of conduction is high but the reception of the electrode is less. Thus, it is sure that the addition of leaf vein in the insulating matrix has got a favourable effect on conduction. However, a proper interfacing methodology to drain the charges in the electrode is in demand for a better conduction to occur. Figure 4.39 shows the dielectric performance of these membranes which again confirms that only interfacial capacitance is dominant by the low frequency dispersion of the dielectric profile. Further to look into a possibility that the huge resistances may emerge due to agglomeration of salt, the FTIR is analysed for any alkali metal bonding.

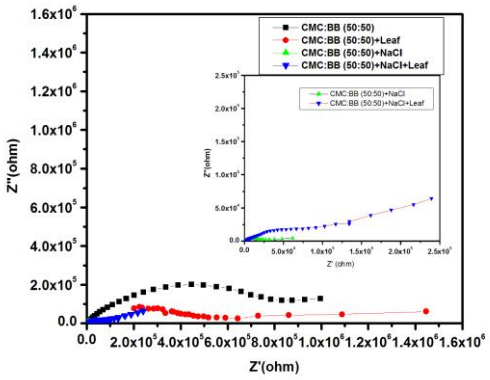

Figure 4.38 Comparision of Nyquist plot of CMC:BB (50:50) membrane with leaf and NaCl

Table 4.5 Comparision of CMC:BB (50:50) membrane with leaf and NaCl

S. No	Ratio of NaCl (g)	Leaf	Thickness of the membrane 10^{-3} m	Overlapped area of the film 10^{-4} m^2	R1 (Ω)	R2 (Ω)	R3 (Ω)	CPE1-T (µF)	CPE1-P	CPE2-T (µF)	CPE2-P	DC Conductivity (Sm^{-1})
1.	-	-	0.140	4	4.47	722550	-	1.6841	0.59	25.389	0.34	0.388 $x10^{-6}$
2.	-	Leaf double casted	0.250	4	10	600910	-	0.5893	0.37	63.121	0.40	1.25 $x10^{-6}$
3.	0.09	-	0.216	4	69.8	2223	17122	31.1	0.71	49.7	0.62	27 $x10^{-6}$
4.	0.09	Leaf double casted	0.228	4	1575	8620	85477	3.5388	0.62	11.337	0.54	5.7 $x10^{-6}$

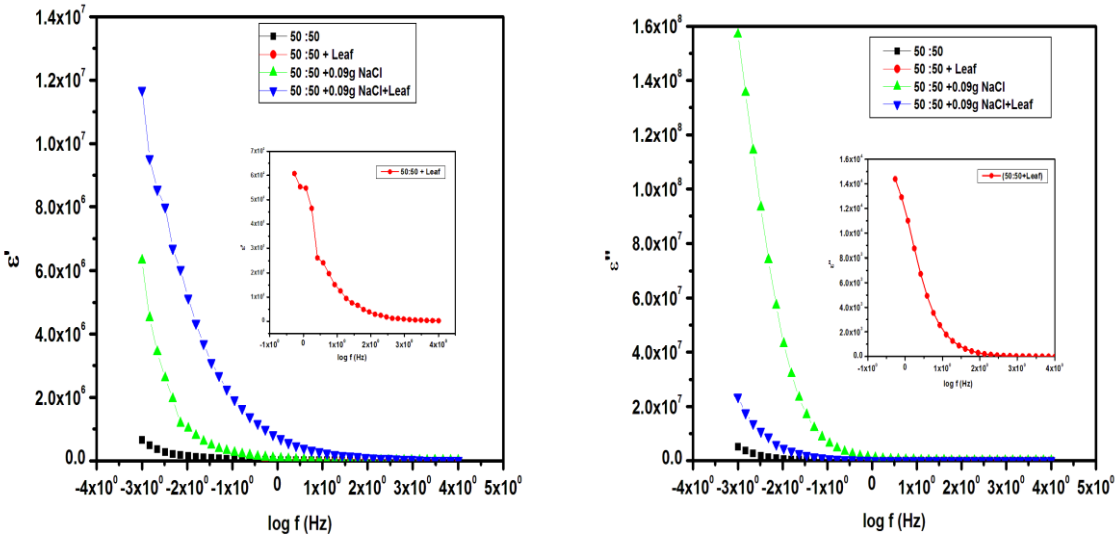

(a) (b)

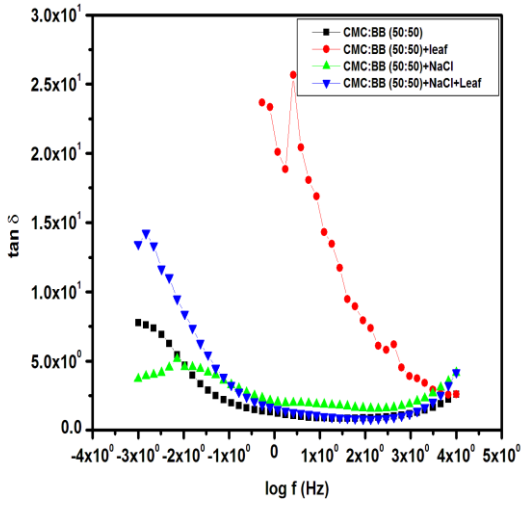

(c)

Figure 4.39(a) Dielectric constant (b) Dielectric loss and (c) tan δ of the various concentration of Leaf composited membrane

4.3 FOURIER TRANSFORM INFRARED SPECTROSCOPY (FTIR)

Fourier Transform Infrared Spectroscopy (FTIR) provides the specific information about the vibrational modes of chemical bonding and molecular structures. Figure 4.40 shows the FTIR spectra comparing the pristine CMC, pristine BB, CMC:BB (50:50) ratio and CMC:BB (50:50) with leaf vein , CMC:BB(50:50) with NaCl 0.09g and CMC:BB (50:50) with NacL (0.09g) and Leaf vein. The assignments of the absorption due to the different vibrational state in the FTIR spectra are listed in the Table 4.6. Majority of the FTIR vibrations are observed with the CMC or Bovine Bone. No minor peaks of NaCl could be identified since the concentration of NaCl is too low in the membrane. There appears some shift due to the addition of either leaf vein or NaCl in the membrane in few peak positions indicating their presence but cannot be taken as confirmation of NaCl in the membrane. However, as no heat or any other treatment except for air drying is carried out in the samples, NaCl added need to be remaining in the membrane. Hence, the results are attributed to the addition of leaf or NaCl as included during preparation itself. It is to be noted that the CMC and BB spectra gets mixed in the membranes and only to show this, independents spectra of CMC and BB are included in the figure. The bands around 1200 to 1400cm^{-1}, corresponding to CH and CN bond stretching, are intense in the CMC pure spectra but they all got suppressed in the BB included membranes. These got completely suppressed in NaCl added membrane but got a bit prominent when included with both leaf vein and NaCl. Thus, these CH and CN bonds are bound when they are formed as membranes. Hence, it can be understood that the CMC and BB gets engaged through weaker bonds and thus how a complex membrane which can be a standalone film for handling [98-100].

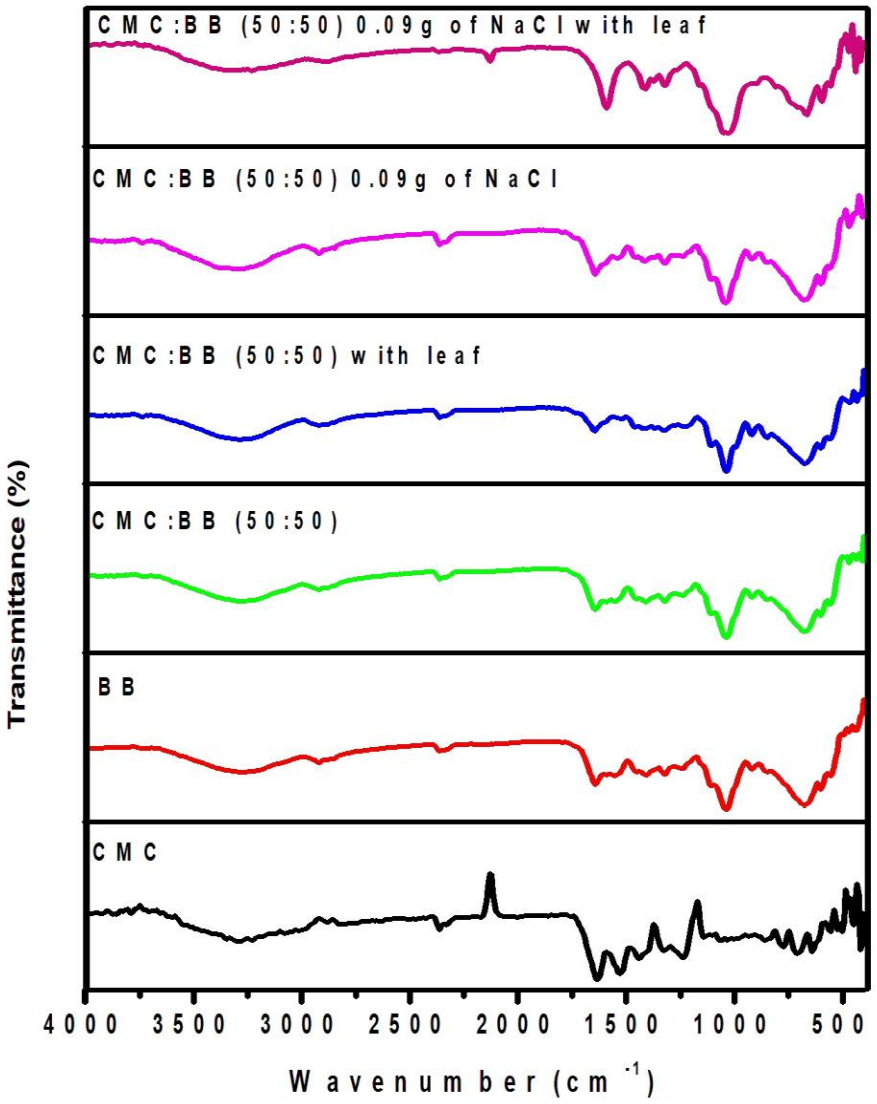

Figure 4.40FTIR spectra comparing the pure CMC, pure BB, CMC:BB (50:50), CMC:BB (50:50) with Leaf vein, CMC:BB (50:50) with NaCl, and CMC:BB(50:50) with NaCl and Leaf vein

Table: 4.6 Table 4.6 FTIR Assignments table for variety of CMC:BB Membranes under study

Wave number (cm^{-1})	**Assignment/vibration**					
	CMC	**BB**	**CMC:BB (50:50)**	**CMC:BB+Leaf (50:50+Leaf)**	**CMC:BB+NaCl (50:50+0.09g)**	**CMC:BB+NaCl+Leaf (50:50+0.09g +Leaf)**
620	-	V_4Phosphate	-	-	-	-
660	-	-	-	-	V_4Phosphate	-
663	-	-	-		-	-
664	-	-	-	V_4Phosphate	-	-
685	-	-	V_4Phosphate	-	-	V_4Phosphate
916	-	-	V_4Phosphate	V_4Phosphate	-	-
928	-	-	-	-	V_4Phosphate	-
1026	-	-	-	V_3 Phosphate	-	-
1031	C-O Stretching	-	-	-	-	-
1034	-	-	C-O Stretching	-	-	-
1043	-	-	-	-	C-O Stretching	-

Wave number (cm^{-1})	Assignments /vibration					
	CMC	**BB**	**CMC:BB (50:50)**	**CMC:BB+Leaf (50:50+Leaf)**	**CMC:BB+NaCl (50:50+0.09g)**	**CMC:BB+NaCl+Leaf (50:50+0.09g +Leaf)**
1050						C-O Stretching of CMC polysaccharide skeleton
1228	-	-	Amide III combined effect of C-N stretching and N-H in-plane bending	-	-	-
1231	-	-	-	Amide III combined effect of C-N stretching and N-H in-plane bending	Amide III combined effect of C-N stretching and N-H in-plane bending	-
1316-1329	O-H Stretching in plane and symmetic C-H Stretching	-	O-H Stretching in plane and C-H symmetric Stretching	O-H Stretching in plane and symmetric C-H Stretching -	O-H Stretching in plane and symmetric C-H Stretching	O-H Stretching in plane and C-H symmetric Stretching

Wave number (cm^{-1})	**Assignments /vibration**					
	CMC	**BB**	**CMC:BB (50:50)**	**CMC:BB+Leaf (50:50+Leaf)**	**CMC:BB+NaCl (50:50+0.09g)**	**CMC:BB+NaCl+Leaf (50:50+0.09g +Leaf)**
1413	v_3 Carbonate vibration	-	-	v_3 Carbonate vibration	-	v_3 Carbonate vibration
1420	-	V3 Carbonate vibration	-	-	-	-
1434	-	V3 Carbonate vibration	-	-	-	-
1440	-	-	V3 Carbonate vibration	-	-	-
1515 - 1535	-	Vibrations from amide II bending vibration from N-H groups	-	-	Vibrations from amide II bending vibration from N-H groups	Vibrations from amide II bending vibration from N-H groups
1540	-	-	Vibrations from amide III plane of C-N and N-H groups	-	-	-

Wave number (cm^{-1})	**Assignments /vibration**					
	CMC	**BB**	**CMC:BB (50:50)**	**CMC:BB+Leaf (50:50+Leaf)**	**CMC:BB+NaCl (50:50+0.09g)**	**CMC:BB+NaCl+Leaf (50:50+0.09g +Leaf)**
1580	Presence of COO^-assigned to carboxyl group	-	-	-	-	-
1622	-	C=O stretching of amide I or Hydrogen bond coupled to COO	-	-	-	-
1637 - 1644	-	-	C=O stretching of amide I	C=O stretching of amide I	C=O stretching of amide I	C=O stretching of amide I
2358	-	-	Related to the background CO_2 in the spectrometer	-	-	-

Wave number (cm^{-1})	**Assignments /vibration**					
	CMC	**BB**	**CMC:BB (50:50)**	**CMC:BB+Leaf (50:50+Leaf)**	**CMC:BB+NaCl (50:50+0.09g)**	**CMC:BB+NaCl+Leaf (50:50+0.09g +Leaf)**
2366	-	Related to the background CO_2 in the spectrometer	-	Related to the background CO_2 in the spectrometer	-	-
2373	-	-	-	-	Related to the background CO_2 in the spectrometer	-
2867 – 2925	CH stretching associated with methane ring of hydrogen atom	-	CH stretching associated with methane ring of hydrogen atom	-	CH stretching associated with methane ring of hydrogen atom	CH stretching associated with methane ring of hydrogen atom
3281-3762	OH-Hydroxyl group	OH-Hydroxyl group	OH-Hydroxyl group	OH-Hydroxyl group	OH-Hydroxyl group	OH-Hydroxyl group

CHAPTER-V

5.1 Summary and Conclusion:

The optimization of CMC:BB membranes at different ratios are made and found that 50:50 is more suitable ratio in terms of conductivity with low solution or electrolytic conduction, optimal insulating matrix resistance and interfacial resistance. An electrolytic salt, which is a very common one, NaCl is used to disperse in the membrane for improving the electrolytic conduction. Out of the different ratios of NaCl added to the membrane, 0.09g yielded better results and hence further analyses are made using CMC:BB (50:50) with 0.09g of NaCl. The conductivity of the membrane got improved and further attempt on including a leaf vein resulted in equivalent conduction corresponding to the NaCl added matrix. The impedance data are analysed also for the NaCl and Leaf vein added CMC:BB membrane. The addition of NaCl and Leaf vein and Leaf vein alone showed impedances due to the interface indicating that the rate of charge transfer is faster in the insulating matrix compared to the electrode-electrolyte interface. Hence, the conduction of CMC:BB with NaCl resulted in $27x10^{-6}$ Sm^{-1}, one order less conduction ($5.7x10^{-6}$ Sm^{-1}) for the NaCl with Leaf added to CMC:BB membrane , CMC:BB with leaf showed a conductivity of 1.25 $x10^{-6}Sm^{-1}$ compared to the lowest conductivity of $0.388x10^{-6}Sm^{-1}$. The dielectric relaxation studies ensured the interfacial resistance and also assured that no insulation matrix relaxations occurred indicating that the electrolytic conduction occurred in the membrane. FTIR results also affirmed that NaCl did not agglomerate in the medium. Thus, in the present work, the leaf vein reinforced CMC:BB membrane with an electrolytic salt , NaCl, is analysed and found favourable for supercapacitor applications.

REFERENCE

[1] A. Burke, Analysis of Hybrid Rechargeable Energy Storage Systems in Series- In Hybrid Electric Vehicles Based on Simulations, Electrochemiaca Acta 53 (2007) 1083–1091.

[2] Partice Simon,Yury Gogotsi, Materials for electrochemical capacitors, A nature research Journal 7 (2008) 845-854.

[3] D. Connolly, A Review of Energy Strorage Technologies (2009).

[4] Schmidt-Rohr, Klaus, How Batteries Store and Release Energy: Explaining Basic Electrochemistry, Journal of Chemical Education 95 (2018) 1801–1810.

[5] Pistoia, Gianfranco , Batteries for Portable Devices, Elsevier *(* 2016).

[6] Khurmi, R. S, Material Science S (2014).

[7] Schmidt-Rohr, K , How Batteries Store and Release Energy: Explaining Basic Electrochemistry, J. Chem. Educ. 95 (2018) 1801-1810.

[8] M. Jayalakshmi , M. Palaniappa, K. Balasubramanian, Single Step Solution Combustion Synthesis of ZnO/carbon Composite and its Electrochemical Characterization for Supercapacitor Application, Int. J. Electrochem. Sci., 3 (2008) 96 – 103.

[9] Tehrani, Z.,Thomas, D.J., Korochkina, T., Phillips, C.O., Lupo, D., Lehtimäki, S.,O.Mahony, J., Gethin, D.T., Large-area printed supercapacitor technology for low-cost domestic green energy storage, Energy 118 (2017) 1313–1321.

[10] P. Sharma, T.S. Bhatti, A review on electrochemical double-layer capacitors, Energy Conversion and Management 51 (2010) 2901.

[11] Partice Simon,Yury Gogotsi, Materials for electrochemical capacitors, A nature research Journal 7 (2008) 845-854.

[12] G. Wang, L. Zhang, J. Zhang, A review of electrode materials for electrochemical supercapacitors, Chemical Society Reviews 41 (2012) 797-828.

[13] Becker, HI , Low voltage electrolytic capacitor, US Patent 2800616 (1957).

[14] R. Kötz, P.W. Ruch, D. Cericola, Aging and failure mode of electrochemical double layer capacitors during accelerated constant load tests, In Journal of Power Sources 195 (2010) 923-928.

[15] Y.-H. Lin, T.-Y. Wei, H.-C. Chien, S.-Y. Lu, Manganese Oxide/Carbon Aerogel Composite: an Outstanding Supercapacitor Electrode Material, Adv. Energy. Mat. 1 (2011) 901-907.

[16] N.B. Trung, T.V. Tam, H.R. Kim, S.H. Hur, E.J. Kim, W.M. Choi, Three-dimensional hollow balls of graphene–polyaniline hybrids for supercapacitor applications, Chem. Eng. J. 255 (2014) 89-96.

[17] N.S. Choi, Z. Chen, S.A. Freunberger, X. Ji, Y.K. Sun, K. Amine, G. Yushin, L.F. Nazar, J. Cho, P.G. Bruce, Challenges facing lithium batteries and electrical double-layer capacitors, Angew. Chem. Int. Ed. 51 (2012) 9994-10024.

[18] B.Dyatkin, V.Presser, M.Heon, M. R. Lukatskaya, M.Beidaghi, Y.Gogotsi, Development of a green supercapacitor composed entirely of environmentally friendly materials. ChemSusChem 6(2013) 2269-2280.

[19] Becker, H.I., Low voltage electrolytic capacitor, United States Patent Office 7 (1957) 23.

[20] Ho, J., Jow, R., Boggs, S, Historical Introduction to Capacitor Technology, IEEE Electrical Insulation Magazine. 26 (2010) 20–25.

[21] A brief history of supercapacitors, Batteries & Energy Storage Technology (2014).

[22] Rightmire, Robert A., Electrical energy storage apparatus (1966).

[23] J. G. Schindall, The Change of the Ultra-Capacitors, IEEE Spectrum (2007).

[24] Conway, Brian Evans , Electrochemical Supercapacitors: Scientific Fundamentals and Technological Applications , Springer 978 (1999)1–8.

[25] Conway, Brian Evans, Transition from Supercapacitor to Battery Behavior in Electrochemical Energy Storage, J. Electrochem. Soc. 138 (1991) 1539–1548.

[26] A. M. Namisnyk, A survey of electrochemical supercapacitor technology (2003).

[27] Aiping Yu, Victor Chabot, and Jiujun Zhang, Electrochemical supercapacitors for energy storage and delivery fundamentals and applications (2013).

[28] Conway, BE, Birss, V & Wojtowicz, J , The Role and utilization of pseudocapacitance for energy storage, Journal of Power Sources 66 (1997) 1-14.

[29] Ruch, PW, Kötz, R & Wokaun, A , Electrochemical characterization of single-walled carbon nanotubes for electrochemical double layer capacitors using non-aqueous electrolyte, Electrochimica Acta 54 (2009) 4451– 4458.

[30] Braun, A, Bartsch, M, Merlo, O, Schnyder, B, Schaffner, B, Kotz, R, Haas, O & Wokaun, A , Exponential growth of electrochemical double layer capacitance in glassy carbon during thermal oxidation 41 (2003) 759–765.

[31] Zheng, JP, Huang, J & Jow, TR, The limitations of energy density for electrochemical capacitors, Journal of Electrochemical Society 144 (1997) 2026 – 2031.
[32] Zhang, LL & Zhao, XS, Carbon-based materials as supercapacitor electrodes, Chem. Soc. Rev., 38 (2009) 2520–2531.
[33] E. Gongadze, S. Petersen, U. Beck, U. van Rienen, Classical models of the interface between an electrode and an electrolyte, Research gate (2015).
[34] B. Conway, V.Birss, J. Wojtowicz, The role and utilization of pseudocapacitance for energy storage by supercapacitors, Journal of Power Sources 66 (1997) 1.
[35] J.R. Miller, P. Simon, Fundamentals of electrochemical capacitor design and operation, Electrochemical Society Interface 17 (2008) 31.

[36] X.-h. Xia, J.-p. Tu, X.-l. Wang, C.-d. Gu, X.-b. Zhao, Hierarchically porous NiO film grown by chemical bath deposition via a colloidal crystal template as an electrochemical pseudocapacitor material Journal of Materials Chemistry 21 (2011) 671.

[37] C. Arbizzani, M. Mastragostino, L. Meneghello, Polymer-based supercapacitor : A comapritive study, Electrochimica Acta 41 (1996) 21-26.

[38] Maiti, S., A. Pramanik, and S. Mahanty , Extraordinary high pseudocapacitance of metal organic framework derived nanostructured cerium oxide, Chemical Communications 50 (2014) 11717-11720.
[39] C. Ming Chuang, C. W. Huang, H. Teng and J. M. Ting, Effects of Carbon Nanotube Grafting on the Performance of Electric Double Layer Capacitors, Energy & Fuels 24 (2010) 6476-6482.
[40] Liu, J, Essner, J & Li, J, Hybrid supercapacitor based on coaxially coated manganese oxide on vertically aligned carbon nanofiber arrays, Chem. Mater 22 (2010) 5022-5030.
[41] Y. Gogotsi and P. Simon, Science, True Performance Metics in Elcetrochemical Energy Storage 334 (2011) 917–918.
[42] A. Burke, Analysis of Hybrid Rechargeable Energy Storage Systems in Series Plug –In Hybrid Electric Vehicles Based on Simulations, Electrochim. Acta,. 53 (2007) 1083–1091.
[43] K. Naoi, S. Ishimoto, J. I. Miyamoto and W. Naoi, Second generation nanohybrid supercpacitor: Evolution of capacitive energy storage Energy Environ. Sci., 5 (2012) 9363–9373.
[44] M. Lu, F. Beguin and E. Frackowiak, Supercapacitors: Materials, Systems and Applications, John Wiley & Sons, 2013.

[45] J. Chmiola, G. Yushin, Y. Gogotsi, C. Portet, P. Simon and P. L. Taberna, Anomalous Increase in Carbon Capacitance at Pore Sizes Less than 1 Nanometer, Science 313 (2006) 1760–1763.

[46] L. L. Zhang and X. S. Zhao, A review of electrode materials for electrochemical supercapacitors, Chem. Soc. Rev., 38 (2009) 2520–2531.

[47] A. Burke, J. Power Sources, Ultracapacitors: why, how, and where is the technology 91 (2000) 37–50.

[48] A. Burke and M. Miller, The Power Capability of Ultracapacitors and Lithium Battries for Electric and Hybrid Vehicle Applications, J. Power Sources, 196 (2011) 514–522.

[49] Aiping Yu, Victor Chabot, and Jiujun Zhang, Electrochemical supercapacitors for energy storage and delivery fundamentals and applications (2013).

[50] L. L. Zhang and X. S. Zhao, Carbon based materials as supercapacitor electrodes, Chem. Soc. Rev, 38 (2009) 2520–2531.

[51] Cheng Zhong, Yida Deng, Wenbin Hu, Jinli Qiao, Lei Zhang ,Jiujin Zhang, A review of electrolyte materials and compositions for electrochemical supercapacitors, Chem. Soc. Rev., 44 (2015) 7484-7539.

[52] Kotz, R, M. Carlen, Principles and applications of electrochemical capacitors, Electrochemica Acta 45 (2000) 2483-2498.

[53] Vieira, D.F, Avellaneda, C.O. and Pawlicka A., Conductivity study of a gelatin-based polymer electrolyte, Electrochimica Acta, 53 (2007) 1404-1408.

[54] Avellanedaa, C.O., Vieirac, D.F., Kahlouta, A.A., Heusinga, S., Leiteb, E.R., Pawlicka, A. and Michel A., All solid-state electrochromic devices with gelatin-based electrolyte, Solar Energy Materials and Solar Cells, 92 (2008) 228–233.

[55] Andrade, J., Raphael, E. and Pawlicka, A., Plasticized pectin-based gel electrolytes, Electrochimica Acta, 54 (2009) 6479-6483.

[56] Khiar, A.S.A. and Arof, A.K., Conductivity studies of starch-based polymer electrolytes, Ionics, 16 (2010) 123–129.

[57] Rozely, F.M.S., Marcondes, P. S., Agostini, D., Ferreira, J., Emerson, M. G., Pawlicka, A. and Douglas, C., Amylopectin-rich starch plasticized with glycerol for polymer electrolyte application, Solid State Ionics, 181 (2010) 586-591.

[58] Tiwari ,T., Srivastava, N. and Srivastava, P. C., Electrical transport study of potato starch-based electrolyte system, Ionics, 17 (2011) 335-360.

[59] Leones, Sentanin, F., Rodrigues, L.C., Ferreira, R.A.S., Marrucho, I.M., Esperança, J.M.S.S., Pawlicka, A., Carlos L.D. and Silva M.M., Novel polymer electrolytes based on gelatin and ionic liquids, Optical Materials, 35 (2012) 187–195.

[60] Sit Y.K, Samsudin, A.S. and Isa M.I.N, Ionic conductivity study on hydroxyethyl cellulose (HEC) doped with NH4Br based biopolymer electrolytes, Research Journal of Recent Sciences, 1 (2012) 16-21.

[61] Noor, I.S.M., Majid, S.R., Arof, A.K., Djurado, D., Neto, S. C. and Pawlicka A., Characteristics of gellan gum–LiCF3SO3 polymer electrolytes, Solid State Ionics, 225 (2012) 649-653.

[62] Ramlli, M.A. and Isa, M.I.N., Conductivity study of carboxyl methyl cellulose solid biopolymer electrolytes (SBE) doped with ammonium fluoride, Research Journal of Recent Sciences,. 2277 (2013) 2502-2509.

[63] M. N. Chai, M. I. N. Isa, The Oleic Acid Composition Effect on the Carboxymethyl Cellulose Based Biopolymer Electrolyte, Scientific research, 3 (2013), 1-4

[64] Shukur, M. F., Ibrahim, F.M., Majid, N. A., Ithnin, R. and Kadir, M.F.Z., Electrical analysis of amorphous corn starch-based polymer electrolyte membranes doped with LiI, The Royal Swedish Academy of Sciences Physica Scripta, 88 (2012) 025601-025608.

[65] Rani ,M.S.A, Rudhziah, S., Azizan, A. and Mohamed N.S, Biopolymer electrolyte based on derivatives of cellulose from kenaf bast fiber, Polymers, 6 (2014) 2371-2385.

[66] Ramlli, M.A. and Isa, M.I.N., Conductivity study of carboxyl methyl cellulose solid biopolymer electrolytes (SBE) doped with ammonium fluoride, Research Journal of Recent Sciences ISSN, 2277 (2014) 2502-2509.

[67] Shukuret M. F, Y.M Ysof, Electrical analysis of amorphous corn starch-based polymer electrolyte membranes doped with LiI, The Royal Swedish Academy of Sciences Physica Scripta, 88, (2014) 025601-025608.

[68] Arora, N., Kumar, R. and Kumar, A., Transport studies of Xanthan Gum based gel electrolytes containing ammonium chloride salt, International Journal of Research in Engineering and Technology, 4 (2014) 68-71.

[69] Vijaya, N., S. Selvasekarapandian, S., Pandi, D.V., Sindhuja, S., Arun, A. and Karthikeyan, S., Bio – polymer pectin based proton conducting polymer electrolyte, Asian Conference on Solid State Ionics (2014).

[70] Leones, R., Botelho, M. B. S., Sentanin, F., Cesarino, I., Pawlicka, A., Camargo, A. S. S.D. and Silva, Pectin-based polymer electrolytes with Ir (III) complexes, Molecular Crystals and Liquid Crystals, 604 (2014) 117-125.

[71] Sudhakar, Selvakumar, M. and Bhat, D.K., Lithium salts doped biodegradable gel polymer electrolytes for supercapacitor application, Journal of Material Environment Science 6 (2015) 1218-1227.

[72] Zhu, Y.S., Xiao, S.Y., Li, M.X., Chang, Z., Wang, F.X., Gao, J. and Wu, Y.P., Natural macromolecule based carboxymethyl cellulose as a gel polymer electrolyte with adjustable porosity for lithium ion batteries, Journal of Power Sources, 288 (2015) 368–375.

[73] Sohaimy, M. I. H. and Isa M. I. N., Conductivity and dielectric analysis of cellulose based solid polymer electrolytes doped with ammonium carbonate (NH4CO3), Applied Mechanics and Materials, 719-720 (2015) 67-72.

[74] Sudhakar, Y.N., Selvakumar, M. and Bhat, D.K., Preparation and characterization of phosphoric acid-doped hydroxyethyl cellulose electrolyte for use in supercapacitor, Materials for Renewable and Sustainable Energy, 4 (2015) 10-18.

[75] Ledwon, P. Andrade, J.R., Lapkowski, M. and Pawlicka, A., Hydroxypropyl cellulose-based gel electrolyte for electrochromic devices, Electrochimica Acta, 159 (2015) 227-233.

[76] Kavitha, S., Vijaya, N., Pandeeswari, R. and Premalatha, M., Vibrational, electrical and optical studies on pectin- based polymer electrolyte, International Research Journal of Engineering and Technology, 3 (2016) 1385-1390.

[77] M.N.Chai, Iaha, Novel Proton Conducting Solid Bio-polymer Electrolytes Based on Carboxymethyl Cellulose Doped with Oleic Acid and Plasticized with Glycerol, Scientific reports, 6 (2016) 1-6.

[78] Ahmad, N.H., Isa, Ionic conductivity and electrical properties of carboxymethyl cellulose-NH4Cl solid polymer electrolytes, Journal of Engineering Science and Technology, 11, (2016) 839 - 847.

[79] Teoh, K. H., Lim, C.S., Liew, C.W. and Ramesh S., Preparation and performance analysis of barium titanate incorporated in corn starch-based polymer electrolytes for electric double layer capacitor application, Journal of Applied. Polymer Science, 133 (2016) 43275-43286.

[80] HemalathaR, Radha, K.P. and Jesintha, L.R., AC impedance, FTIR studies of biopolymer electrolyte potato starch: NH_4SCN, International Journal of Multidisciplinary Education and Research, 1 (2016) 01-03.

[81] Samsuddin, A.S A.S., Khairul, W.M. and Isa M., Characterization on the potential of carboxy methylcellulose for application as proton conducting biopolymer electrolytes, Journal of Non-crystalline solids, 358 (2016) 1104-1110.

[82] M A Saadiah, Chao L.Z., Electrical study on Carboxymethyl Cellulose-Polyvinyl alcohol based bio-polymer blend electrolytes, Materials Science and Engineering 342 (2018) 012045.

[183] P.Perumal,P Christopher Selvin, S Selvasekarapandian, Characterization of biopolymer pectin with lithium chloride and its applications to electrochemical devices, International Journal of Ionics, 24 (2018) 3559-3570.

[84] N.A.M Noor, I.S.M., Majid, S.R., Arof, A.K., Investigation on transport and thermal studies of solid polymer electrolyte based on carboxymethyl cellulose doped ammonium thiocyanate for potential application in electrochemical devices 5 (2019) 6745.

[85] M. Muthukrishnan, Kumari, Synthesis and characterization of pectin-based biopolymer electrolyte for electrochemical applications, International Journal of Ionics, 25 (2019) 203-204.

[86] P Perumal, P Christopher Selvin, S Selvasekarapandian, P Sivaraj, KP Abhilash, V Moniha, R Manjula Devi, Plasticizer incorporated, novel eco-friendly bio-polymer based solid bio-membrane for electrochemical clean energy applications, Polymer degradation and stability, 159 (2019) 45-53.

[87] S. Mohajer, M. Rezaei, S.F. Hosseini, Physico-chemical and microstructural propertiesof fish gelatin/agar bio-based blend films, Carbohydr. Polym. 157 (2017) 784–793.

[88] Moore, D. M. and R. C. Reynolds, Jr.. X-Ray diffraction and the identification and analysis of clay minerals. 2nd Ed. Oxford University Press, New York 1997.

[89] D. R. Lide, ed., CRC Handbook of Chemistry and Physics, 75th ed., Boca Raton, FL: CRC Press, 1994, 9–79.

[90] R. M. Silverstein, G. C. Bassler, T. C. Morrill, Spectrometric Identification of Organic Compounds, 4th ed., New York: Wiley, 1981, 166.

[91] IUPAC Compendium of Chemical Terminology, 2nd Edition, 1997.

[92] K. S. Cole, R. Cole, Journal of chemical Physics 9 (1941) 341.

[93] C. Gabrielli, Identification of Electrochemical Processes by Ltd., Farnborough, UK (1980).

[94] A. J. Bard, L.R. Faulkner, Electrochemical Methods, John Wiley & Sons, New York 1980, Chapter 9.

[95] M. N. Chai, M. I. N. Isa, The Oleic Acid Composition Effect on the Carboxymethyl Cellulose Based Biopolymer Electrolyte, Journal of Crystallization Process and Technology, 3 (2013) 1-4.

[96] M.A. Ramlli, M.N. Chai and M.I.N. Isa, Influence of propylene carbonate as a plasticizer in CMC-OA based biopolymer electrolytes: conductivity and electrical study, Advanced Materials Research 802 (2013) 184-188.

[97] M A Saadiahand, A S Samsudin,Electrical study on Carboxymethyl Cellulose-Polyvinylalcohol based bio-polymer blend electrolytes, IOP Conf. Series: Materials Science and Engineering 342 (2018) 012045.

[98] M.A.S.P. Nur Hazirah, M.I.N. Isa, N.M. Sarbon, Effect of xanthan gum on the physical and mechanical properties of gelatin-carboxymethyl cellulose film blends, Food Packaging and Shelf Life 9 (2016) 55–63.

[99] Ali Hebeish, S. Sharaf, Novel nanocomposite hydrogel for wound dressingand other medical applications, Royal Society of Chemistry, 5 (2015) 103036

[100] Xanes and Ftir study on dried and calcined bones by jayapradhi rajendran (2011).